CRANFIELD UNIVERSITY

Emanuele Pagone

Techno-Economic Environmental Risk Analysis of Sustainable Power Systems

School of Aerospace, Transport and Manufacturing

Doctor of Philosophy
Academic Year: 2017–2018

Supervisor: Prof Pericles Pilidis
January 2018

CRANFIELD UNIVERSITY

School of Aerospace, Transport and Manufacturing

Doctor of Philosophy Full Time

Academic Year 2017-2018

Emanuele Pagone

Techno-Economic Environmental Risk Analysis of Sustainable Power Systems

Supervisor: Prof Pericles Pilidis
January 2018

Typeset in LaTeX 2_ε.

Emanuele Pagone: *Techno-Economic Environmental Risk Analysis of Sustainable Power Systems,* Doctor of Philosophy thesis,

Abstract

Sustainable engine systems are undoubtedly one of the main topics at the centre of the recent scientific debate. A significant number of novel thermodynamic concepts, partly based on gas turbine engines, are available in the open scientific literature and have been scarcely investigated. Cranfield University has developed an integrated, modular, multi-disciplinary framework of computational software called Techno-economic Environmental Risk Analysis (TERA) to assess complex, thermodynamic cycles from an integrated point of view.

The present study completes a TERA work on sustainable power systems in two steps. Initially, the entire TERA methodology is applied to the aviation field with the integration of a set of modules to investigate three novel, turbofan, aircraft engines. Namely, the mentioned concepts are featured by: a counter-rotating core for short range (GTCRSR), an active core for short range (GTACSR), and an inter-cooler for Long Range (GTICLR). The optimised design specifications of the GTCRSR engine show a reduction of more than 7% of block fuel in comparison to the reference engine, more than 6% for the GTACSR and almost up to 5% for the GTICLR.

Subsequently, a library of electric power generation future technology concepts has been built to be merged in the TERA for energy framework, developing the relevant computational codes. The power plants chosen encompass different domains of the field and are: the Advanced Zero Emissions Power plant — AZEP (carbon capture and storage concept); a supercritical steam turbine power plant (for nuclear applications); a land-based wind farm working in synergy with a conventional power plant. Multiple, specific control strategies for the fossil fuel and nuclear power plant have been identified to handle the power output down to 60% of the design point for the AZEP and slightly below 80% for the nuclear cycle. Hourly performance simulations of typical days representative of each season of the wind farm in combination to conventional gas turbine engines have been investigated for different size (from 223 MW to 5 MW at full load).

To Giovanni.

Contents

List of Figures

List of Tables

Acronyms

EVA Environmental Assessment of Novel Propulsion Cycles. 56

PROOSIS Propulsion Object-Oriented Simulation Software. 53

AGR Advanced Gas-cooled Reactor. 19

ASU Air Separation Unit. 37, 38

AZEP Advanced Zero Emissions Power plant. xii, xiii, xv, xxii, 5, 7, 9, 11–16, 31, 32, 34, 37, 79, 80, 83–87, 104, 105

BHX Bleed gas Heat exchanger. 11, 13–16, 32, 34

BWR Boiling Water Reactor. 19

CAEP Committee on Aviation Environmental Protection. 57

CCS Carbon Capture and Storage. 2, 5, 7, 31, 61, 104

CFD Computational Fluid Dynamics. 41

COT Combustor Outlet Temperature. 80

DDICLR Direct Drive Inter-Cooled for Long Range. 64

DOC direct operating costs. 57

FAR Federal Aviation Regulation. 64

GFR Gas-cooled Fast Reactor. 17

GIF Generation IV International Forum. 17, 25, 39

GTACSR Geared Turbofan with Active Core for Short Range. 5, 53, 62, 64, 103, 104

GTCRSR Geared Turbofan with Counter-Rotating core for Short Range. 5, 53, 61, 103, 104

GTHTR300 300 MW Gas Turbine High Temperature Reactor. 23

GTICLR Geared Turbofan Inter-Cooled for Long Range. 5, 53, 64, 104

GTMHR Gas Turbine Modular Helium Reactor. 24

GWP Global Warming Potential. 57, 62

HAWT Horizontal Axis Wind Turbine. 50

HRSG Heat Recovery Steam Generator. 12, 14, 15, 32, 37, 51, 52, 74, 105

HTHX High Temperature Heat exchanger. 12, 14, 15, 32, 34

HTR-10 10 MW High Temperature gas-cooled Reactor. 24

HTR-10GT 10 MW High Temperature gas-cooled Reactor Gas Turbine. 24

IAPWS International Association for the Properties of Water and Steam. 44, 52

ICAO International Civil Aviation Organization. 57

IGCC Integrated Gasification Combined Cycle. 8

IPCC Intergovernmental Panel on Climate Change. 1, 2

JAERI Japan Atomic Energy Research Institute. 23

LFR Lead-cooled Fast Reactor. 17

LMTD logarithmic mean temperature difference. 34, 36, 40, 52

LTHX Low Temperature Heat exchanger. 12, 32, 34

LWR Light Water Reactor. 17, 19

MCM Mixed Conductive Membrane. xiii, 11, 16, 32, 36, 37, 80, 82, 83, 87

MSR Molten Salt Reactor. 17

NASA National Aeronautics and Space Administration. 34, 52

NEWAC NEW Aero Engine Core concepts. 4, 5, 53, 57, 61, 64, 103

NREL National Renewable Energy Laboratory. 51

NWTC National Wind Technology Center. 51

OEM Original Equipment Manufacturer. 57, 64

OKBM Experimental Design Bureau of Machine Building (in Russian). 23, 24

PEHX Post Expansion Heat exchanger. 16, 34

PFD Process Flow Diagram. ix, 9, 10, 24, 32, 34, 38, 39, 53, 79, 88, 90, 92

PWR Pressurized Water Reactor. 19

SCWR Supercritical Water-cooled Reactor. 5, 7, 17, 39, 44, 61, 88, 90, 92, 94, 104, 105

SFR Sodium-cooled Fast Reactor. 17

TERA Techno-economic Environmental Risk Analysis. 3–5, 53, 58, 103, 104

UHC Uncombusted Hydrocarbons. 83

VHTR Very High Temperature Reactor. 17, 19

VIGV variable inlet guide vanes. 15, 37, 74, 76, 77, 80, 87

VITAL Environmentally Friendly Aero Engine. 53

Nomenclature

A	Area
c_p	Specific heat at constant pressure
c_v	Specific heat at constant volume
η	Efficiency
f	Composition gravimetric fraction
F	Faraday constant
Γ	Turbine non-dimensional mass flow
γ	Heat capacity ratio
h	Specific enthalpy
j	Molar flux
π	Compressor pressure ratio
P	Mechanical power
p	Pressure
Q	Heat
$\dot{Q}$	Thermal flow
$\mathcal{R}$	Ideal gas constant
σ	Electric conductivity
T	Temperature
U	Overall heat transfer coefficient

Υ	AZEP flue gas loop fraction of the inlet mass flow
W	Mass flow
x	Heat exchanger non-dimensional abscissa

Chapter 1

Introduction

1.1 Background

Earth's surface temperature increase has become a scientific evidence in the last decades and it is often referred to as "global warming". The Intergovernmental Panel on Climate Change (IPCC) accounted for an increase of $0.74 \pm 0.18\,^{\circ}\mathrm{C}$ in the 20th century [43].

Although the scientific community has different estimates on the future increase rate of the temperature [69], there is a very broad agreement in considering human activity the cause of the phenomenon. Specifically, the large scale combustion of fossil fuels and deforestation have increased the concentration of greenhouse gases in the atmosphere [62], triggering the global warming process.

The main effect of this process is a change in the climate of the planet, implying a rise in the sea level, a significant change in the current model of precipitation, with the probable extension of subtropical deserts [57]. Aside these consequences, the higher concentration of carbon dioxide (the most important anthropogenic greenhouse gas) in the atmosphere determines an acidification of the oceans, threatens living beings, and reduces agricultural and fishing productivity.

In this picture, the sheer increase in World's population, with a constantly growing part of people consuming quickly natural resources (and emitting more greenhouse gases), introduces an additional challenge for the future well-being of mankind. Furthermore, considering the finite and (in many cases) *non* renewable nature of all natural resources, it is undeniable that the current technical, economical, environmental, and social status needs to evolve to face new challenges.

Sustainability is the concept responding to this requirement. According to

its most famous definition (given by the Brundtland Commission of the United Nations in 1987), "sustainable development is development that meets the needs of the present without compromising the ability of future generations to meet their own needs" [82].

Sustainability implies the ability to endure in the long-term as a species together with Earth's ecosystems, and its practices improve the *resilience* of living organisms on our planet i.e., helps them to react more effectively when environmentally stressed by sudden changes [86].

Considering the importance of global warming and the more general problem of fast consumption of natural resources, many actions have been elaborated to counteract the ongoing trend. Options include:

- carbon dioxide and other pollutant emissions taxation (with potential trade of CO_2 emissions);
- promotion of more efficient technologies;
- reduction of deforestation in developing countries;
- *geo-engineering* i.e., deliberately modify the global climate system;
- substitute the current dominant sources of energy with renewable or low-carbon alternatives;
- intergovernmental actions.

The most notable intergovernmental effort on global scale is the Kyoto Protocol and, later, the European Union approved the "Climate Change Package" with additional actions [69].

Among many options in the geo-engineering family, one that found favour with the IPCC is Carbon Capture and Storage (CCS). The basic concept of this option is to capture carbon dioxide and to store it in a geological, mineral, or oceanic, insulated place [6, 58].

Looking at carbon dioxide emissions on global scale (Figure 1.1), electricity and heat production together with the transport sector are the two main contributors. Similar conclusions can be drawn looking at the European Union data [27]. Thus, power generation and civil aeronautic industry (important subsets of the cited sectors) are strategic fields to counteract the global warming issue and are at the centre of many governmental and intergovernmental activities as well as future plans. Given these preliminary conditions, there is a strong interest in the academic and industrial research about these highly competitive industry domains.

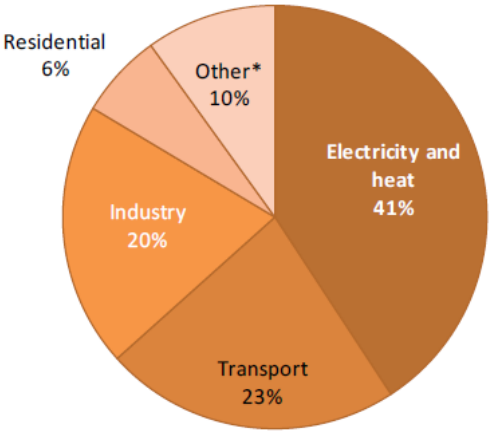

Figure 1.1. World CO_2 emissions by sector in 2009 [44].

Especially civil aviation, although it does not account for the main part of transport emissions share, has experienced a rapid growth in the industry with a relevant increase in pollution. In the European Union, greenhouse gas emissions attributable to aviation have increased by 87% between 1990 and 2006 [29].

Also the later increase in the cost of oil has pushed the aeronautical research towards innovation and performance enhancement. This is because the only viable option in the short-medium term to reduce greenhouse gas emissions in the aircraft industry is the development of more efficient technologies.

The increase in the cost of oil has important consequences also for the power generation sector, with even more challenging scenarios in the view of the current steep increase in energy demand [69].

Many novel concepts have been conceived to address the presented request in innovation, both in the aviation and the power generation sector of engine systems. Given the large number of alternatives and their complexity, there is no complete and deep knowledge in the scientific literature on some promising, advanced power plants.

1.2 Aim and Objectives

This project aims to analyse a number of power plants from a multi-disciplinary point of view. The strategy adopted is called Techno-economic Environmental Risk Analysis (TERA). This approach has been developed at Cranfield University throughout two decades of research and allows to explore the design space of power plants according to different criteria.

TERA comprises a module for each criterion considered. In principle, according to its acronym, it covers the following areas

- performance,
- economic viability,
- emissions,
- technological risk.

TERA has been applied to different fields of gas turbine application and it has been adapted to their specific characteristics (aviation [67, 14], marine [81], industrial sector [60, 36]). Moreover, it reached a different degree of maturity in every sector according to the time invested in its implementation. Thus, a different set of modules for each field of application is available.

The present project covers the entire TERA strategy in two steps, adapting the general methodology to the two main areas that constitute the project: aviation and power generation. A contribution in the integration of all modules has been offered in the NEW Aero Engine Core concepts (NEWAC) project, taking advantage of its maturity and its TERA for aviation package.

A larger effort is being invested in the enhancement of the "TERA for energy" framework.[1] The main goal is the development of a reliable off-design computational code that is currently missing. This will allow an assessment and comparison of the different options and further, multi-disciplinary analyses in the form of a new TERA release.

The basic research questions that characterise this project are:

- How does the design space of aero-propulsion concepts look like according to several, multi-disciplinary degrees of freedom?
- What is the off-design performance of novel electric power generation cycles?

This project is funded partly by the EU programme NEWAC [63], and partly by E.ON UK Limited.

1.3 Scope

The project investigates in the aeronautical field three novel engine configurations. They all have in common the geared turbofan concept, i.e. the implementation of a reduction gear train placed on the engine shaft to allow an optimal rotational speed of the fan, the compressor and the turbine.

[1] this is the TERA package developed for power generation applications

- Geared Turbofan with Counter-Rotating core for Short Range (GTCRSR): the core of this engine has two independent shafts rotating in opposite direction implementing several stages of counter-rotating blades.

- Geared Turbofan with Active Core for Short Range (GTACSR): the core of this engine is controlled actively during all phases of the flight mission to minimise the tip clearance of rear stages, to control the surge of the front stages and to optimise for every phase the cooling blade mass flow.

- Geared Turbofan Inter-Cooled for Long Range (GTICLR): the core of this engine is inter-cooled between groups of compression stages.

The contribution of the author is oriented towards the integration of several TERA modules, to allow the production of results by other members of the NEWAC working team.

In the power generation field has been completed the development of the off-design performance tool for a number of different concepts in the following areas.

CCS advanced cycles: the Advanced Zero Emissions Power plant (AZEP).

Nuclear: a supercritical steam power plant inspired by the Supercritical Water-cooled Reactor (SCWR).

Wind: a land-based wind farm working in synergy with a conventional power plant.

Conventional: two combined cycle, reference engines. Namely, a simple, topping gas turbine cycle and a re-heat one.

1.4 Thesis Structure

The contents of the present work comprise

1. a concise *executive summary*;

2. a *list* of the contents and other useful elements (e.g., figures, tables, acronyms, ...);

3. an *introductory* chapter (the present) where the research background, its goals, and other relevant information is provided;

4. a chapter dedicated to the description of the *methodology* adopted to undertake the research;
5. final *results* for every power plant investigated;
6. a summary of *conclusions*;
7. suggestions for *further work*;
8. bibliographic *references*.

Chapter 2

Literature survey

2.1 Low/Zero Carbon Power Plant Concepts

The project presented in this work encompasses a range of different power plant concepts with low or zero carbon dioxide emissions. All them are novel concepts based on turbine engines.

Namely, the concepts analysed are

- the Advanced Zero Emissions Power plant (AZEP), an oxy-fuel thermodynamic cycle belonging to the Carbon Capture and Storage (CCS) family;
- the Supercritical Water-cooled Reactor (SCWR) concept, an advanced nuclear power plant based on steam turbine engines;
- a wind farm working in synergy with a conventional power plant.

2.2 Carbon capture concepts for power generation

There are several strategies that has been investigated for the CO_2 capture in the power generation field, but there is a general agreement [37, 5, 21, 61] in dividing them in three main categories:

- pre-combustion capture;
- oxy-fuel combustion;
- post-combustion capture.

The first category includes a number of processes (steam reforming, gasification, partial oxidation [37, 21]) that aim to the transformation of the fuel in a mixture of CO_2 and H_2 (in same cases also CO), using the latter as a fuel and separating the CO_2 before the combustion with a chemical or a physical method [32]. The Integrated Gasification Combined Cycle (IGCC) concept is the most promising in this field also thanks to the research efforts invested on it [80]. A number of demonstrations plants showed technology readiness for an upcoming industrial implementation [73].

The oxy-fuel principle operates the combustion in a pure (or almost pure) oxygen environment (achieving, in this way, also the advantage to avoid the production of nitrogen and sulphur oxides), and requires the recirculation of the exhaust gas in order to dilute the reactive mixture and obtain, after the combustion, an acceptable temperature [5, 80]. In all these concepts the flue gas is basically constituted by steam and carbon dioxide, so it is simple to separate the steam by condensation [80, 37]. A first pilot power plant has been set up in September 2008 [34] but some other demonstrative projects are planned to be started in the near future [73]. There are several options to carry out the oxy-fuel combustion, they will be described in the next section.

The post-combustion processes are the most mature: they exploit physical or chemical techniques in order to capture the CO_2 from the exhaust gas of a conventional combustion. The main problem of this principle is the low concentration of carbon dioxide that requires the use of large and expensive devices [37] affecting remarkably also the thermodynamic performance of the power plant because of the pressure loss through them [5]. The aforementioned techniques vary from the chemical absorption [80] (the most popular choice), physical absorption or adsorption and the use of solid chemicals [37, 5] until the application of membranes or distillation processes [73, 61]. The first pilot power plant of this family started to operate on March 2006, and several other demonstrative projects are ongoing or planned to be completed in the next years [73].

All the described strategies are energy demanding and require also, in many cases, a significant aggravation for the capital costs of the power plant. In fact the pre-combustion processes reduce the heating value of the fuel, the oxy-fuel approach requires efforts for the oxygen production and the post-combustion option involves energy also for the regeneration of the chemicals, used in the most popular choice [61].

2.2.1 Oxy-fuel Cycles

The oxygen-fuel combustion has been applied to the glass melting and the steel and aluminium industry [21], and just recently it has started to be

considered for power generation applications [41]. The options available in this field are several and comprise (among others less important) [41, 61]

- the semi-closed cycle (also known as the "oxy-fuel combined cycle");
- the Chemical Looping Combustion cycle;
- the electrochemical reactions in fuel cells;
- the AZEP cycle.

The common feature of them is the composition of the exhaust gas that comprises mainly steam and carbon dioxide.

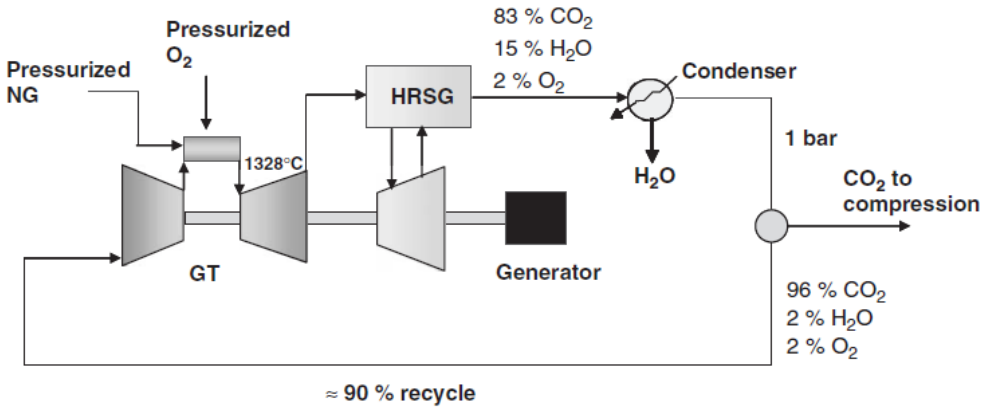

Figure 2.1. A simple Process Flow Diagram (PFD) of the "oxy-fuel combined cycle" concept [50].

The semi-closed cycle concept (Figure 2.1) shows several similarities with the conventional combined cycle: the heat of the exhaust gas is released in a Heat Recovery Steam Generator after the combustion process. The main difference of this power plant, compared to a conventional one, is the reaction with the fuel that is carried out with pure oxygen. As shown in Figure 2.1, there is a large quantity (about the 90%) of flue gas recirculated at the inlet of the compressor, in order to lower the combustor outlet temperature to an acceptable value.

The oxygen supplied for the reaction is produced in a dedicated device (the air separation unit) with a cryogenic process that results in a loss of electrical efficiency of about ten percent [37]. Moreover, there are also studies on chemical cycles for oxygen generation [5]. The concept with the cryogenic air separation unit implements an already mature technology which, despite its lower efficiency, makes it attractive.

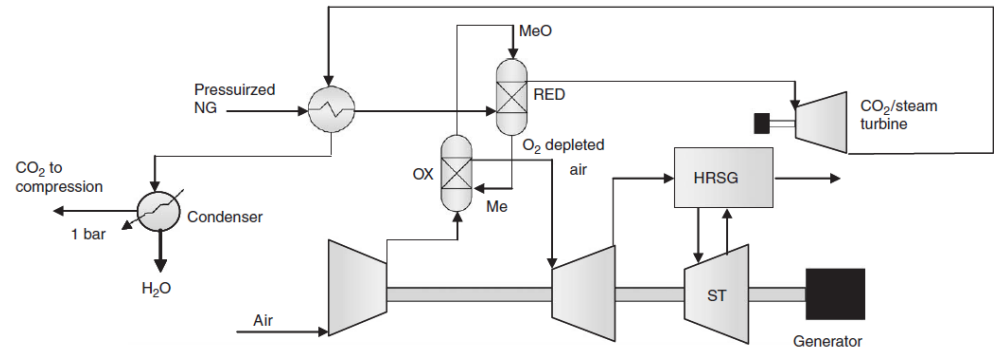

Figure 2.2. PFD of the Chemical Looping Combustion cycle [50].

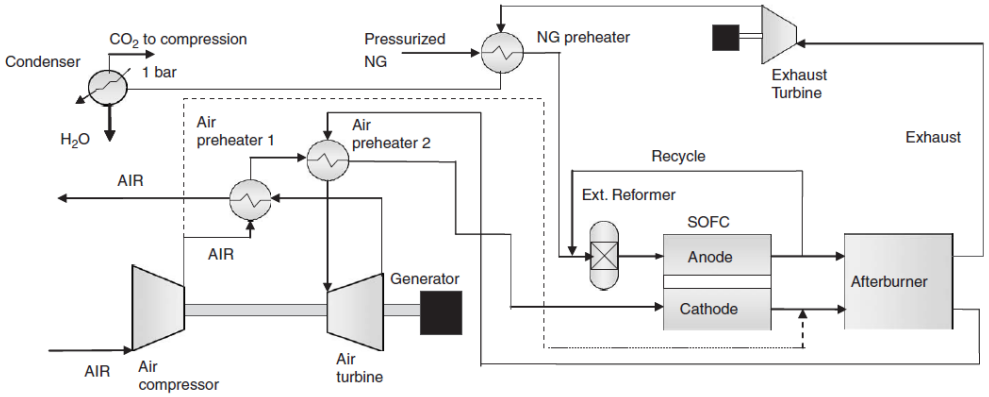

Figure 2.3. Integration of a Solid Oxide Fuel Cell (SOFC) with a gas turbine (simplified PFD) [50].

In the Chemical Looping Combustion concept (Figure 2.2), the oxy-fuel process is carried out by an oxygen carrier (a metal oxide) that circulates between two reactors, one for the oxidation and the other for the reduction. The reactors environment is kept as close as possible to the thermodynamic equilibrium [50]. The power plant is completed by two turbines (namely, for the oxygen-depleted air and the CO_2/H_2O streams) and a steam bottoming cycle.

In another oxy-fuel option (Figure 2.3), a Solid Oxide Fuel Cell can operate the reaction of the air (previously compressed and pre-heated) with fuel; the device uses the oxygen in the air stream. It is important that the anode and cathode flows stay separated to obtain only steam and carbon dioxide in the exhaust mixture, allowing the CO_2 capture simply by steam condensation. An afterburner is needed (as well as a stream of air bled from the compressor)

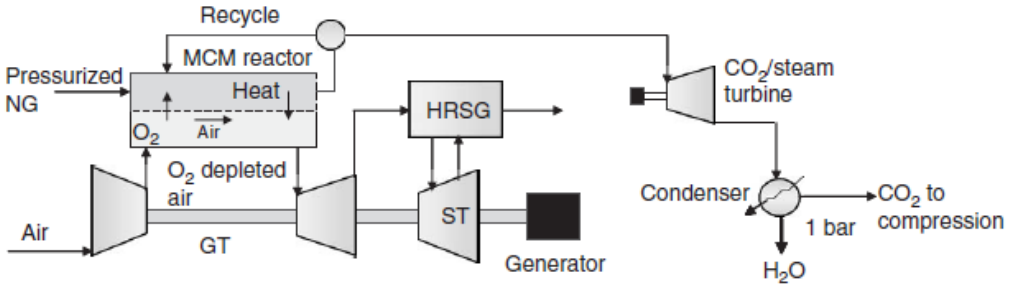

Figure 2.4. A simple PFD of the Advanced Zero Emissions Power plant concept [50].

to complete the oxidation of the fuel, that is just partially carried out in the fuel cell [50].

Finally, the AZEP will be discussed thoroughly in the next section; a very brief and simple description will be given. The cycle (Figure 2.4) adopts a special membrane to substitute a conventional combustor; so the new device operates the separation of the oxygen from the air, the combustion of the fuel with pure oxygen and, finally, transfers the heat of combustion to the oxygen-depleted air. The power plant usually integrates a steam bottoming cycle and one or two turbines for the oxygen-depleted air and the CO_2/H_2O flows.

A great deal of efforts is being invested to increase the working temperature of the membrane, for the relevant large benefits on the cycle performance.

2.2.2 The Advanced Zero Emissions Power plant

The AZEP cycle is one of the most promising oxy-fuel concepts and only some studies have investigated its potential in the open literature. Most of them do not provide off-design results and a complete picture of the computational assumptions for all key components.

The AZEP concept was conceived in 2001 by Norwegian company Norsk Hydro ASA and after a promising result derived by a feasibility study, a development project was started with a consortium of partners (including ALSTOM, Norsk Hydro, Borsig, Eni Tecnologie, KTH) [78].

In the previous section the basics of this novel cycle have shown, so now it will be presented a more comprehensive process flow sheet (Figure 2.5) where the membrane is sketched in more detail. As represented, the "membrane reactor" comprises a Mixed Conductive Membrane (MCM) together with a catalytic combustor and a Bleed gas Heat exchanger (BHX). As detailed in

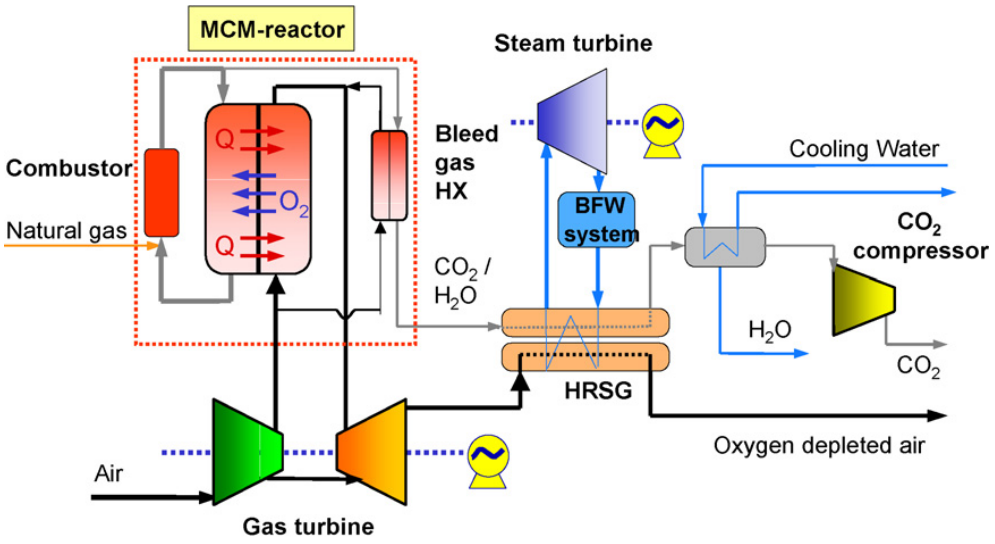

Figure 2.5. The PFD of the AZEP cycle basic concept [79].

Figure 2.6, the central device of the membrane reactor is actually made up of three parts: a Low and High Temperature Heat Exchanger (respectively LTHX and HTHX) and the membrane itself that performs at the same time the oxygen mass transfer and the heat exchange.

The insertion of the Low Temperature Heat exchanger (LTHX) and the High Temperature Heat exchanger (HTHX), respectively before and after the membrane is necessary to keep its temperature as constant as possible at the optimal value for the oxygen transport, preserving the integrity of the device (e.g. 900 °C–1050 °C [79]). According to the physical principle underlying the device behaviour, the higher is the temperature of the membrane, the higher is the mass of the oxygen depleted from the compressed air (the transferred flow rate is an exponential function of temperature). Thus, it is desirable to work at the highest possible temperatures to reduce the membrane exchange area [38]. Unfortunately, there are constraints due to thermal degradation of the device that is subject to a mechanical stress (creep effects, first of all) and the membrane working temperature has to be lower than a conventional gas turbine firing temperature. Thus, the HTHX is necessary to reduce the difference between the combustor outlet temperature of a conventional power plant and the turbine inlet temperature of the AZEP cycle [38, 28, 50, 61, 33, 21, 37]. This limitation turns out in the constitutional disadvantage of the AZEP concept versus the conventional thermodynamic cycle.

Moreover, comparing Figure 2.4 to Figure 2.5, it could be observed that in the second diagram the stream of flue gas is conveyed to the Heat Recovery

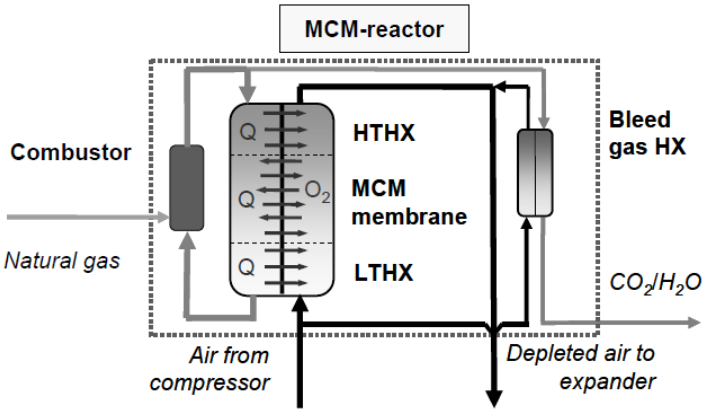

Figure 2.6. A detailed view of the membrane reactor [61].

Steam Generator (HRSG) instead of being expanded in a CO_2/H_2O turbine (first diagram). The two figures represent different implementations of the AZEP cycle: the concept with the flue gas turbine is stated to be better performing than the other, but it requires the development of a novel kind of gas turbine working with a significantly different mixture of gas than the conventional nitrogen-based air turbines [37, 33]. Moreover, a CO_2/H_2O turbine is not available at the moment on the market and its development would require great efforts in terms of time and money. Hence, the layout of Figure 2.5 it is more interesting in the short term, even if it achieves reduced performance, and in fact it is the most investigated in the literature.

Another option often considered alongside the "standard" AZEP cycle, is the modification of the layout with the insertion of a conventional afterburner before the expansion of the oxygen-depleted stream (Figure 2.7). In fact, the air at the outlet of the membrane still retains a quantity of oxygen capable to react with additional fuel, increasing the turbine inlet temperature and reaching values close to the conventional case. This improves the performance of the power plant, but it makes impossible to capture *all* the generated CO_2. For this reason, this concept is usually called "AZEP 85%" since the plant is able to capture approximately the 85% of the carbon dioxide originated in the energy conversion process [61, 50].

The BHX is adopted to increase slightly the inlet temperature at the turbine of the oxygen-depleted air stream, but mainly to reduce the temperature of the flue gas that could be unacceptable for the Heat Recovery Steam Generator or (if present) for the CO_2/H_2O turbine.

The literature values available prescribe that about 10% of the bled flow is conveyed to the BHX, a range of 30%–50% of the oxygen present in the air is, on the whole, transferred to the oxy-fuel combustor in the membrane

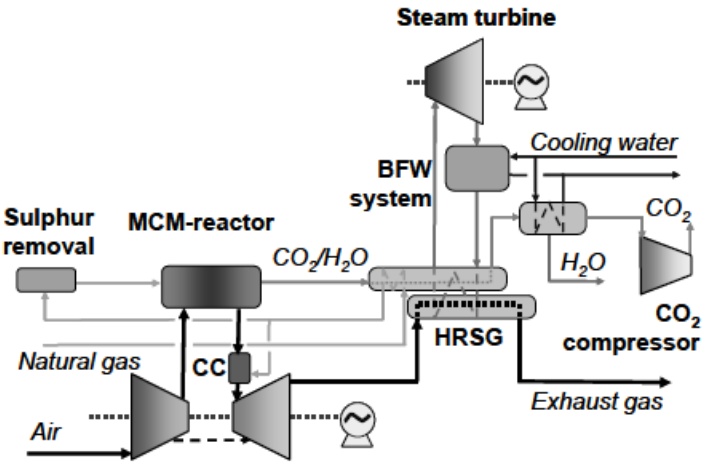

Figure 2.7. The alternative AZEP layout with a conventional afterburner before the expansion of the oxygen-deplated air flow [61].

(with a concentration of about 10% of O_2 at the combustor inlet) and about the 90% of the flue gas is recirculated via the HTHX to the membrane and then to the combustor [38].

Considering the variety of different layouts available for the AZEP concept, the few studies in the open literature reflect this multitude of options. Thus, the AZEP literature is non homogeneous (as well as scarce) concerning the power plant layout considered, the aspects of its behaviour investigated, and the accuracy of the model used.

A first study [28] reports a penalty of 4.5 percentage points for the thermal efficiency of a 50 MW combined cycle plant, according to the AZEP 100% layout, and less than 3.0 points for the AZEP 85%; there are no specifications about the bottoming cycle characteristic parameters. It is also considered a 400 MW combined cycle computation, where the reference engine is a Siemens V94.3A plant. It results in a higher reduction in the efficiency (compared to the smaller size case) that is 4.5 percentage points for the AZEP 85% concept and it is not specified in the 100% CO_2 capture case. The concentration of the NO_x in the oxygen-depleted stream is claimed to be lower than 1 ppm in volume in the AZEP 100% layout.

In this work the flue gas goes to the HRSG *without* any CO_2/H_2O turbine and that the compression of the CO_2 for the storage is included in the overall balance. Other useful assumptions reported in the paper are the plant pressure ratio of about 18, approximately 10% of oxygen concentration in the recirculation flow, the pressure difference over the membrane below 0.5 bar, about 10% of the flue gas conveyed to the BHX, the outlet temperature

of the oxygen-depleted air from the HTHX that is about 1200 °C and the specification that the CO_2 is first compressed from the flue gas pressure, liquefied and then pumped to 100 bar.

Other investigations [50] report a thermal efficiency of 50% for the AZEP 100% and 53% for the AZEP 85%, while the reference engine, GE9351FA, holds 57%. The bottoming cycle modelled is a triple pressure steam plant with reheat, where the pressure levels are 111, 27 and 4 bar and it is supposed to have a turbine able to expand the oxy-fuel combustion exhaust gas with a polytropic efficiency of 87%. The authors do not specify the output power but include in the performance computation the energetic cost of CO_2 preparation for storage. This is operated by four inter-cooled stages of compression to 200 bar.

In another paper [61], it is investigated again the effect of power plant size on the performance, while comparing the conventional combined cycle and the AZEP without CO_2/H_2O turbine. A 50 MW plant is referred to the conventional Siemens SGT800 gas turbine coupled with a dual pressure steam cycle (80 bar and 510 °C for the high pressure level). The AZEP 100% has 4.6 points of reduction in the thermal efficiency, while the AZEP 85% (with a turbine inlet temperature of 1327 °C) results in less than three percentage points of penalty. The reference plant for the 400 MW is a Siemens SGT5-4000F engine with a triple pressure HRSG with reheat of about 130, 30, 5 bar and 560, 545, 240 °C. The AZEP 100% gives a too low exhaust gas temperature for the triple pressure bottoming cycle, so it is used the dual pressure reference cycle of the 50 MW case. The results show a reduction of more than eight percentage points for the efficiency. The AZEP 85%, instead, exhibits a penalty of about 4%. The power output reduction is about a quarter of the reference case in the AZEP 100% and, respectively, 10 and 100 MW for the 50 and 400 MW for the AZEP 85%.

A similar study [33] was carried out in comparison with a conventional Siemens V94.3A combined cycle with an efficiency of 57.9% and considers again the AZEP layout without the CO_2/H_2O turbine. For what concerns the 100% case (with a turbine inlet temperature of 1200 °C) the efficiency drops of 8.3 percentage points, instead in the AZEP 85%, the efficiency is claimed to be 53.4%.

To the knowledge of the author, there is only one comprehensive study undertaken so far that has investigated the off-design performance of this concept [16]. The power plant selected is a 30.4 MW AZEP 85% engine with a BHX and without CO_2/H_2O turbine, a compressor featured with variable inlet guide vanes (VIGV), and a dual pressure steam bottoming cycle (80 bar and 5 bar). At design-point, considering a reference engine with same turbine inlet temperature and inlet mass flow, the AZEP shows 47.1% of overall efficiency

(versus 53.3% of the conventional plant) and about 6 MW of penalty for the power output (36.2 MW in the reference cycle). This work is very interesting also for the comprehensive and accurate description of the operation and material constraints of the MCM and the power plant.

The same author undertook a number of other complementary studies regarding the dynamic behaviour of the MCM and the entire power plant, as well as the operation stability and the component degradation [15, 17, 18, 19].

There is just another work available in the open literature investigating the off-design of the AZEP concept [40], but it is considered far less comprehensive.

Although other studies could be referenced [71, 70, 54, 21] the common problem faced when browsing the literature data on this topic, is the lack of specification for some computational assumptions and (most important) the effect that the main cycle parameters determine to the performance of the power plant.

Another aspect neglected in the open literature is a methodical comparison among the different layouts available, as well as a sensitivity analysis for these AZEP power plants. This missing study has been carried out by the author [68] in 2009 with the development of a computational code (written in Fortran 95) called eAZEP. This computer program allows the user to simulate, in a modular fashion, a number of different layouts for the AZEP 100% at design-point. Alongside the layouts including or excluding the BHX and the CO_2/H_2O turbine, an original family of options has been introduced with the conception of another heat exchanger, the Post Expansion Heat exchanger (PEHX) [68]. There are two journal papers under preparation based on the results of this study.

Subsequently, at Cranfield University, Gianvito Ciavarella [12] and Jon Freire [34] (with the collaboration of the author) extended and refined eAZEP introducing the off-design performance feature (Ciavarella) and the AZEP 85% (Freire) mainly reproducing the layouts investigated in the scientific literature.

2.3 Nuclear Power Plants

2.3.1 Background

Nuclear energy is a complementary option to contribute to sustainable energy as it is a low carbon technology. There is a strong debate on its present state-of-the-art reliability, and a part of the public opinion claims (as well as a part of scientists) it is not able to provide an acceptable level of risk, as the recent Fukushima accident has proven. Moreover, there are doubts on the economic feasibility of these power plants, especially considering the

remaining availability of cheap uranium supplies. However, efforts towards a new generation of nuclear power plants are necessary, especially considering the huge challenge for the power generation sustainability with the forthcoming increase in energy demand (see Section 1.1).

Historically, mankind has just recently exploited nuclear power with the creation of the first fission-based reactor in the early Forties of the last century. In the subsequent decades, the industrial implementation of first generation reactors took place. The deployment of nuclear power technology on industrial scale is usually considered starting from 1970, with the commissioning of the majority of power plant nowadays still operating (mainly belonging to the Light Water Reactor (LWR) family described below) [83]. The most successful commercial phase in history of nuclear power is usually considered ranging between the Seventies and the Nineties, when the so-called "second generation" of power plant was sustained by the huge investments in the nuclear sector because of the Cold War.

With the collapse of the USSR, a new phase of nuclear generation is usually considered, with a significantly lower number of power plant commissioned. The causes of this reduction could be mainly addressed to the effect on the public opinion of the Chernobyl disaster, and the end of the Cold War (with its relevant economic investments). Generation III is characterised by enhanced concepts of commercially successful power plants and it is supposed to last until 2020 or 2030. By that time, it is expected most of the nuclear power plants currently in operation to be at their decommissioning phase.

With the purpose to replace the old power plants with a new Generation IV, an international research body called Generation IV International Forum (GIF) has been established in 2001 among ten countries (including the UK): Argentina, Brazil, Canada, France, Japan, the Republic of Korea, the Republic of South Africa, Switzerland, and the United States [83]. The organisation aims to address most of the critical problems or limitations of power plant present state-of-the-art (Figure 2.8) taking into account also the entire fuel cycle. More precisely, GIF aims to reduce drastically the amount of waste produced by the energy conversion process, to allow flexibility of operation (an important feature for the recent market deregulation), to implement safety passive systems (more reliable), to keep a strict control on nuclear material inventories with the use of protective systems in case of natural disasters or terrorist attacks [52, 83].

GIF selected six families of novel/advanced concept for nuclear power generation to focus the research effort. Namely, they are the Gas-cooled Fast Reactor (GFR), the Lead-cooled Fast Reactor (LFR), the Molten Salt Reactor (MSR), the Sodium-cooled Fast Reactor (SFR), the SCWR, and the Very High Temperature Reactor (VHTR) [35, 83]. In a later phase, just three or two

Goals for Generation IV Nuclear Energy Systems

Sustainability–1 *Generation IV nuclear energy systems will provide sustainable energy generation that meets clean air objectives and promotes long-term availability of systems and effective fuel utilization for worldwide energy production.*

Sustainability–2 *Generation IV nuclear energy systems will minimize and manage their nuclear waste and notably reduce the long-term stewardship burden, thereby improving protection for the public health and the environment.*

Economics–1 *Generation IV nuclear energy systems will have a clear life-cycle cost advantage over other energy sources.*

Economics–2 *Generation IV nuclear energy systems will have a level of financial risk comparable to other energy projects.*

Safety and Reliability–1 *Generation IV nuclear energy systems operations will excel in safety and reliability.*

Safety and Reliability–2 *Generation IV nuclear energy systems will have a very low likelihood and degree of reactor core damage.*

Safety and Reliability–3 *Generation IV nuclear energy systems will eliminate the need for offsite emergency response.*

Proliferation Resistance and Physical Protection–1 *Generation IV nuclear energy systems will increase the assurance that they are a very unattractive and the least desirable route for diversion or theft of weapons-usable materials, and provide increased physical protection against acts of terrorism.*

Figure 2.8. Main goals of the Generation IV International Forum [83].

most promising concepts will be selected for the industrial implementation.

The majority of world's operating power plants is currently based on steam cycles and, mainly because of its working fluid high inertia, they do not exhibit load flexibility. The technological family of these engines is referred to as LWR, comprising the Pressurized Water Reactor (PWR) (the most common type[1]) and the Boiling Water Reactor (BWR) concepts. The PWR is an *indirect* cycle i.e., it has two separated loops, one going through the reactor and one for power generation (Figure 2.9). Both loops uses de-mineralised and de-ionised water, and they are linked by a steam generator. Water in the reactor loop does not boil completely because the pressure is high enough (usually $150 - 160$ bar [26]) to avoid steaming. On the contrary, BWR plants are direct cycles (just one loop) where water changes phase when it gets in contact with the reactor. To allow steaming, pressure in a BWR circuit is approximately half of the value in a PWR reactor loop [26] .

At the time of early prototypes of the nuclear industry (Generation I), power plants with reactor loops based on carbon dioxide or helium were considered. In particular, the Magnox reactor (conceived in the Fifties by a joint effort of the French and the UK government) used CO_2 at 20 bar and 400 °C to cool the reactor achieving an efficiency of 31%. An enhanced version of the same concept, with better construction materials, allowed an increase in temperature and pressure of the CO_2 (40 bar and 650 °C) leading to an increase in efficiency to almost 40% [47]. Both in the Magnox and its evolutionary concept — known as Advanced Gas-cooled Reactor (AGR) — the power generation cycle was still based on steam.

Concepts of the VHTR family (more precisely, *direct*, closed gas turbine cycles) are of strong industrial and academic interest mainly driven by the higher efficiency that could be achieved (there are no losses due to the heat transfer between the loops), and their load flexibility. On the other hand, direct cycles require higher cost for the containment of the radioactive working fluid that is in contact with the fissionable material [39].

The basic principle of a closed gas turbine cycle shows many analogies with a simple steam turbine cycle. Gas is initially compressed and then heated by a reactor. Afterwards, expansion takes place in a turbine reducing the temperature and the pressure of the working fluid and generating useful work (converted, in this case, in electrical power by a generator). Finally, the cycle initial temperature is restored by means of a pre-cooler to prepare the gas to start a new cycle (Figure 2.10). This simple process is very rarely implemented because of its low efficiency, thus a complication of the aforementioned process is always pursued (see Sections 2.3.4 and 2.3.3) to

[1] see `http://world-nuclear.org/NuclearDatabase/rdResults.aspx?id=27569`

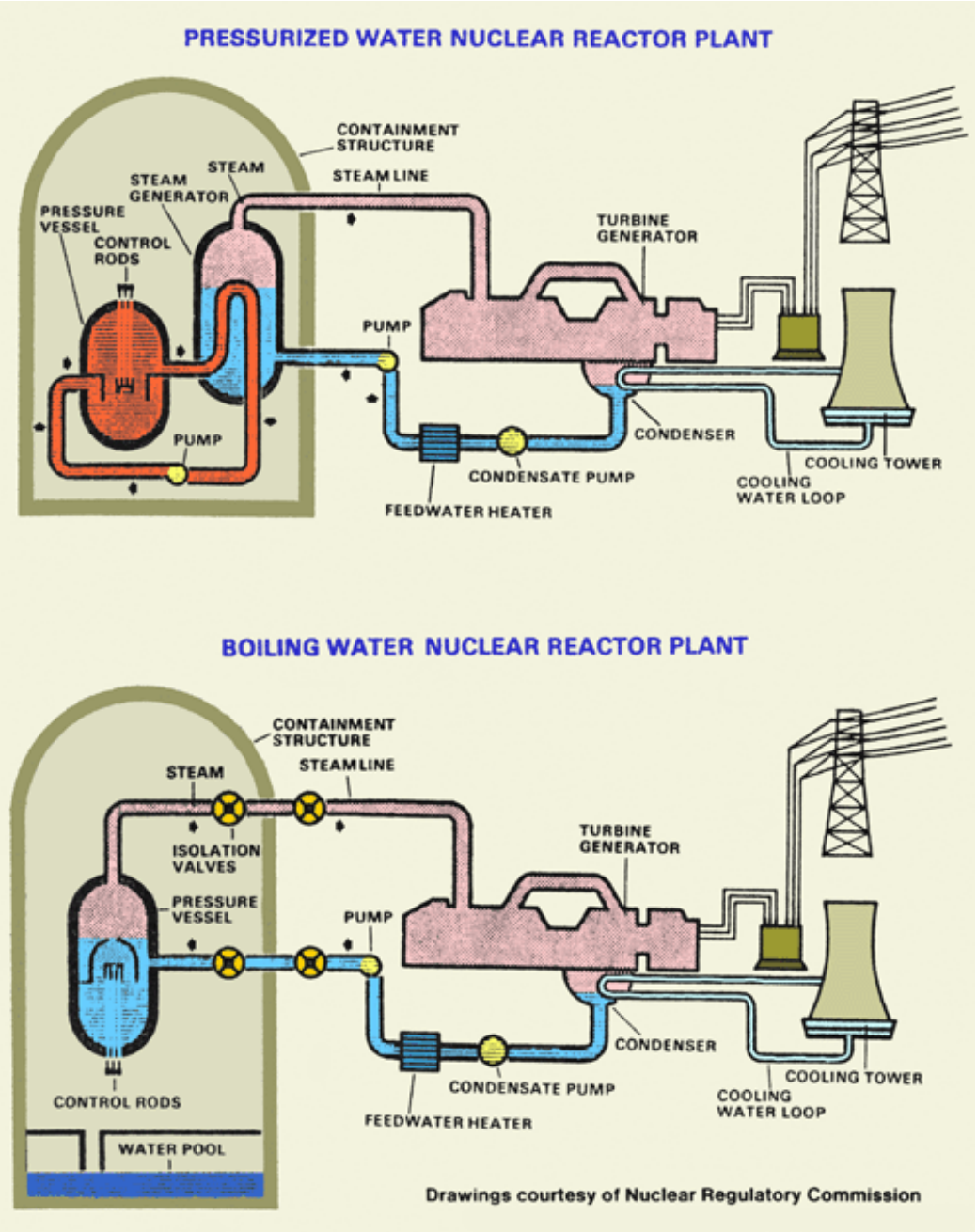

Figure 2.9. PWR and BWR power plant schematic.

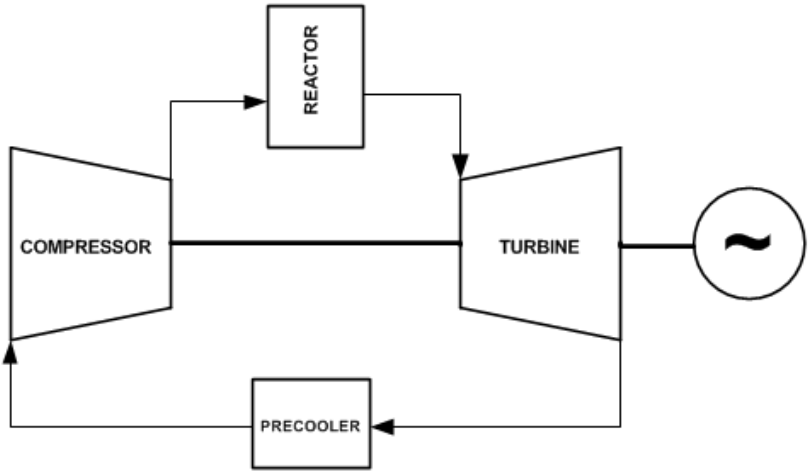

Figure 2.10. The PFD of a basic closed gas turbine cycle [39].

accomplish better performance.

2.3.2 Working Fluids

Historically, *helium* and *carbon dioxide* have been the most studied working fluids for gas-based power plants and this interest is still ongoing in the scientific community. Both gases are attractive because of their thermodynamic properties.

Helium behaves almost like an ideal gas at any working condition and it manifests an high heat capacity ratio γ

$$\gamma = \frac{c_p}{c_v} \tag{2.1}$$

where c_p and c_v are respectively the specific heat at constant pressure and at constant volume. For helium $\gamma = 1.66$ can be sensibly considered a constant at any operating condition as a consequence of its ideal gas behaviour. It could be proved that an higher heat capacity ratio allows, in a compression process, to obtain an higher outlet temperature, for a given pressure ratio [39]. This reduces the quantity of heat (and, in turn, the quantity of fuel) necessary to reach the temperature at the inlet of the turbine in a power plant cycle. Similarly, for a given pressure ratio in an expansion process, a higher capacity ratio dictates a lower outlet temperature (with a consequent lower loss in the pre-cooler of a closed gas turbine cycle). As a result, for a fixed temperature ratio, helium has almost five times the specific power output of

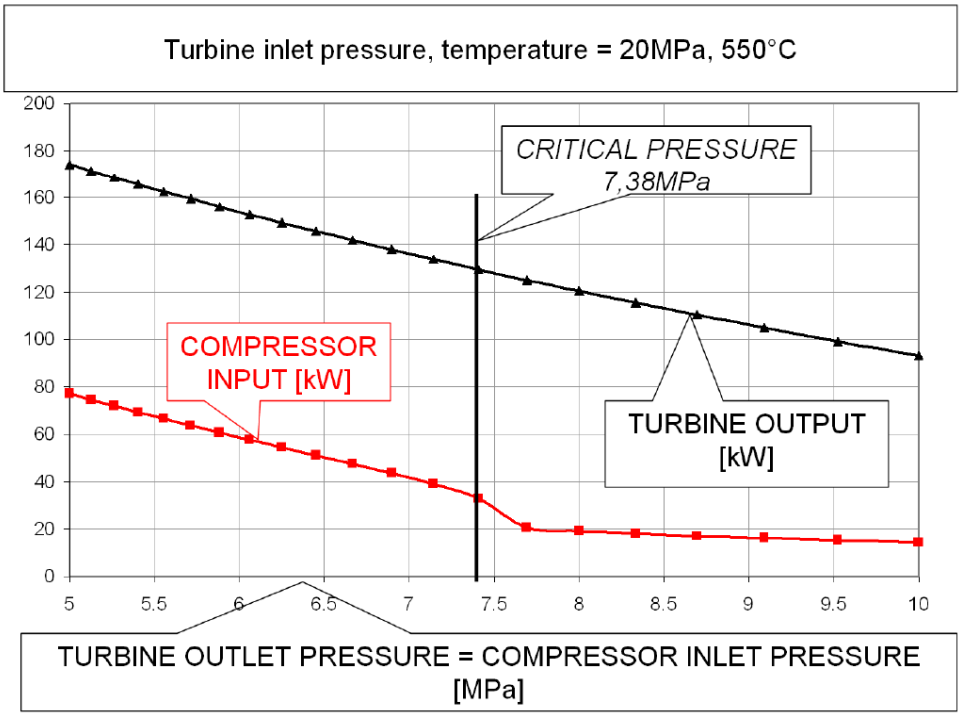

Figure 2.11. Reduction in the CO_2 compression work at quasi-critical conditions. The expansion work is not affected. [49].

the corresponding air-based gas turbine cycle. Moreover, it has five times air's thermal conductivity allowing to design more compact heat exchangers.

On the other hand, although helium provides inherently an higher specific work, its lower density than air imposes a severe penalty to the actual output work. Thus, it is necessary to increase the minimum cycle pressure at much higher values than ambient (e.g. 35 bar [39]) to overcome this problem.

Carbon dioxide has a critical point relatively close to ambient conditions (at 31 °C and 73.8 bar), so it allows to compress the gas at nearly critical conditions, where the compression work reduces significantly. Profitably, the turbine work is not affected by the supercritical conditions, because the temperature at the reactor outlet is much higher than critical (Figure 2.11).

One drawback, from the modelling point of view, is that CO_2 does not behave like an ideal gas, especially at the lower temperatures of the cycle. Hence, the calculation of its properties is dependent on temperature *and* pressure. Moreover, the sharp variability of the CO_2 properties at conditions close to the critical point, has an important, detrimental effect on the efficiency of recuperators that are almost always used in CO_2-based cycles. In fact, the specific heat at constant pressure is very high on the cold side of the

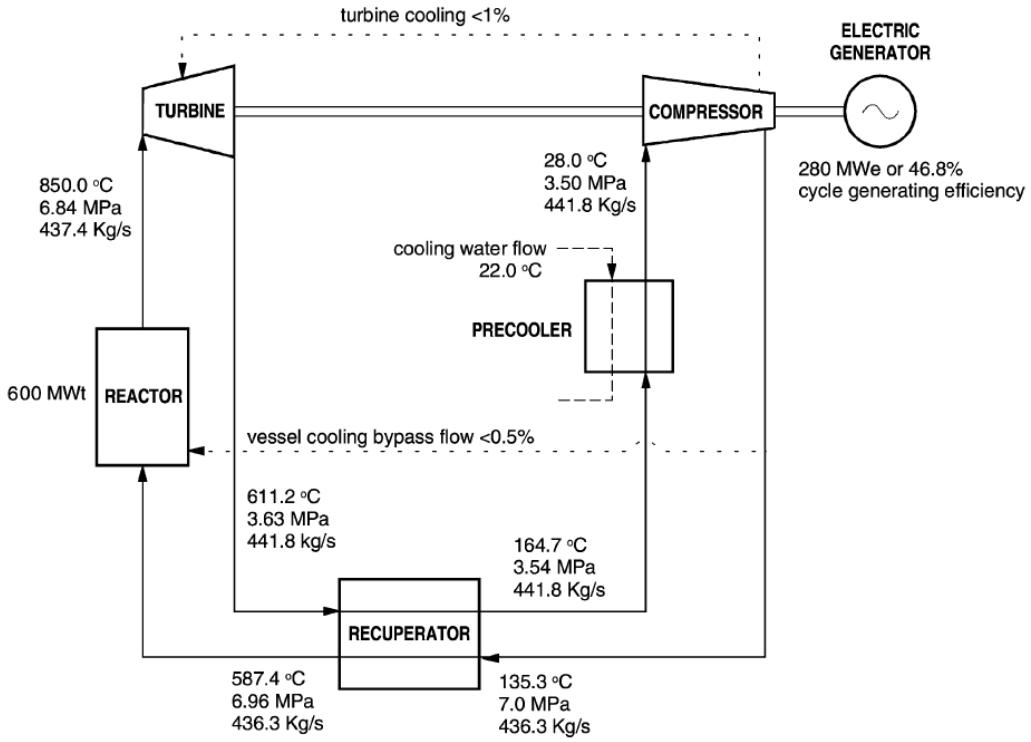

Figure 2.12. The PFD of the GTHTR300 [88].

recuperator, hindering the fluid heating [39].

2.3.3 Helium Direct Cycles

Helium-based gas turbine engines have been more studied in the past than carbon dioxide cycles, because it is not necessary to bring the working fluid to critical point, an "extreme" condition on a thermodynamic and fluid-mechanic point of view.

The recent state-of-the-art in research could be isolated in a few programmes undertook by

- the Japan Atomic Energy Research Institute (JAERI),
- the USA General Atomics and the Russian Federation Experimental Design Bureau of Machine Building (in Russian) (OKBM) jointly,
- the Chinese Institute of Nuclear and New Energy Technology.

JAERI started in 2001 a programme called 300 MW Gas Turbine High Temperature Reactor (GTHTR300) with the goal to produce by 2010 a first

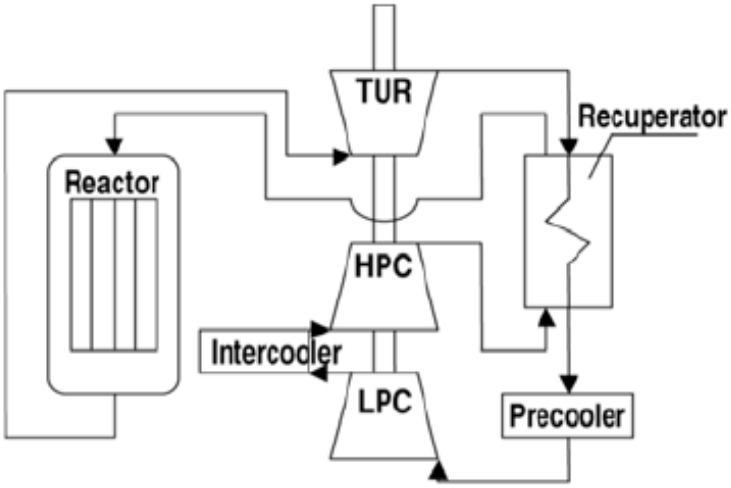

Figure 2.13. The PFD of the GTMHR [4].

prototype, and have the concept ready for the industrial implementation by 2020. The engine is a simple recuperated gas turbine closed cycle with almost 300 MW of power output (Figure 2.12). The cycle has a pressure ratio of 2, reactor outlet temperature of 850 °C, and claims to have an overall cycle efficiency of 46.8% [88].

The General Atomics and OKBM programme is called Gas Turbine Modular Helium Reactor (GTMHR) and it aims to enhance an indirect cycle conceived in the late Eighties. The old concept couples the helium cycle with a steam turbine loop, providing 350 MW of the reactor thermal power with efficiency 38%. Differently, the new direct cycle is an intercooled, recuperated gas turbine power plant (Figure 2.13) with reactor outlet temperature 850 °C and estimated cycle efficiency 50.3% [4].

In 2003 the Chinese Institute of Nuclear and New Energy Technology started operating successfully "the first modular high temperature gas-cooled reactor (...) worldwide" [45] called 10 MW High Temperature gas-cooled Reactor (HTR-10). This power plant is an indirect cycle comprising an helium and steam loop. Afterwards, the Institute decided to launch a new programme called 10 MW High Temperature gas-cooled Reactor Gas Turbine (HTR-10GT), modifying the concept with an helium direct cycle. The PFD shows it is an intercooled, recuperated gas turbine engine with an additional temperature moderator to keep the reactor inlet temperature below the limits of its material (Figure 2.14). The pressure ratio of the power plant is 2.5, the overall thermal efficiency is 21.44%, and power output is slightly lower than 6 MW [45]. The power claimed in the name of the programme is the reactor thermal power (10 MW).

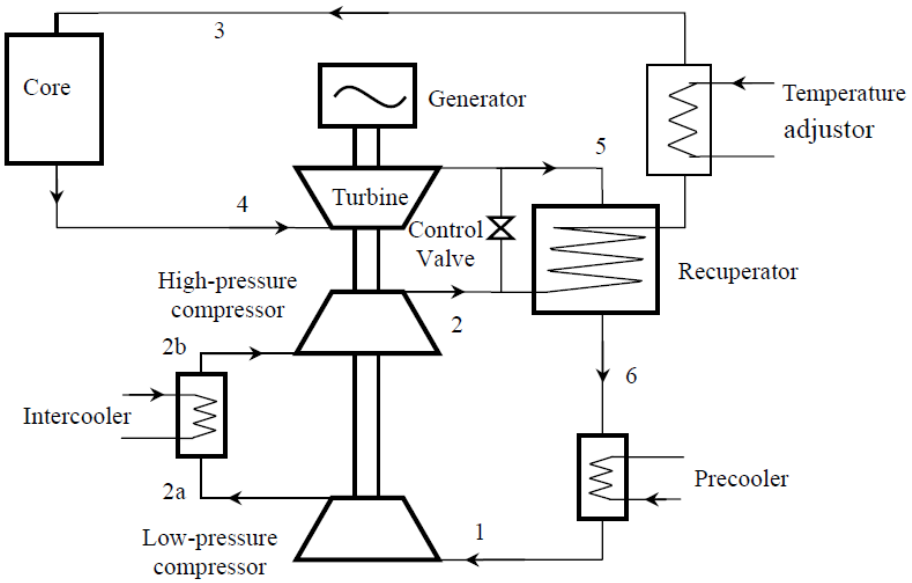

Figure 2.14. The PFD of the HTR-10GT [45].

2.3.4 Carbon Dioxide Direct Cycles

First concepts of carbon dioxide-based cycles could be traced back since the Forties and had been considered until the Seventies, almost always exploiting condensation cycles. The main limitations that prevented their commercial success were technological. In particular, the low efficiency of CO_2-based turbomachinery and lack of maturity in compact reactor design were two of the main issues [25]. Recently, the GIF reconsidered this option in the supercritical version, since the mentioned technological problems could be addressed thanks to the latest scientific progress. The typical power plant layouts studied for CO_2-based direct cycles are presented, sorted by increasing complexity.

The simplest layout is a recuperated gas turbine cycle (Figure 2.15). Typical parameters describing this concept are turbine pressure ratio 3.0, turbine inlet temperature 550 °C with a thermal efficiency slightly higher than 38% [49].

The previous concept could be improved trying to equalise the heat capacity of the quasi-critical fluid at the cold inlet of the recuperator (see Section 2.3.2). One option is to use a low and a high temperature recuperator, working also at different pressures on the hot side by means of an additional compressor between the two heat exchangers (Figure 2.16). This increased complexity in the power plant allows an increase of about 3% [49] in the thermal efficiency of the cycle (compared with the recuperated concept). This

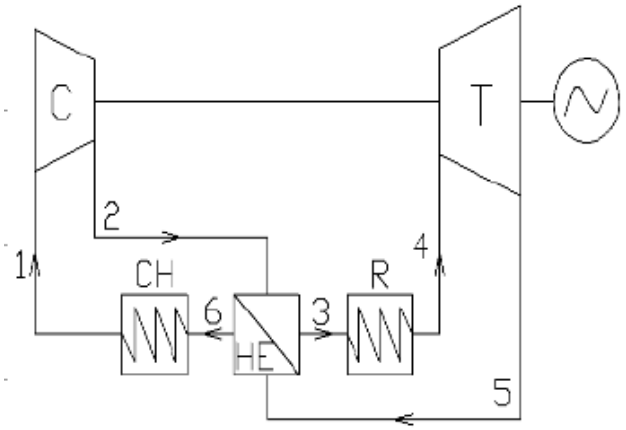

Figure 2.15. The PFD of a recuperated gas turbine cycle based on carbon dioxide. R: reactor, HE: heat exchanger (recuperator), CH: chiller (pre-cooler) [49].

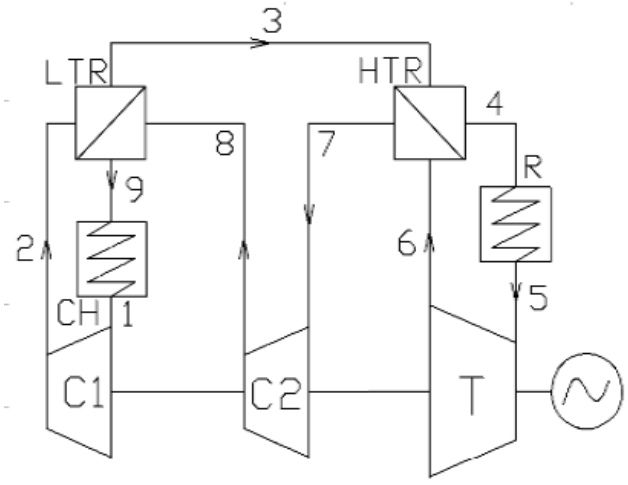

Figure 2.16. The PFD of a pre-compression, carbon dioxide, gas turbine cycle. R: reactor, CH: chiller (pre-cooler), LTR: Low Temperature Recuperator, HTR: High Temperature Recuperator [49].

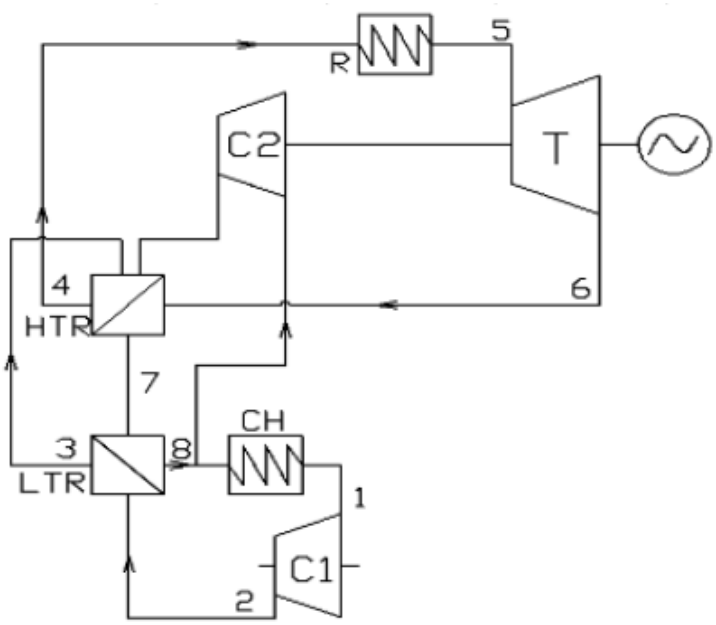

Figure 2.17. The PFD of a re-compression, carbon dioxide, gas turbine cycle. R: reactor, CH: chiller (pre-cooler), LTR: Low Temperature Recuperator, HTR: High Temperature Recuperator [49].

layout is often referred to as pre-compression cycle.

Another way to increase the recuperated heat is to rearrange the same pre-compression layout components differently, and reduce the mass flow on the cold side of the low temperature recuperator. This is achieved splitting and re-compressing a part of the working fluid mass flow before the pre-cooling (Figure 2.17). The mixing of the re-compressed, split mass flow takes place on the cold side of the high temperature recuperator. In this concept (called re-compression cycle), the pressure ratio of the additional compressor is quite low (differently than the pre-compression case) because the dominant effect is the different mass flow on the sides of the low temperature recuperator. This strategy to improve the heat recuperated is more efficient than the pre-compression, and it leads to a further increase of about 1% in the thermal efficiency.

It is possible to introduce an additional turbine in the re-compression layout expanding initially the gas heated by the recuperators, and then exploit in the main turbine the heat released in the reactor (Figure 2.18). This layout takes the name of split expansion cycle. Unfortunately, this complication does not increase the performance of the power plant, showing (on the contrary) a thermal efficiency comparable to the pre-compression case (about 41% [49]).

Finally, it is possible to combine pre-compression and re-compression using

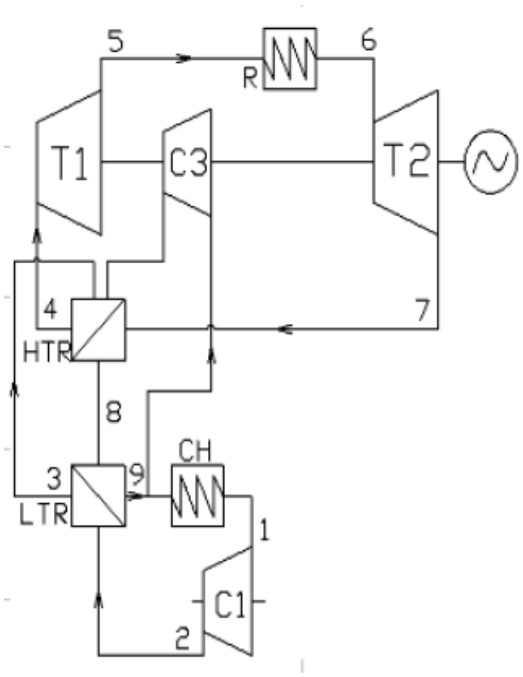

Figure 2.18. The PFD of a split expansion, carbon dioxide, gas turbine cycle. R: reactor, CH: chiller (pre-cooler), LTR: Low Temperature Recuperator, HTR: High Temperature Recuperator [49].

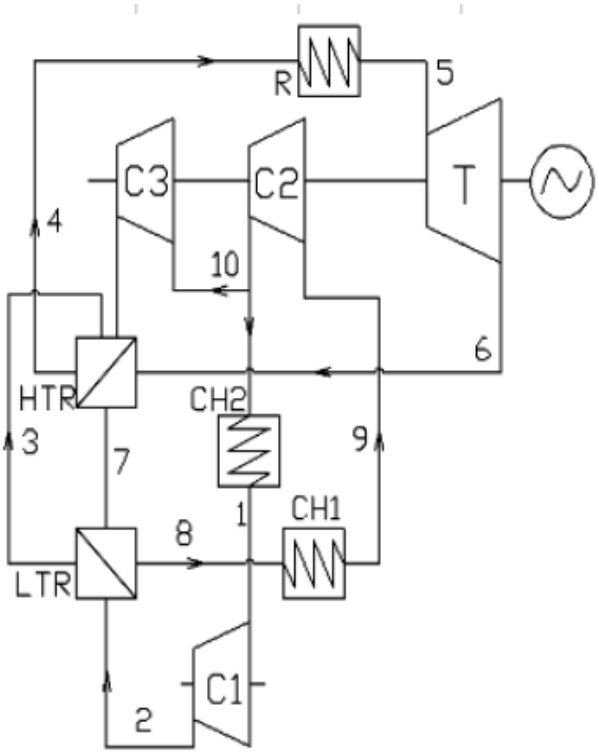

Figure 2.19. The PFD of a partial cooling, carbon dioxide, gas turbine cycle. R: reactor, CH: chiller (pre-cooler), LTR: Low Temperature Recuperator, HTR: High Temperature Recuperator [49].

three compressors and two pre-coolers (Figure 2.19). This is known as the partial cooling cycle and it is the most complicated power plant with the highest efficiency (up to 44%, in study [49]).

The scientific community is currently investigating the best performing concepts (re-compression and partial cooling cycles). An interesting, recent study considered the effect of intercooling and reheat to the re-compression cycle. Considered a fixed reactor outlet temperature of 750 °C, thermal efficiency ranges between 46% (simple re-compression layout and pressure ratio 3.1) and 50% (intercooled, reheated, re-compression cycle with pressure ratio 5.0) [89].

Another, older study simulated a simple re-compression cycle (called "partial pre-cooling" in the text) obtaining a cycle efficiency close to 46%. Computational assumption included: pressure ratio 3.3, reactor outlet temperature 650 °C, and turbine inlet pressure 70 bar [47].

Although the re-compression layout is more attractive for the reduced complexity, there is no clear picture in the open literature on the best layout. A study claims the re-compression cycle to have higher efficiency at design-point, while at part-load the partial cooling concept shows higher efficiency [49].

2.3.5 Cycles Selected

There is no evidence showing which family of cycles is better. A comparison of helium and carbon dioxide cycles requires to reconsider some of the fluids properties.

On the one hand, carbon dioxide seems more suitable for future nuclear power plants. Compared with helium, CO_2 has higher heat transfer coefficient, higher heat transport capacity (both features useful to design compact and efficient reactors and heat exchangers), longer depressurization time (allowing an easier design of passive safety systems), lower leakages problems (because of the higher molecular weight), and it is 250 times cheaper per unit weight [47].

On the other hand, helium-based cycles have been historically implemented before CO_2-based power plants. This is because helium requires simpler power plants and less demanding technological features for the components, reducing capital and maintenance costs. In summary, carbon dioxide seems to be the best working fluid for gas turbine, nuclear power plants in the long-term, but at the moment it does not appear clearly predominant over helium.

In 2011 work on cycles based on both working fluids has started at Cranfield University by Filip Grochowina (with the collaboration of the author) developing a preliminary model of the selected cycles for design-point and off-design behaviour. The computational code is written in Fortran 95 and it provided preliminary results [39].

Chapter 3

Methods

3.1 Power Generation Engine Systems: Performance

3.1.1 Carbon Capture and Storage Cycles: Advanced Zero Emissions Power Plant

The Advanced Zero Emissions Power plant (AZEP) cycle is one of the most promising Carbon Capture and Storage (CCS) concepts and only a few studies have investigated its potential in the open literature. Most of them do not provide off-design results and a complete picture of the computational assumptions for all key components (Section 2.2.2).

In broad terms, the cycle (Figure 3.1) adopts a special membrane (the "MCM reactor") to substitute a conventional combustor. Thus, the new device operates the separation of the oxygen from the air, the combustion of the fuel with the extracted oxygen and, finally, transfers the heat of combustion to the

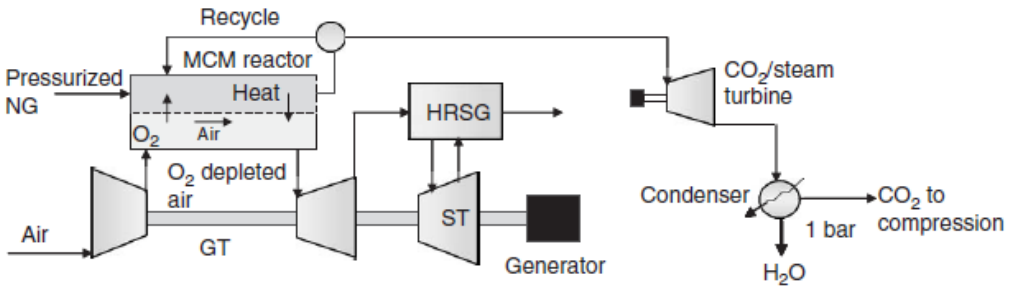

Figure 3.1. A simple PFD of the AZEP concept [50].

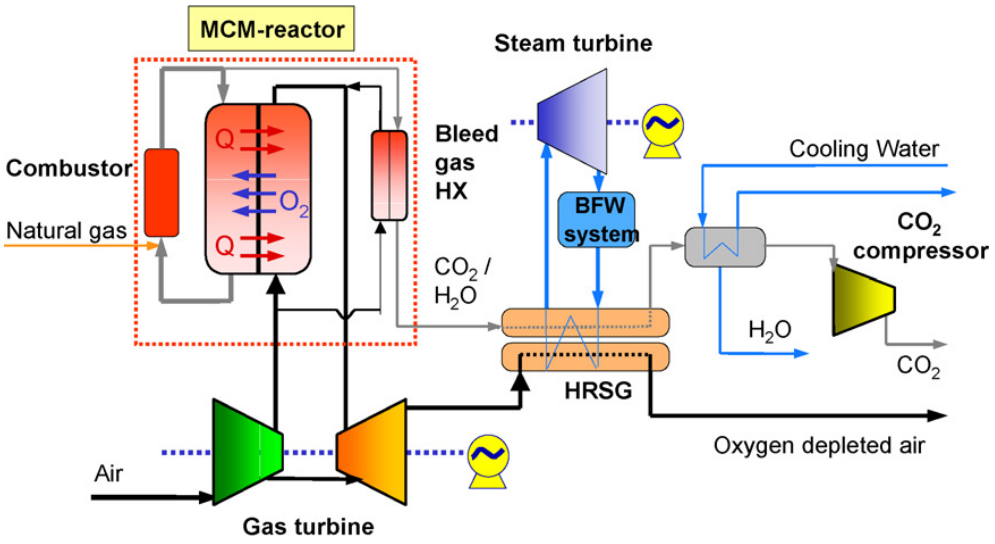

Figure 3.2. The PFD of the AZEP cycle basic concept [79].

oxygen-depleted air. The power plant usually integrates a steam bottoming cycle and one or two turbines for the oxygen-depleted air and the CO_2/H_2O flows (all represented in the figure).

A more detailed look at its Process Flow Diagram (PFD) (Figure 3.2) reveals that the "MCM reactor" comprises a Mixed Conductive Membrane (MCM), a catalytic combustor, and a Bleed gas Heat exchanger (BHX). As detailed in Figure 3.3, the central device of the membrane reactor is actually made up of three parts: a Low Temperature Heat exchanger (LTHX), a High Temperature Heat exchanger (HTHX), and the membrane itself that performs at the same time oxygen mass transfer and heat exchange.

Moreover, comparing Figure 3.1 to Figure 3.2, it can be observed that in the second diagram the stream of flue gas is conveyed to the Heat Recovery Steam Generator (HRSG) instead of being expanded in a CO_2/H_2O turbine (Figure 3.1). The two figures represent different configurations of the AZEP cycle.

Another option often considered alongside the "standard" AZEP cycle, is a modified layout with the insertion of a conventional afterburner before the expansion of the oxygen-depleted stream (Figure 3.4). In fact, the outlet membrane air still retains a quantity of oxygen capable to react with additional fuel, increasing the turbine inlet temperature and reaching values close to the conventional case. This improves the power plant performance, but it makes impossible to capture all the generated CO_2. For this reason, this concept is usually called "AZEP 85%" because it is possible to capture approximately 85% of the carbon dioxide originated in the energy conversion process [61, 50].

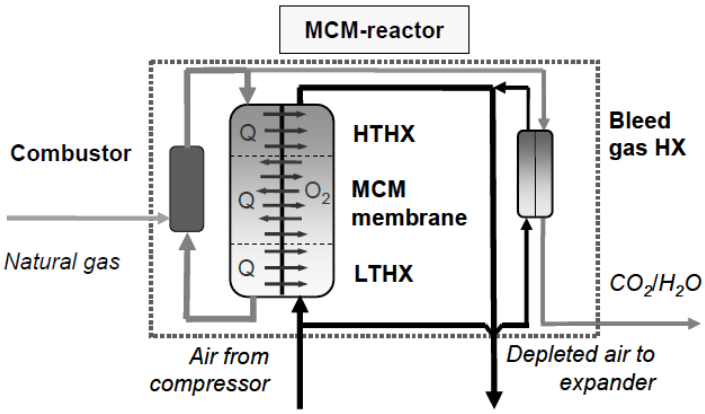

Figure 3.3. A detailed view of the membrane reactor [61].

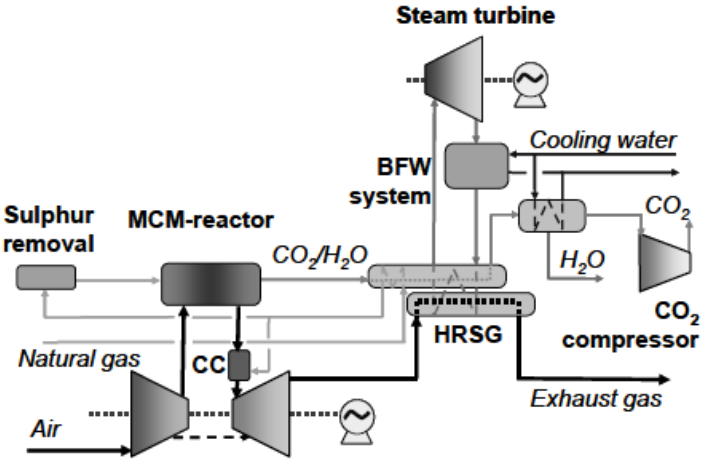

Figure 3.4. The alternative AZEP layout with a conventional afterburner before the expansion of the oxygen-depleted air flow [61].

In 2009, the author (in the scope of his Master by Research course) developed a computational code written in Fortran 95 called eAZEP. This computer program allows the user to simulate in a modular fashion a number of different layouts for the AZEP 100% at design-point [68].

Alongside the layouts including or excluding the BHX and the CO_2/H_2O turbine, an original family of configurations has been introduced with the conception of another heat exchanger, the Post Expansion Heat exchanger (PEHX) [68]. According to the information in the open literature, eAZEP is the only computational program developed directly in a programming language without making use of any commercial, mathematical or thermo-physical, simulation tool. This unique feature yields its high flexibility.[1]

Subsequently, the MSc students Gianvito Ciavarella (in 2010) and Jon Freire (in 2011), with the collaboration of the author, extended and refined eAZEP introducing the off-design performance feature [12] and the AZEP 85% [34], respectively.

Thus, the methodology adopted for the AZEP power plants is completely described in the Master by Research thesis of the author [68]. The *application* of the same methodology has received some minor amendments in the cited subsequent studies by Ciavarella and Freire [12, 34].

The last incarnation of the AZEP *combined cycle* PFD comprises stations with different kind of working fluids: mixtures of carbon dioxide and water vapour, standard air and oxygen depleted air, fuel (natural gas), pure oxygen, and water or steam (Figure 3.5).

eAZEP currently handles the modelling of the topping AZEP cycle, and it is connected to the steam, bottoming cycle described in Section 3.1.4. The reader is encouraged to refer to the relevant section for information on the steam cycle methodology.

eAZEP calculations are based on a zero-dimensional model of perfect gases (or mixtures of them) with the specific heat dependent on temperature only

$$\begin{cases} c_p = c_p(T) = {}^{\mathrm{d}h}/_{\mathrm{d}T} \\ c_v = c_v(T) = {}^{\mathrm{d}u}/_{\mathrm{d}T} \end{cases} \tag{3.1}$$

A polynomial expression developed by NASA is chosen to describe their variability [90].

The heat exchangers design criterion is based on the ε-N_{tu} method [53, 46, 76] for perfect counter-current devices. However, some small changes had been introduced by Ciavarella to improve the convergence robustness of eAZEP. More specifically, only the LTHX and HTHX are resolved at design-point according to the logarithmic mean temperature difference (LMTD)

[1] There are two journal papers currently under review based on the results of this study

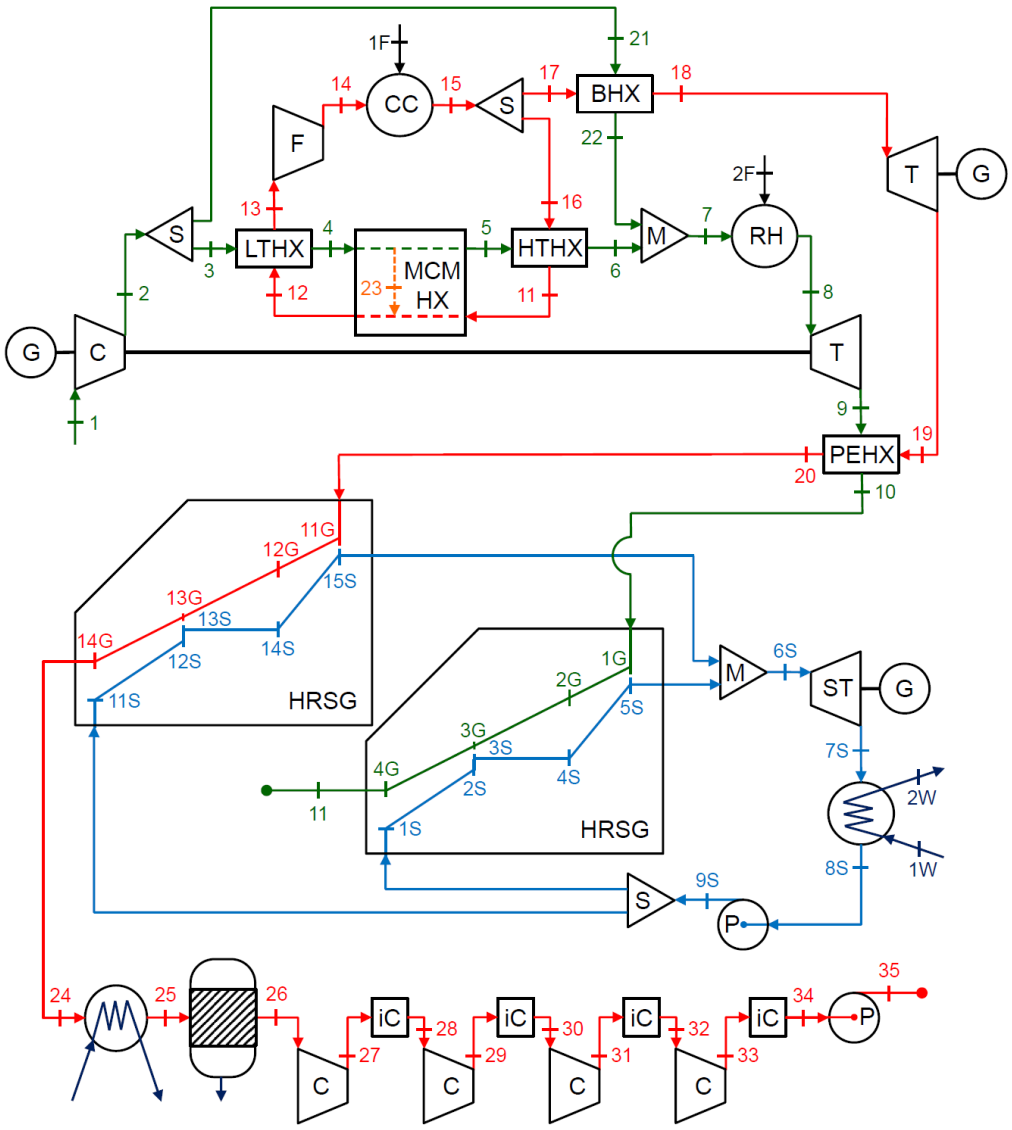

Figure 3.5. Complete PFD of the AZEP combined cycle as modelled by eAZEP (currently the steam, bottoming cycle is simulated by another piece of software connected to eAZEP) [34].

method [53, 46, 76], while at off-design the original ε-N_{tu} strategy is adopted. If the heat capacity rates of the fluids are very similar, the ε-N_{tu} method could not converge at off-design. When this condition is detected, eAZEP uses again the LMTD method. This amendment trades numerical efficiency and accuracy for robustness [12].

The transfer of oxygen in the MCM is modelled by the Nernst-Einstein formula, a simple case of integration of the Wagner equation [77, 8, 55].

$$j_{\mathrm{O}_2} = \frac{\sigma\,\mathcal{R}\,T}{4\,L\,n^2\,\mathrm{F}^2}\,\ln\frac{p^{\mathrm{F}}_{\mathrm{O}_2}}{p^{\mathrm{P}}_{\mathrm{O}_2}} \tag{3.2}$$

where

j_{O_2} is the oxygen flux (mol/(m^2 s));

σ is the membrane *electric* conductivity (S/m);

$\mathcal{R}$ is the ideal gas constant (J/(mol K));

T is the membrane *absolute* temperature (K);

L is the membrane thickness (m);

n is the valency number of the element permeated (in this case we deal with oxygen, then, $n = 2$) (0);

F is the Faraday constant (mol/C);

$p^{\mathrm{F}}_{\mathrm{O}_2}$ is the partial pressure of the oxygen on the *feed* side (Pa);

$p^{\mathrm{P}}_{\mathrm{O}_2}$ is the partial pressure of the oxygen on the *permeate* side (Pa).

All quantities varying across the membrane are evaluated by a lumped approach.

The solving strategy is based on a sequential, iterative process to resolve the system of non-linear equations describing the power plants behaviour. The root-finding algorithm for each equation resolved in turn is based on the Brent method, coupled with two bracketing strategies. The convergence criterion is based on a non-dimensional error [72, 59].

Three off-design control strategies to meet the required electrical grid load are implemented in eAZEP [12, 34]:

- fuel control in the main combustor chamber;

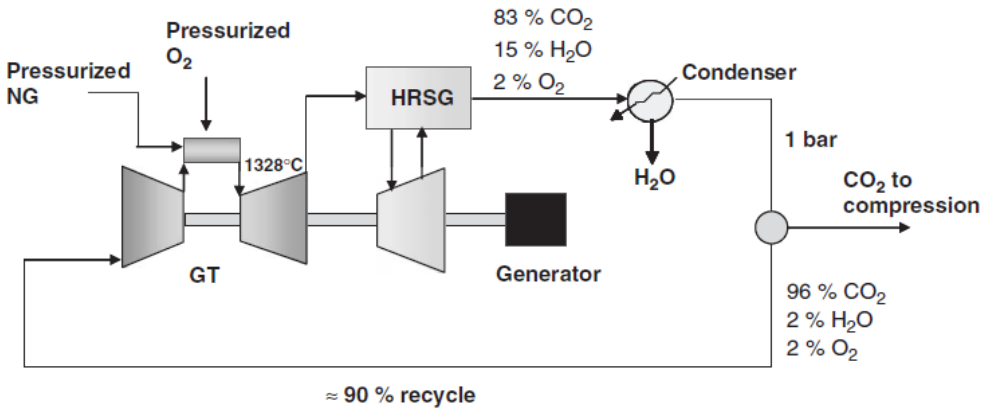

Figure 3.6. A simple PFD of the oxy-fuel combined cycle concept [50].

- control of mass flow at the inlet of the main compressor by means of variable inlet guide vanes (VIGV);
- fuel control in the re-heater (AZEP 85% only).

Additional off-design controls are implemented [12, 34]

- to keep the MCM operating temperature within the optimal range (handling the combustor chamber exit temperature and the sweep gas ratio);
- to limit the mechanical stress on the membrane (adjusting the sweep gas loop operating pressure);
- to guarantee a minimum excess of oxygen in the combustion chamber.

Oxy-fuel Combined Cycle

Also the oxy-fuel combined cycle concept shows several similarities with a conventional combined cycle: the heat of the exhaust gas is released in a HRSG, but the fuel oxidation is operated by *pure* oxygen produced in a dedicated device (Figure 3.6). This component performs a cryogenic process with an estimated loss in the electrical efficiency of about 10% [37], although there are also studies that substitute the cryogenic process with chemical cycles [5]. The device that supplies oxygen to the oxy-fuel combined cycle combustor is often referred to as Air Separation Unit (ASU).

Moreover, this thermodynamic cycle recirculates about 90% of flue gas at the compressor inlet to dilute the combustive mixture and lower the combustor outlet temperature to an acceptable value.

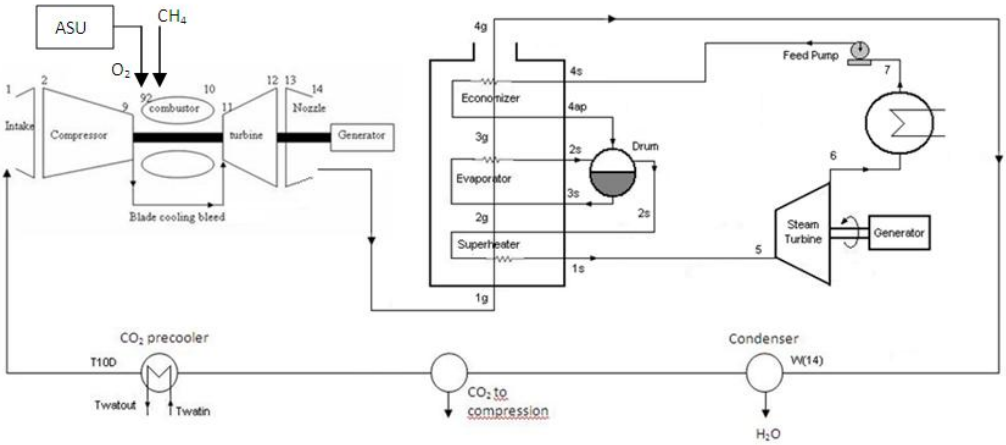

Figure 3.7. General layout of the oxy-fuel combined cycle [9].

There have been some studies at Cranfield University on this cycle performance [56, 2], and the current adopted methodology has been developed by Francisco Carrillo Romero for his final MSc thesis [9]. Carrillo modified a computational code written in Fortran programming language called Variflow, initially developed in 1999 by Codeceira Neto [13] mainly exploiting the software fluids model.

The PFD of the oxy-fuel combined cycle model includes both the topping, gas-turbine and the bottoming, steam cycle (Figure 3.7) however, the steam cycle simulation tool is detailed in Section 3.1.4. The two pieces of software are not completely integrated yet.

Concerning the oxy-fuel cycle only, the underlying simulation assumptions (mainly derived by the program Variflow) include

- a zero-dimensional model of all working fluids as perfect gases,
- perfect, complete combustion in the combustion chamber,
- mean temperature method to calculate the temperature and pressure ratio of turbomachinery,
- the turbine is always considered chocked i.e., the non-dimensional mass flow is constant,
- the ASU performs a cryogenic, staged, compression process [2].

The solving process does not need any iterative strategy so that the non-linear equations of the power plant can be solved in turn, directly.

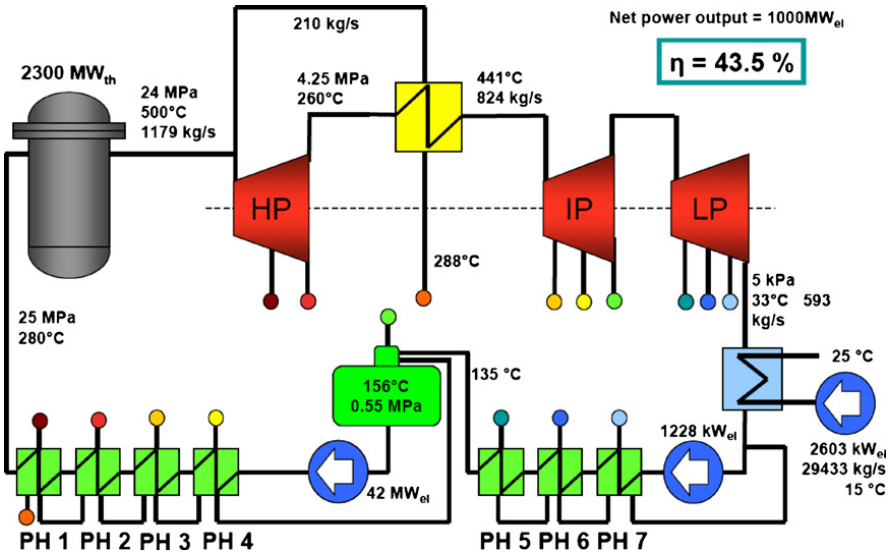

Figure 3.8. Complete layout of the SCWR concept with key parameters and performance data [75].

3.1.2 Nuclear Cycles

Nuclear energy is a complementary option to contribute to sustainable energy because it is a low carbon technology. A strong effort towards innovation is ongoing in the international scientific community to select the best candidate cycles for the forthcoming generation of engine systems (Section 2.3).

SCWR Power Plant

The Supercritical Water-cooled Reactor (SCWR) is one of the concepts identified by Generation IV International Forum (GIF) as candidate for future generations of nuclear power plants [35, 83]. Figure 3.8 summarises, alongside the plant layout, the key data of the cycle, i.e. main parameters and expected performance. The model developed in this study is an approximation of the concept shown including all its major features. This is visually represented in the PFD of the model (Figure 3.9).

In principle, the relevant methodology can be adopted from the steam plant simulation theory (Section 3.1.4) but, in this case, the supercritical working fluid behaves quite differently than water/steam at ordinary conditions of steam turbine power plants. Hence, a new methodology has been developed, although it has been limited to the components that are sensitive to the supercritical steam properties.

In particular, the modelling of the fluid heat transfer requires particular

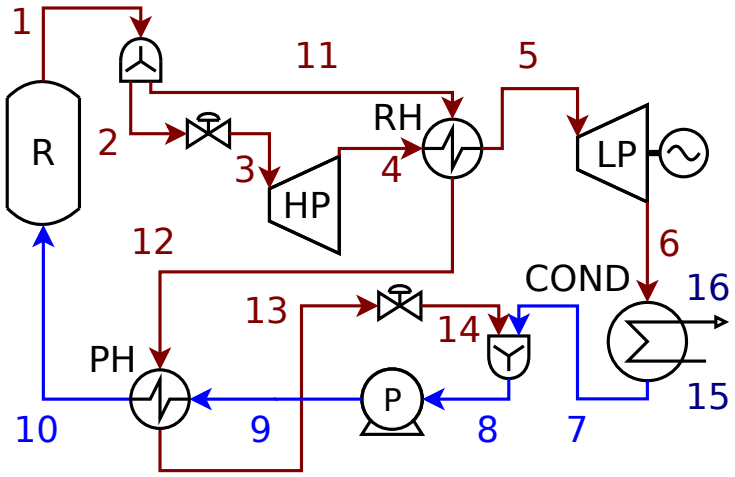

Figure 3.9. Process Flow Diagram of the SCWR cycle computational code.

attention, whereas the electronic library chosen to estimate the properties of the water and steam (Section 3.1.4) is still deemed adequate because of the high accuracy of the model that it implements [85]. All heat exchangers (namely, the re-heater, the pre-heater, and the condenser) are directly dependent on this new heat transfer model.

Moreover, the reactor and the steam turbine arrangement are other specific features of this cycle that will be discussed as well.

Heat exchangers: background In process engineering, a simplified approach to heat exchangers modelling is usually pursued. The most popular methods (e.g. LMTD, ε-N_{tu}, P-N_{tu}), among other simplifications, assume a constant value of the fluid specific heat in the development of their expressions [53, 46].

In this case, on the trail of the LMTD method, a more accurate expression of heat transfer is developed considering specific heat and, thus, specific enthalpy dependent both on temperature *and pressure*. This feature is an original contribution to knowledge.

In fact, a similar model has been developed for supercritical water in the scientific literature, but it takes into account only the effect of temperature on the fluid properties [74]. Similarly, a few accurate models based on empirical,

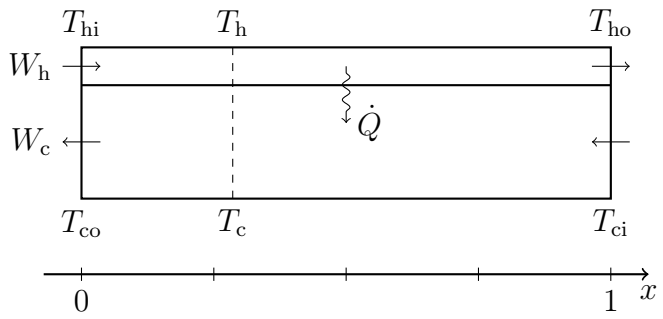

Figure 3.10. A simplified sketch of the modelled heat exchanger.

semi-empirical or Computational Fluid Dynamics (CFD) simulations are available in the literature (Cheng offers a good review [11]) but they require knowledge of the specific geometry being modelled losing generality and (in many cases) requiring significantly higher computational effort.

Heat exchangers design-point: preliminary assumptions A perfect, counter-current, single-tube heat exchanger is considered (Figure 3.10). The following quantities are inputs:

- W_c, cold fluid mass flow;
- W_h, hot fluid mass flow;
- T_{hi}, inlet hot fluid temperature;
- T_{ci}, inlet cold fluid temperature;
- T_{co}, outlet cold fluid temperature.

Whereas the expected outputs are:

- UA, the area-overall heat exchange coefficient product;
- T_{ho}, outlet hot fluid temperature.

Heat exchangers design-point: derivation The sought heat transfer expression is first obtained considering both streams properties dependent on temperature only. Subsequently, the model will be extended to the general case (thermodynamic properties dependent on temperature *and pressure*).

First of all, the specific enthalpies h are easily calculated from the relevant known temperatures by means of their gas model (e.g. the eAZEP gas model library described in Section 3.1.1):

$$h_{\mathrm{hi}} = h_{\mathrm{gas}}\left(T_{\mathrm{hi}}\right) \tag{3.3}$$
$$h_{\mathrm{ci}} = h_{\mathrm{gas}}\left(T_{\mathrm{ci}}\right) \tag{3.4}$$
$$h_{\mathrm{co}} = h_{\mathrm{gas}}\left(T_{\mathrm{co}}\right) \tag{3.5}$$

Considering a *generic*, infinitesimal element of the heat exchanger, the first law of thermodynamics for both fluids (first two equations), and the heat exchange equation (last one) can be written

$$\begin{cases} -\mathrm{d}\dot{Q} = W_{\mathrm{h}}\,\mathrm{d}h_{\mathrm{h}} \\ \mathrm{d}\dot{Q} = -W_{\mathrm{c}}\,\mathrm{d}h_{\mathrm{c}} \\ \mathrm{d}\dot{Q} = UA\,\left(T_{\mathrm{h}} - T_{\mathrm{c}}\right)\,\mathrm{d}x \end{cases} \tag{3.6}$$

In the third equation x is the non-dimensional abscissa describing the fluids position through the heat exchanger between the two ends ($x \in [0, 1]$).

Combining the third and the second equation,

$$UA\,\left(T_{\mathrm{h}} - T_{\mathrm{c}}\right)\,\mathrm{d}x = -W_{\mathrm{c}}\,\mathrm{d}h_{\mathrm{c}}$$

it is obtained

$$UA\,\mathrm{d}x = -\frac{W_{\mathrm{c}}\,\mathrm{d}h_{\mathrm{c}}}{T_{\mathrm{h}} - T_{\mathrm{c}}}$$

Integrating across the whole heat exchanger, the expression reads

$$\int_0^1 UA\,\mathrm{d}x = -\int_{h_{\mathrm{co}}}^{h_{\mathrm{ci}}} \frac{W_{\mathrm{c}}\,\mathrm{d}h_{\mathrm{c}}}{T_{\mathrm{h}} - T_{\mathrm{c}}}$$

Assuming (to a first approximation) UA constant and independent on x, and observing that W_{c} is not dependent on the fluid enthalpy, the formula reads

$$UA \int_0^1 \mathrm{d}x = W_{\mathrm{c}} \int_{h_{\mathrm{ci}}}^{h_{\mathrm{co}}} \frac{\mathrm{d}h_{\mathrm{c}}}{T_{\mathrm{h}} - T_{\mathrm{c}}}$$

and finally we obtain the first formula to be used operatively

$$\boxed{UA = W_{\mathrm{c}} \int_{h_{\mathrm{ci}}}^{h_{\mathrm{co}}} \frac{\mathrm{d}h_{\mathrm{c}}}{T_{\mathrm{h}} - T_{\mathrm{c}}}} \tag{3.7}$$

Although in the last equation the integral should be evaluated numerically, there is no information on T_{h} and T_{c} (i.e. the temperatures of hot and cold fluid across the heat exchanger). Hence, the unknowns of Equation (3.7) are

1. UA,
2. T_h,
3. T_c.

There are two trivial equations to be added to the system

$$\boxed{h_\mathrm{h} = h_\mathrm{gas}\left(T_\mathrm{h}\right)} \tag{3.8}$$

$$\boxed{h_\mathrm{c} = h_\mathrm{gas}\left(T_\mathrm{c}\right)} \tag{3.9}$$

Equation (3.8) introduces a fourth unknown: h_h (in fact, h_c is the integration variable of Equation (3.7) and it is *not* unknown).

Thus, an additional, final equation is necessary to close the mathematical model of the heat exchanger. It is obtained combining the first and the second equations of system (3.6), i.e. writing the energy balance of the component

$$W_\mathrm{h}\,\mathrm{d}h_\mathrm{h} = W_\mathrm{c}\,\mathrm{d}h_\mathrm{c}$$

and integrating from the first end of the heat exchanger ($x = 0$) to a generic point (see Figure 3.10)

$$\int_{h_\mathrm{hi}}^{h_\mathrm{h}} W_\mathrm{h}\,\mathrm{d}h_\mathrm{h} = \int_{h_\mathrm{co}}^{h_\mathrm{c}} W_\mathrm{c}\,\mathrm{d}h_\mathrm{c}$$

or, equally

$$\int_{h_\mathrm{h}}^{h_\mathrm{hi}} W_\mathrm{h}\,\mathrm{d}h_\mathrm{h} = \int_{h_\mathrm{c}}^{h_\mathrm{co}} W_\mathrm{c}\,\mathrm{d}h_\mathrm{c}$$

The analytical result of integration is exactly the last formula required to close the mathematical modelling problem

$$\boxed{W_\mathrm{h}\left(h_\mathrm{hi} - h_\mathrm{h}\right) = W_\mathrm{c}\left(h_\mathrm{co} - h_\mathrm{c}\right)} \tag{3.10}$$

Summarising, the required system of equations reads

$$\begin{cases} UA = W_\mathrm{c}\displaystyle\int_{h_\mathrm{ci}}^{h_\mathrm{co}} \frac{\mathrm{d}h_\mathrm{c}}{T_\mathrm{h} - T_\mathrm{c}} \\ h_\mathrm{h} = h_\mathrm{gas}\left(T_\mathrm{h}\right) \\ h_\mathrm{c} = h_\mathrm{gas}\left(T_\mathrm{c}\right) \\ W_\mathrm{h}\left(h_\mathrm{hi} - h_\mathrm{h}\right) = W_\mathrm{c}\left(h_\mathrm{co} - h_\mathrm{c}\right) \end{cases} \tag{3.11}$$

Heat exchangers design-point: gas-water heat exchanger In the previous section, it has been assumed that the specific enthalpy is dependent on temperature only. In the SCWR case there is water and steam flowing and exchanging heat then, according to the formulation provided by the International Association for the Properties of Water and Steam (IAPWS) is necessary to take into account also the effect of pressure. Hence, the water/steam specific enthalpy is dependent on temperature *and pressure* [85].

Especially at (quasi) supercritical conditions the effect of pressure is not negligible (it could introduce errors up to 50% for the calculation of specific enthalpy[2]). Looking at the derivations in the previous section, there are just a few equations dependent on the model of specific enthalpy. These equations can be simply substituted by a more accurate formulation without affecting the congruity of the previous derivation.

In practice, if the cold fluid is water/steam (subscript "w") and the hot fluid is a gas (subscript "g"), the previous system (3.11) becomes

$$\begin{cases} UA = W_{\mathrm{w}} \displaystyle\int_{h_{\mathrm{wi}}}^{h_{\mathrm{wo}}} \frac{\mathrm{d}h_{\mathrm{w}}}{T_{\mathrm{g}} - T_{\mathrm{w}}} \\ h_{\mathrm{g}} = h_{\mathrm{gas}}\left(T_{\mathrm{g}}\right) \\ h_{\mathrm{w}} = h_{\mathrm{iapws}}\left(T_{\mathrm{w}}, p_{\mathrm{w}}\right) \\ W_{\mathrm{g}}\left(h_{\mathrm{gi}} - h_{\mathrm{g}}\right) = W_{\mathrm{w}}\left(h_{\mathrm{wo}} - h_{\mathrm{w}}\right) \end{cases} \tag{3.12}$$

Unfortunately, looking carefully at the last result, an additional unknown appears: p_{w} (third equation). Thus, an additional equation must be provided to describe the pressure distribution across the heat exchanger of water/steam. A number of tests have been run to appreciate the sensitivity of the results on the pressure distribution across the device. Comparing a linear distribution to exponential functions with different power-laws has shown a relative insensitivity of the outputs on the type of pressure distribution (maximum error reported of around 1%). Thus, considering the degree of approximation of the present model, a quasi-linear behaviour is deemed satisfactory.

$$\boxed{p_{\mathrm{w}} = \frac{T_{\mathrm{gi}} - T_{\mathrm{g}}}{T_{\mathrm{gi}} - T_{\mathrm{go}}}\, p_{\mathrm{wi}}} \tag{3.13}$$

According to the previous equation, the pressure drop will follow the same trend of the gas temperature drop. Although not very accurate, this assumption is deemed consistent with the targeted accuracy of the model.

[2]comparison of IAPWS specific enthalpy at critical temperature calculated at critical and sea level standard pressure

Moreover, considering also the substituting equations for the calculation of the water/steam enthalpy

$$h_{\mathrm{wi}} = h_{\mathrm{iapws}}\left(T_{\mathrm{wi}}, p_{\mathrm{wi}}\right) \tag{3.14}$$

$$h_{\mathrm{wo}} = h_{\mathrm{iapws}}\left(T_{\mathrm{wo}}, p_{\mathrm{wo}}\right) \tag{3.15}$$

two additional parameters must be known at the starting of the solving procedure: the inlet and outlet pressure of water/steam (p_{wi}, p_{wo}), or the inlet pressure and the pressure drop across the heat exchanger on the water/steam side (p_{wi}, Δp_{w}).

Summarising, for a gas-water heat exchanger, the input quantities are:

- W_{w}, water/steam mass flow;
- W_{g}, gas mass flow;
- T_{gi}, inlet gas temperature;
- T_{wi}, inlet water/steam temperature;
- T_{wo}, outlet water/steam temperature;
- p_{wi}, inlet water/steam pressure;
- p_{wo}, outlet water/steam fluid pressure.

The calculated outputs are:

- UA, the area-overall heat exchange coefficient product;
- T_{go}, outlet gas temperature.

The five unknowns are

1. UA,
2. T_{g},
3. T_{w},
4. p_{w},
5. h_{g}.

and the final solving system of equations reads

$$\begin{cases} UA = W_{\mathrm{w}} \displaystyle\int_{h_{\mathrm{wi}}}^{h_{\mathrm{wo}}} \frac{\mathrm{d}h_{\mathrm{w}}}{T_{\mathrm{g}} - T_{\mathrm{w}}} \\ h_{\mathrm{g}} = h_{\mathrm{gas}}\left(T_{\mathrm{g}}\right) \\ h_{\mathrm{w}} = h_{\mathrm{iapws}}\left(T_{\mathrm{w}}, p_{\mathrm{w}}\right) \\ W_{\mathrm{g}}\left(h_{\mathrm{gi}} - h_{\mathrm{g}}\right) = W_{\mathrm{w}}\left(h_{\mathrm{wo}} - h_{\mathrm{w}}\right) \\ p_{\mathrm{w}} = \dfrac{T_{\mathrm{gi}} - T_{\mathrm{g}}}{T_{\mathrm{gi}} - T_{\mathrm{go}}}\, p_{\mathrm{wi}} \end{cases} \tag{3.16}$$

Heat exchangers design-point: water-water model For a water-water heat exchanger, a similar expression could be easily derived considering the additional input parameters and opportunely changing some equations in a similar fashion as done in the previous section.

For the sake of brevity, just the resulting final system of equations with a list of the input and output quantities will be presented.

Input quantities:

- W_{c}, cold water/steam mass flow;
- W_{h}, hot water/steam mass flow;
- T_{hi}, inlet hot water/steam temperature;
- T_{ci}, inlet cold water/steam temperature;
- T_{co}, outlet cold water/steam temperature;
- p_{ci}, inlet cold water/steam pressure;
- p_{hi}, inlet hot water/steam pressure;
- p_{co}, outlet cold water/steam fluid pressure.
- p_{ho}, outlet hot water/steam fluid pressure.

Output quantities:

- UA, the product area-overall heat exchange coefficient;
- T_{ho}, outlet hot water/steam temperature.

List of the six unknowns:

1. UA,
2. T_{h},
3. T_{c},
4. p_{h},
5. p_{c},
6. h_{h}.

Solving system of equations:

$$\begin{cases} UA = W_{\mathrm{c}} \displaystyle\int_{h_{\mathrm{ci}}}^{h_{\mathrm{co}}} \frac{\mathrm{d}h_{\mathrm{c}}}{T_{\mathrm{h}} - T_{\mathrm{c}}} \\ h_{\mathrm{h}} = h_{\mathrm{iapws}}\left(T_{\mathrm{h}}, p_{\mathrm{h}}\right) \\ h_{\mathrm{c}} = h_{\mathrm{iapws}}\left(T_{\mathrm{c}}, p_{\mathrm{c}}\right) \\ W_{\mathrm{h}}\left(h_{\mathrm{hi}} - h_{\mathrm{h}}\right) = W_{\mathrm{c}}\left(h_{\mathrm{co}} - h_{\mathrm{c}}\right) \\ p_{\mathrm{h}} = p_{\mathrm{hi}} + \dfrac{h_{\mathrm{h}} - h_{\mathrm{hi}}}{h_{\mathrm{ho}} - h_{\mathrm{hi}}}\left(p_{\mathrm{ho}} - p_{\mathrm{hi}}\right) \\ p_{\mathrm{c}} = p_{\mathrm{ci}} + \dfrac{h_{\mathrm{c}} - h_{\mathrm{ci}}}{h_{\mathrm{co}} - h_{\mathrm{ci}}}\left(p_{\mathrm{co}} - p_{\mathrm{ci}}\right) \end{cases} \tag{3.17}$$

If T_{ho} is an *input* quantity (instead of T_{co}) and T_{co} is an *output* (instead of T_{ho}), an equivalent solving system can be obtained:

$$\begin{cases} UA = W_{\mathrm{h}} \displaystyle\int_{h_{\mathrm{ho}}}^{h_{\mathrm{hi}}} \frac{\mathrm{d}h_{\mathrm{h}}}{T_{\mathrm{h}} - T_{\mathrm{c}}} \\ h_{\mathrm{h}} = h_{\mathrm{iapws}}\left(T_{\mathrm{g}}, p_{\mathrm{h}}\right) \\ h_{\mathrm{c}} = h_{\mathrm{iapws}}\left(T_{\mathrm{c}}, p_{\mathrm{c}}\right) \\ W_{\mathrm{h}}\left(h_{\mathrm{hi}} - h_{\mathrm{h}}\right) = W_{\mathrm{c}}\left(h_{\mathrm{co}} - h_{\mathrm{c}}\right) \\ p_{\mathrm{h}} = p_{\mathrm{hi}} + \dfrac{h_{\mathrm{h}} - h_{\mathrm{hi}}}{h_{\mathrm{ho}} - h_{\mathrm{hi}}}\left(p_{\mathrm{ho}} - p_{\mathrm{hi}}\right) \\ p_{\mathrm{c}} = p_{\mathrm{ci}} + \dfrac{h_{\mathrm{c}} - h_{\mathrm{ci}}}{h_{\mathrm{co}} - h_{\mathrm{ci}}}\left(p_{\mathrm{co}} - p_{\mathrm{ci}}\right) \end{cases} \tag{3.18}$$

Heat exchangers off-design: model description The off-design case can be resolved simply applying the same system of equations obtained for the design-point, but with a different set of inputs and unknowns. In fact, after the design-point calculation all geometric parameters are determined and assumed constant.

Thus, for a gas-gas heat exchanger, system (3.11) can be resolved to determine the off-design value of the following unknowns

1. h_{co},
2. T_{h},
3. T_{c},
4. h_{h}.

It should be observed that while evaluating the integral at its lower bound (i.e. h_{ci}), h_{ho} and T_{ho} are obtained as results of the system of equations in the form of h_{h} and T_{h}.

For a gas-water heat exchanger, system (3.16) is resolved to calculate the previously listed four unknowns plus p_{w}. Similarly, to resolve a water-water device, it should be considered system (3.17) with all the previous five unknowns together with p_{h}.

The numerical solution of the systems of equations presented so far is obtained incorporating a numerical integration method (a globally adaptive integrator based on recursive monotone stable formulae [30, 31]) in a root-finding algorithm.

Condenser The mathematical model previously outlined is applied in a slightly different way to simulate the condenser performance.

At design-point condition, system (3.17) is resolved assuming that

- W_{h}, hot water/steam mass flow;
- T_{hi}, inlet hot water/steam temperature;
- T_{ho}, outlet hot water/steam temperature.
- T_{ci}, inlet cold water/steam temperature;
- T_{co}, outlet cold water/steam temperature;
- p_{ci}, inlet cold water/steam pressure;
- p_{hi}, inlet hot water/steam pressure;

- p_{co}, outlet cold water/steam fluid pressure.
- p_{ho}, outlet hot water/steam fluid pressure.

are input quantities, while

- W_{c}, cold water/steam mass flow;
- UA, the product area-overall heat exchange coefficient;

are the outputs. More explicitly, the outlet conditions on the hot side are imposed and the required cold stream mass flow is computed.

The off-design behaviour is again governed by the same equations, but computing the following unknowns

1. W_{c},
2. h_{ho},
3. T_{h},
4. h_{h},
5. p_{c},
6. p_{h},

imposing constant (and equal to the design-point value) the outlet conditions of the cold fluid. To improve the robustness of the off-design calculations, an additional backtracking algorithm is implemented that, upon failure of the full integrating step across the condenser abscissa, repeats the process on increasingly smaller sub-intervals. This technique has proven particularly successful at extreme part-load operating conditions.

Nuclear reactor An accurate simulation of the nuclear reactor would be beyond the scope of this work. Hence, the reactor is assumed as a heat input device able to provide, without restrictions, the thermal power necessary to increase the temperature of the inlet fluid to a dictated outlet value.

Characteristic parameters of its performance are the pressure drop efficiency η_π and the thermal efficiency η_{th} defined as follows

$$\eta_\pi = \frac{p_{\mathrm{o}}}{p_{\mathrm{i}}} \tag{3.19}$$

$$\eta_{\mathrm{th}} = \frac{W_{\mathrm{i}}\,(h_{\mathrm{o}} - h_{\mathrm{i}})}{\dot{Q}_{\mathrm{in}}} \tag{3.20}$$

where p_{o} and p_{i} are the outlet and inlet pressure, h_{o} and h_{i} are the outlet and inlet specific enthalpy, W_{i} is the inlet mass flow, and $\dot{Q}_{\mathrm{in}}$ is the thermal power released by the reactor.

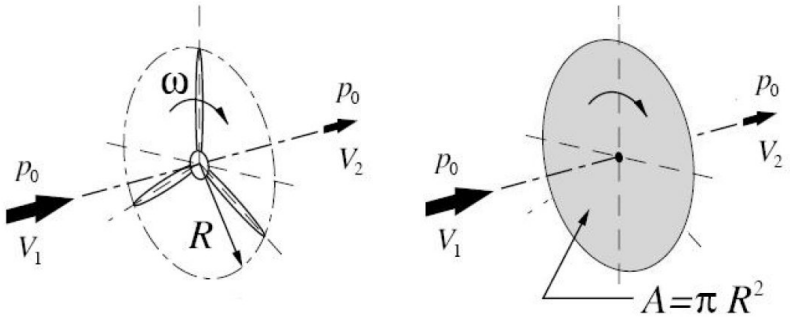

Figure 3.11. Actuator disc model: the turbine is simulated as an infinitely thin disc dictating a step change in the constant velocity along the axis of rotation [22].

Steam turbines The power plant comprises two steam turbines in series (Figure 3.9) assumed to work at choking condition. While predicting the off-design performance, the simulation computer program compares their operating non-dimensional mass flow Γ values

$$\Gamma = \frac{W_{\mathrm{i}} \sqrt{T_{\mathrm{i}}}}{p_{\mathrm{i}}} \tag{3.21}$$

identifying the turbine that dictates the power plant working fluid mass flow. This process ensures that a realistic off-design behaviour prediction is carried out.

3.1.3 Wind Energy

After hydropower, wind energy is currently the most mature renewable technology available. In the present project, a simplified model of a Horizontal Axis Wind Turbine (HAWT) is considered.

A preliminary work, in collaboration with the MSc student Irene De La Torre Mateo, produced a computational code called WindT written in the computer language Fortran 95 [22].

The behaviour of the turbine is simulated according to the actuator disc model (Figure 3.11), assuming the power coefficient at design-point equal to the Betz limit (its theoretical maximum value [42]).

At off-design it is allowed the wind speed to change dictating the variation in the power output, thrust, and torque. When the turbines are in the wind farm arrangement there is an approximate loss of 5% in power output compared to the cumulative power ideally obtained by the same number of isolated turbines [22].

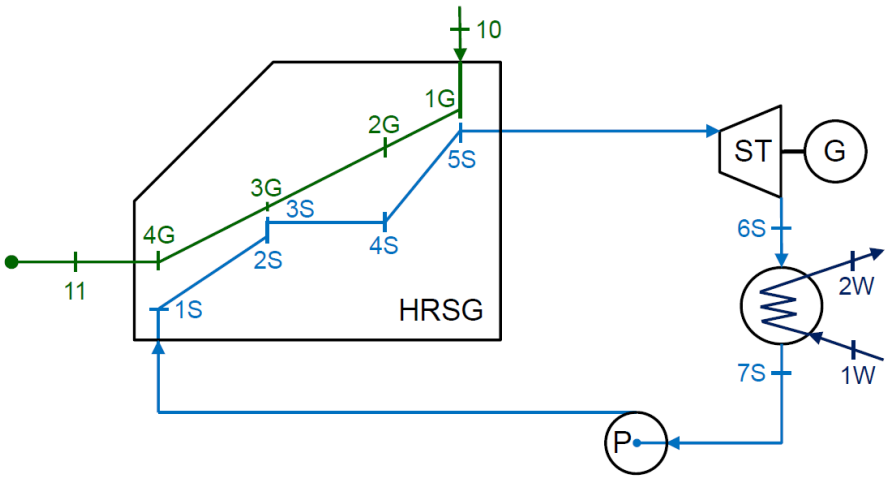

Figure 3.12. Steam plant layout model in the HRSG arrangement [34].

WindT has been validated against the National Wind Technology Center (NWTC) WT_Perf computational code. WT_Perf has been certified by the USA National Renewable Energy Laboratory (NREL) [7].

3.1.4 Steam Power Plants

The reference plants analysed in this project include a conventional, steam cycle exploiting the heat of exhaust gas expelled by another cycle that works at higher temperature.

This combined cycle arrangement is obtained using a HRSG, not burning additional fuel, nor co-generating heat together with electricity for other processes. The current working model of the HRSG is a single-pressure arrangement (Figure 3.12) that is typical of small sized power plants.

In this arrangement, cold water is firstly pumped at high pressure to the HRSG inlet, then it is heated up by the counter-current flow of exhaust gases, it changes phase and it is super-heated to achieve a certain, suitable temperature. Finally, the working fluid is expanded in a turbine (generating electrical power) before to return to the liquid phase and at the initial temperature by means of a condenser.

A Cranfield University legacy, computer code called Steamomatch has been the starting point of the development process that led to the current model of the steam plant. During her PhD course, Giuseppina Di Lorenzo amended parts of the code focussing to the steam turbine and condenser routines [24]. The author, as complementary task of his Master by Research project, adapted the methodology described by Dechamps [23] and re-wrote entirely a single-

pressure, off-design routine producing a preliminary implementation of the mentioned methodology [68].

A joint effort by the MSc students Raquel Avila, Laura Vallejo Sanz, and Jon Freire in collaboration with the author re-wrote and improved the design of large parts of the code [3, 84, 34].

Finally, Karthik Yadiyal provided a further improvement (under the supervision of the author) in the convergence robustness of the single-pressure, off-design routine [87].

The water and steam properties are estimated according to the IAPWS industrial formulation [85], while the NASA model implemented in eAZEP (Section 3.1.1) is used for the hot gas properties. The heat exchangers LMTD design method is used at any working condition to model the HRSG and the condenser behaviour. The steam turbine is considered always chocked at off-design. Finally, the design-point solving process is direct (i.e. not iterative), whereas the off-design routine requires an iterative sequential strategy [87].

3.1.5 Conventional, Reference Power Plants

The reference power plants are combined cycles representative of the current technological state-of-the-art of the electric power generation sector. All simulations are undertaken at steady-state condition. The high-temperature cycle is simulated first and its results are the input of the low-temperature simulation code.

The high-temperature cycle is based on a gas turbine, single-shaft power plants. Specifically, two different layouts are modelled:

- a simple cycle gas turbine inspired by General Electric MS9001FA;
- a re-heat gas turbine based on the concept of Alstom GT26.

The model of the working fluid and power plant components, together with the solving strategy, are adopted from the eAZEP methodology (Section 3.1.1, [68]).

The off-design performance is calculated based on turbomachinery maps imported from Cranfield University legacy simulation code called Turbomatch [20] imposing mass and energy conservation and the same rotational speed.

The architecture of the low-temperature, steam turbine power plant fitted with a HRSG has been chosen in a single-pressure arrangement. This assumption is considered satisfactory to capture the main characteristics of the combined cycle performance without complicating too much the layout.

Moreover, in this way it has been possible to consistently use the same model described in Section 3.1.4.

A complete PFD showing the layout adopted for both power plants is offered in Figure 3.13 for the simple cycle, and 3.14 for the re-heat cycle.

3.2 Aviation Power Plants: Modules Integration

The contribution to the NEW Aero Engine Core concepts (NEWAC) project (a collaborative effort funded by the research and innovation European Framework 6 programme) allowed the author to complete the Techno-economic Environmental Risk Analysis (TERA) exercise with a practical experience of modules integration.

3.2.1 TERA for Aviation

After several years of development at Cranfield University, the TERA package for aviation is a reliable, flexible, multi-disciplinary design support tool to evaluate complex power plants at their early stage of appraisal [67, 64].

In particular, the name has been amended to TERA2020 to emphasise its contribution in the European Union programme "Climate Change Package 20-20-20" (Section 1.1) including additional modules developed by partner European Universities [66].

The complete NEWAC TERA2020 package has a rather complex algorithm (Figure 3.15) inherited from a previous project called Environmentally Friendly Aero Engine (VITAL). The algorithm provides also an approximate view of the data flow, that is of critical importance for integration.

Six modules include the overall capabilities of the tool. A brief description of their methodology will follow (for more details see [66]).

Performance Module

It is the fundamental module of the entire analysis and it starts the computational process. The mathematical modelling tool Propulsion Object-Oriented Simulation Software (PROOSIS)[3] for the Geared Turbofan with Counter-Rotating core for Short Range (GTCRSR) and Geared Turbofan with Active Core for Short Range (GTACSR) configurations has been used. For the Geared Turbofan Inter-Cooled for Long Range (GTICLR) the computational

[3] `http://www.proosis.com/index.php`

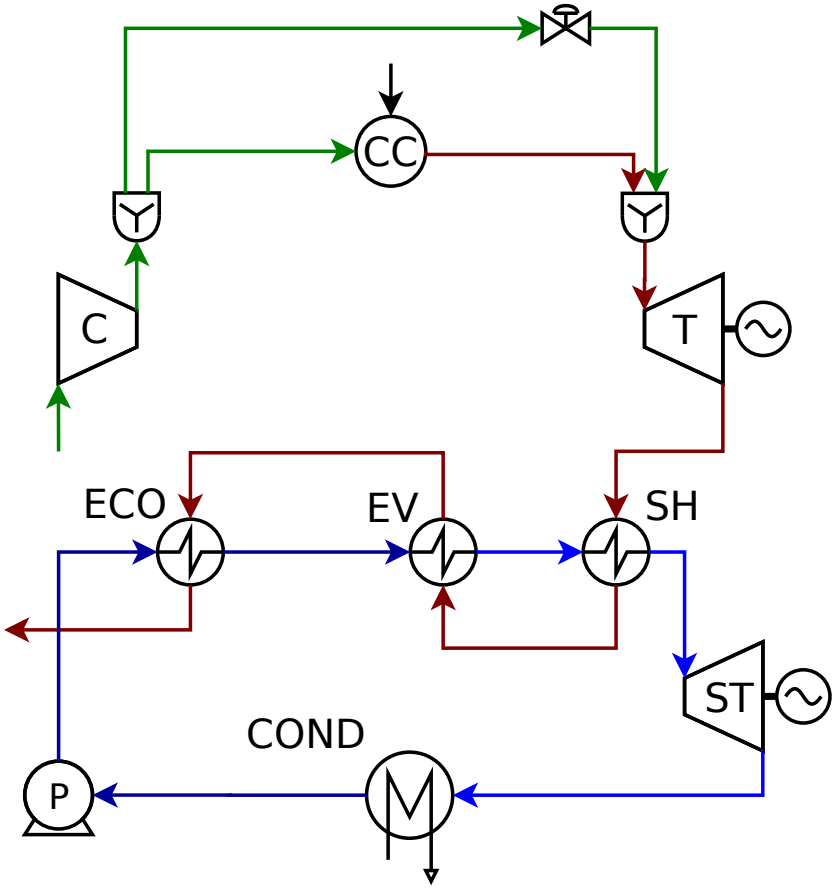

Figure 3.13. Process Flow Diagram of the conventional, combined cycle power plant based on a simple gas turbine cycle.

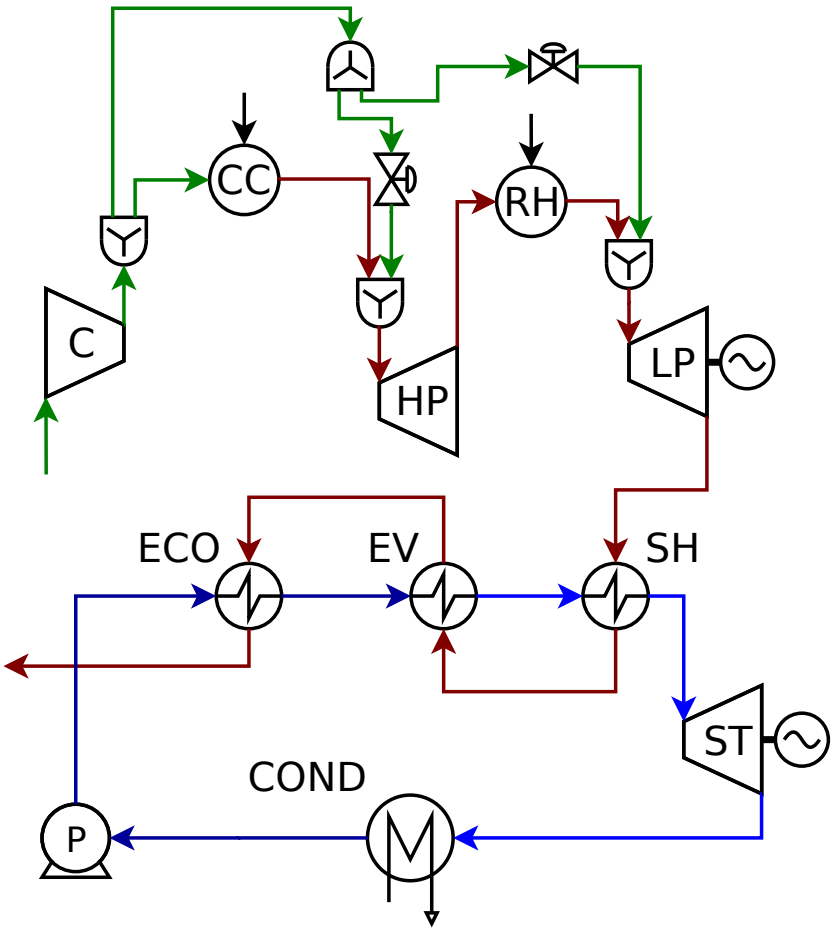

Figure 3.14. Process Flow Diagram of the conventional, combined cycle power plant based on a re-heat gas turbine cycle.

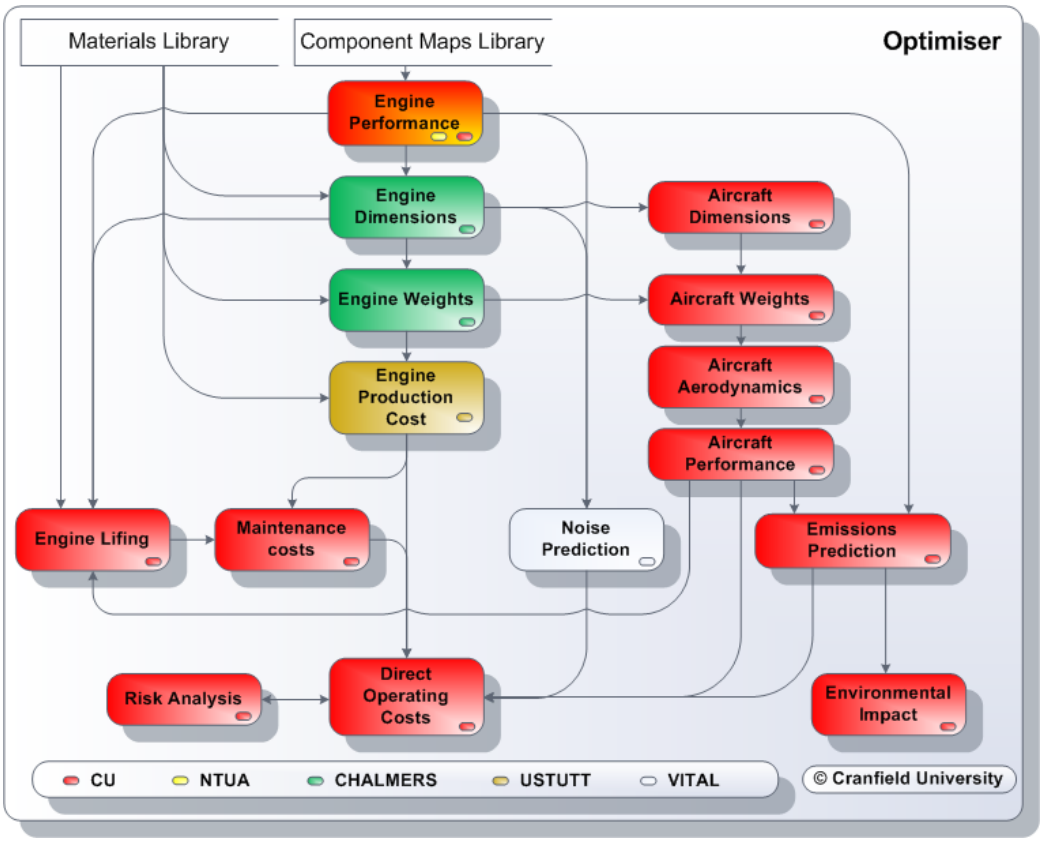

Figure 3.15. Structure and algorithm of the NEWAC TERA2020 package [66].

code called Environmental Assessment of Novel Propulsion Cycles (EVA) [51] has been adopted.

WeiCo Module

The compound name of the module is an abbreviation of weight and costs. Specifically, the weight and dimensions estimation is a contribution of Chalmers University and it is based on the gas path layout evaluated from performance data.

Instead, the University of Stuttgart contributed with a production cost sub-module using a component-by component approach.

Aircraft Module

This is another module developed by Cranfield University. It computes the fuel burnt in the entire flight mission taking into account its different phases.

It depends on both WeiCo and performance module as they provide the necessary inputs.

Noise Module

This module depends on performance and WeiCo data, too. It checks by means of a cumulative analysis the noise impact considering three crucial points: sideline, flyover, and cutback.

The program adopts International Civil Aviation Organization (ICAO) procedures and assesses if the power plant respects the certification limits. The module does not consider the additional noise produced by the heat exchange, auxiliary nozzle, and lean combustion noise although it includes the airframe noise.

Emissions and Environmental Impact Module

A combination of two pieces of software into a single unit originated the emissions module.

Proprietary prediction data and correlations for advanced combustors provided by the NEWAC Original Equipment Manufacturers (OEMs) were used to create a restricted version of this module.

However, another version based on conventional combustors with verified public domain information has been used to calculate the optimisation results. Both versions are dependent on the aircraft and performance data.

The module evaluates the overall production of NO_x, carbon dioxide, and water vapour to assess the Global Warming Potential (GWP) of the concept. A final comparison with the Committee on Aviation Environmental Protection (CAEP) limits completes the appraisal.

Economics Module

This last module computes the direct operating costs (DOC) over a time frame of thirty years. It uses data from all previous modules and takes into consideration many variables including the aircraft utilisation rate, inflation and fuel price, maintenance costs, and taxation for NO_x and noise emissions.

A lifing estimation routine (including creep, fatigue, and oxidation) is embedded to estimate the engine overhaul intervals. Furthermore, a Weibull distribution is used to take into account uncertainty in the failure of other components.

The relevant software is able to perform risk analyses but (because of the moderate computational effort required) it runs too slow for a practical

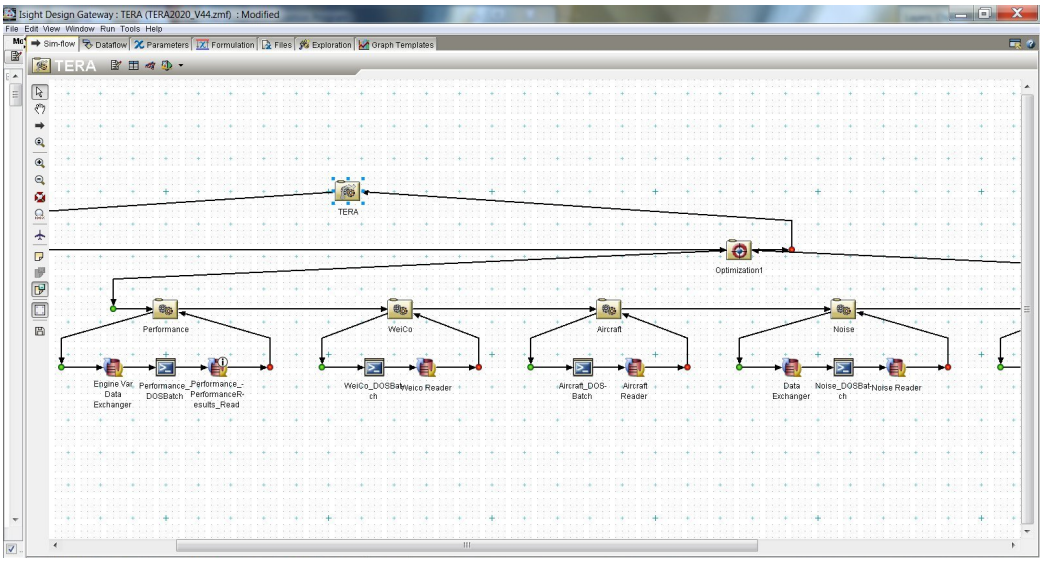

Figure 3.16. Screenshot of Simulia Isight showing part of the TERA2020 integrated structure.

application in a sensitivity analysis or optimisation. Thus, this feature is disabled while running the aforementioned tasks.

3.2.2 Integration Strategy

To carry out the integration of the TERA2020 modules, it has been adopted a commercial software called Simulia Isight[4] able to explore the design space with an optimiser.

The relevant methodology is quite simple. A number of tasks, one for each module, are wired together and executed in turn under the control of an optimiser (Figure 3.16). The initialisation of the calculation procedure is operated by a data exchanger (not visible in the picture). Every task-module runs the corresponding executable file and communicates with the other modules using one or two data exchangers.

To implement in Isight the framework, it has been necessary to create a set of Microsoft Windows batch files to automatically load the correct input files regarding the configurations under investigation and harmonise the file system structure with the internal representation of the relevant Isight project.

Moreover, the amendment of some data exchangers has been necessary to take into account the specific variables of the configurations to be assessed.

[4] `http://www.3ds.com/products/simulia/portfolio/isight-simulia-execution-engine/overview/`

The update of Isight data exchangers has been operated both with the point-and-click interface and modifying directly its behaviour writing code in Java computer language. This last task has been necessary to select the correct flight mission phase, in the aircraft module, while handling the additional variables.

The integration process allowed the update of modules (i.e. WeiCo and economic) with its relevant testing and bug fixing.

Chapter 4

Results

The present chapter will present the following results:

- the novel *aircraft propulsion* cycles developed in the NEW Aero Engine Core concepts (NEWAC) project;
- the conventional, combined cycle, power plants considered as a reference;
- the Carbon Capture and Storage (CCS) concepts;
- the gas turbine nuclear power plants;
- the steam cycle model (the bottoming cycle of the combined cycle arrangements);
- the Supercritical Water-cooled Reactor (SCWR).

4.1 Aircraft Propulsion Power Plants

4.1.1 GTCRSR Concept

The study of the Geared Turbofan with Counter-Rotating core for Short Range (GTCRSR) concept started comparing the performance over the flight mission of the counter-rotating core engine with a conventional one working at the same design-point. Although a benefit of the advanced configuration is observed (Figure 4.1), there is not a large performance improvement (e.g., 1.5% reduction in the block fuel).

The optimised configuration to minimise the block fuel burnt shows much better results with a reduction of almost 7.3% of the optimised parameter,

Parameter	% Deviation
Block Fuel Burn	-1.50
Aircraft Max TO Weight	-0.44
Direct Operating Cost / Year	-0.79
D_p/F_{oo} NO_x CAEP-6 Limit Fraction	0.81
Block Global Warming Potential	-1.21
Plant Production Cost	-5.26

Figure 4.1. Comparison of the performance over an entire flight mission between a conventional and a counter-rotating core engine sharing the same nominal design-point [66].

Parameter	% Deviation
Block Fuel Burn	-7.31
Engine Nacelle Diameter	-6.45
Engine Nacelle Length	-6.54
Aircraft Max TO Weight	-3.05
Direct Operating Cost / Year	-3.36
D_p/F_{oo} NO_x CAEP-6 Limit Fraction	10.67
Block Global Warming Potential	-2.36
Plant Production Cost	-8.91

Figure 4.2. Parameter deviation from the reference, conventional engine of the GTCRSR power plant optimised to minimise the block fuel burnt [66].

a reduction in the operating and production costs, and its Global Warming Potential (GWP). Only the NO_x emissions show an increase (Figure 4.2).

The optimised cycle has a smaller total and core mass flow rate, a lower bypass pressure ratio, and a higher booster and high pressure compressor pressure ratio, with a higher cooling mass flow for the high pressure turbine.

A design-space study in the neighbourhood of the optimal design-point has been performed to give some insight into the optimised engine (e.g., Figure 4.3).

4.1.2 GTACSR Concept

This study extended a previous one still concerning the Geared Turbofan with Active Core for Short Range (GTACSR) configuration [65]. Considering the

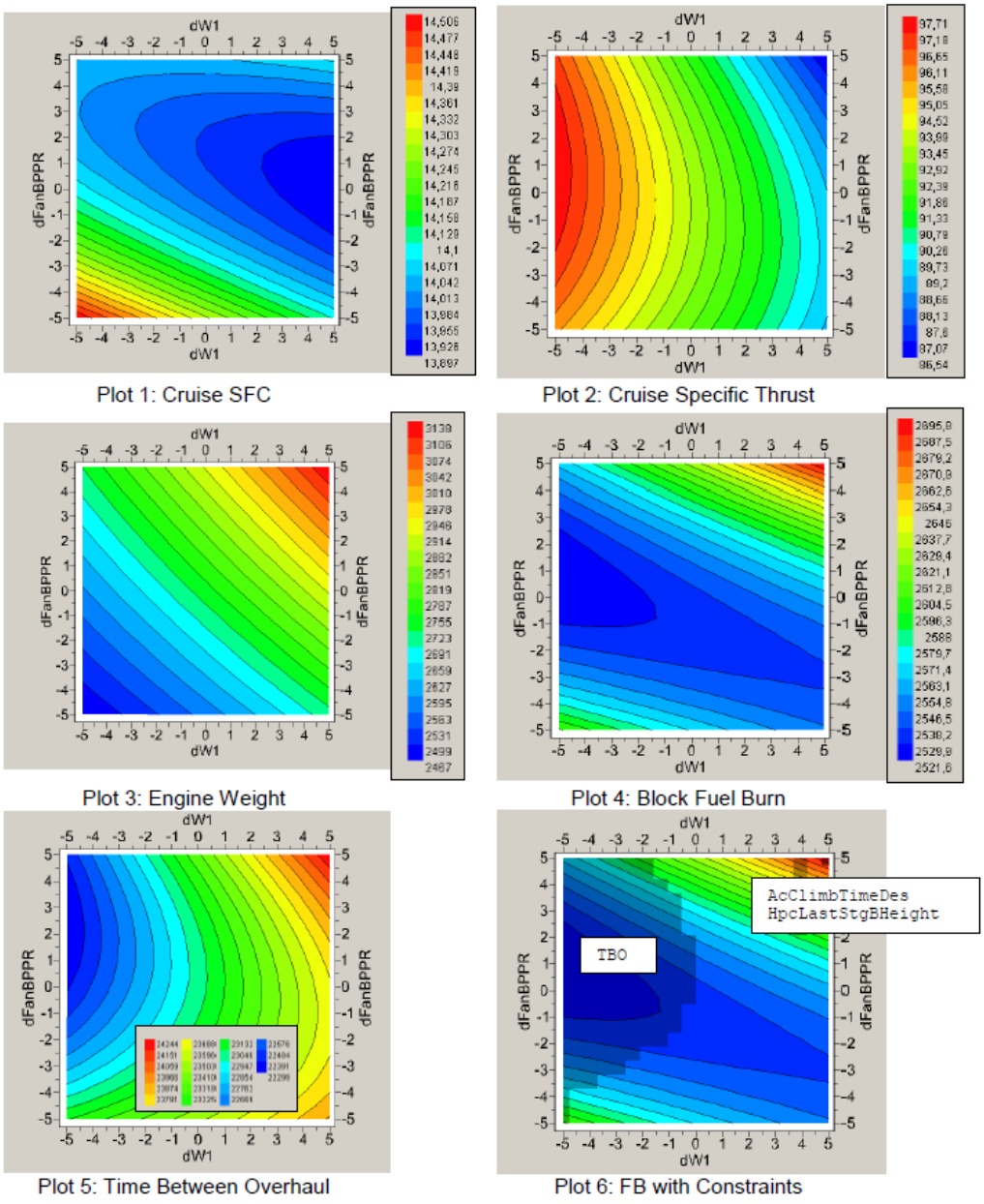

Figure 4.3. Contour plots for the inlet mass flow (dW1) and fan bypass pressure ratio (dFanBPPR) variation in the neighbourhood of the optimised design-point of the GTCRSR concept [66].

Parameter	Changes of GTACSR2 Block fuel optimum Relative to Nominal (%)	GTACSR2 Block fuel optimum
Total inlet mass flow	-18	177.23 kg/s
Core inlet mass flow	-23	12.68 kg/s
Fan pressure ratio	-6	1.49 (Outer Fan PR)
IPC pressure ratio	22	3.2
HPC pressure ratio	-30	10.32
Active Cooling Air Cooler effectiveness	-29	0.39
Active Cooling Air Cooler hot (air) stream mass flow rate	2	0.21
Total Block fuel	-6.3	2423.6 kg

Figure 4.4. Exchange rates and absolute values of design parameters for the GTACSR2 concept [66].

original GTACSR as a reference (called GTACSR1), the overall pressure ratio of the power plant was increased by 10% split between low and high pressure compressor (GTACSR2 concept). The design-point of the compressors has been changed to compensate a reduction in thrust.

The optimisation analysis (aimed to minimise the block fuel burnt) have shown a similar configuration compared to the reference power plant optimised case, with a reduction of just 2% in the block fuel burnt. This reduction, compared to the nominal, reference power plant accounts for 6.3% (Figure 4.4). The main constraint to optimise further the concept was the minimum height of the high pressure compressor blade (Figure 4.5).

Also in this case, an exploration of the design space around the optimal design-point has been undertaken, and a further sensitivity analysis of the optimised concept to small variations of the engine parameters has been performed [66].

4.1.3 GTICLR Concept

A large set of investigations are carried out for the Geared Turbofan Inter-Cooled for Long Range (GTICLR) concept.

An initial recalibration of the nominal Direct Drive Inter-Cooled for Long Range (DDICLR) concept has been operated according to new information supplied by a NEWAC Original Equipment Manufacturer (OEM) partner. The GTICLR concept is derived by the DDICLR and shows a reduction of 2.2% of block fuel at the nominal design [66]. Then, the GTICLR has been resized to match a time to height of 22.5 min and a Federal Aviation

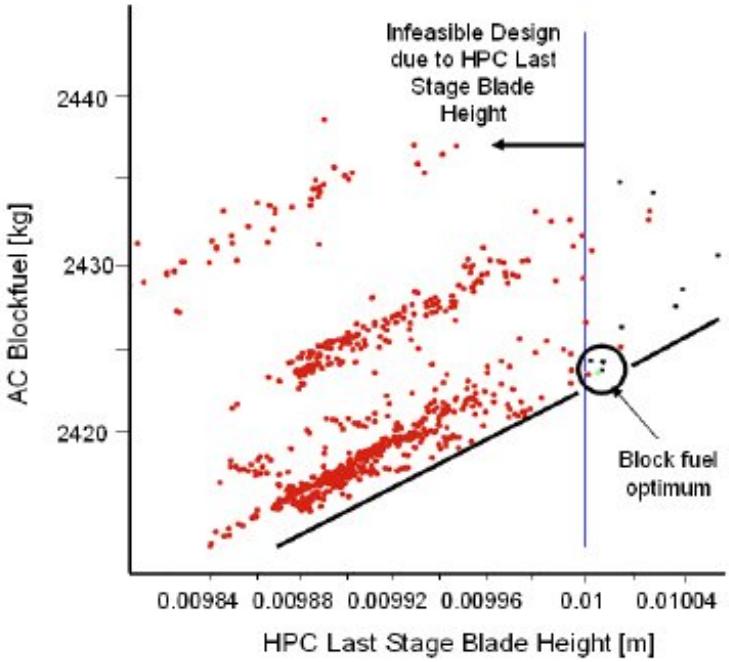

Figure 4.5. Optimisation study to minimise the active core (AC) block fuel varying the high pressure compressor (HPC) blade height in a GTACSR2 concept [66].

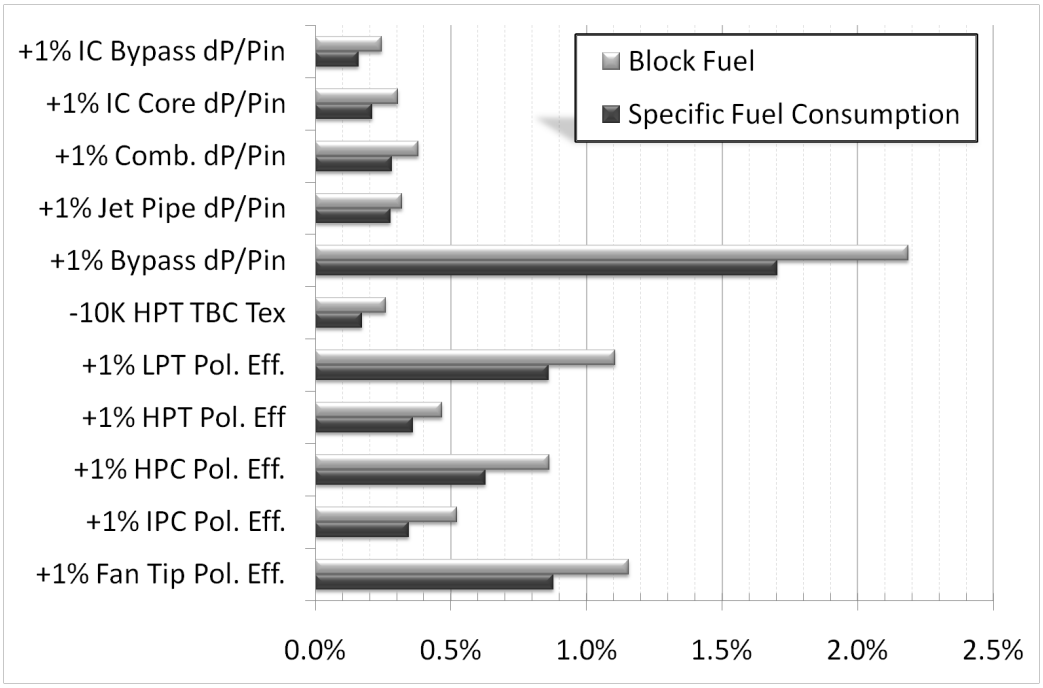

Figure 4.6. Sensitivity analysis of the resized GTICLR concept [66].

Regulation (FAR) take-off distance of 2.5 km. A further improvement in the block fuel burnt of 2.5% has been achieved thanks to the resizing process.

Furthermore, the resized nominal configuration design space has been explored extensively varying the following parameters:

- ideal jet velocity ratio,
- intercooler mass flow ratio,
- overall pressure ratio,
- overall pressure ratio split exponent n,
- fan mass flow,
- intercooler effectiveness at mid-cruise,
- intercooler effectiveness at take-off.

Subsequently, it has been performed a sensitivity analysis of the same resized engine design to appreciate the effect of a number of parameters on the block fuel burnt and the specific fuel consumption (Figure 4.6).

The detrimental effect on the block fuel of the blade height at last stage of the high pressure compressor has been calculated and taken into account for the optimisation studies.

Finally, two sets of the mentioned studies to minimise the block fuel burnt have been carried out: one at fixed thrust levels (Figure 4.7) and the other at fixed customer requirements (Figure 4.8).

Parameter	Units	Range	Resized GTICLR (M49)	Optimal (w/o HPC efficiency penalty)	Optimal (with HPC efficiency penalty)
Fan inlet mass flow (@ TOC)	[kg]	420 ... 560	431.7	559	539.5
Overall pressure ratio (@ TOC)	[-]	70 ... 103	79.5	94.7	83.9
Bypass ratio (@ TOC)	[-]	N/A	11.16	14.35	13.9
Fan tip pressure ratio (@ TOC)	[-]	1.38 ... 1.70	1.589	1.43	1.45
IPC pressure ratio (@ TOC)	[-]	N/A	4.72	3.95	3.13
HPC pressure ratio (@ TOC)	[-]	N/A	12.7	19.7	20.2
Pressure ratio split exponent n (@ TOC)	[-]	0.3 ... 0.45	0.435	0.360	0.337
HPT Blade TBC External Surface Temperature (@ TOC)	[K]	1100 ... 1200	1165	1165	1158
Ideal jet velocity ratio (@ TOC) (@ Mid-Cr)	[-]	0.6 ... 0.8 N/A	0.681 0.825	0.684 0.826	0.683 0.827
Intercooler effectiveness (@ Mid-Cr)	[%]	50 ... 70	60.7	58.6	58.8
Intercooler effectiveness (@ TO)	[%]	60 ... 75	72.1	69.1	68.3
Intercooler mass flow ratio (@ TOC)	[-]	1.00 ... 1.5	1.35	1.13	1.13
Business case block fuel	[kg]	N/A	27125	26370	26455
Business case block fuel (corrected)	[kg]	N/A	27125	26595	26455
Specific fuel consumption (@ Mid-Cr)	[g/(kN*s)] [lb/hr/lbf]	N/A	14.39 508	13.85 0.489	13.87 490
Time to height	[min]	N/A	22.5	22.8	23.0
FAR take-off distance	[m]	N/A	2500	2420	2430
Maximum intercooler auxiliary nozzle area variation	[%]	N/A	32.0	31.7	27.9
HPC last stage blade height	[mm]	N/A	14.6	11.1	13.0
Engine weight	[kg]	N/A	6310	7720	7690
Stage count	[-]	N/A	1-7-9-2-4	1-6-10-2-5	1-5-11-2-5
Production cost	[k€]	N/A	5150	5825	5860

Figure 4.7. Results for the resized GTICLR concept optimised at fixed thrust for minimum block fuel burnt [66].

Parameter	Units	Range	Resized GTICLR (M49)	Optimal (w/o HPC efficiency penalty)	Optimal (with HPC efficiency penalty)
Fan inlet mass flow (@ TOC)	[kg]	420 ... 560	431.7	544	532
Overall pressure ratio (@ TOC)	[-]	70 ... 103	79.5	103	89.8
Bypass ratio (@ TOC)	[-]	N/A	11.16	13.63	13.71
Fan tip pressure ratio (@ TOC)	[-]	1.38 ... 1.70	1.589	1.44	1.46
IPC pressure ratio (@ TOC)	[-]	N/A	4.72	4.04	3.86
HPC pressure ratio (@ TOC)	[-]	N/A	12.7	20.9	18.9
Pressure ratio split exponent n (@ TOC)	[-]	0.3 ... 0.45	0.435	0.359	0.362
HPT Blade TBC External Surface Temperature (@ TOC)	[K]	1100 ... 1200	1165	1180	1170
Ideal jet velocity ratio (@ TOC) (@ Mid-Cr)	[-]	0.6 ... 0.8 N/A	0.681 0.825	0.673 0.818	0.676 0.827
Intercooler effectiveness (@ Mid-Cr)	[%]	50 ... 70	60.7	59.2%	56.9%
Intercooler effectiveness (@ TO)	[%]	60 ... 75	72.1	72.1%	67.0%
Intercooler mass flow ratio (@ TOC)	[-]	1.00 ... 1.5	1.35	1.19	1.15
Business case block fuel	[kg]	N/A	27125	26335	26335
Business case block fuel (corrected)	[kg]	N/A	27125	26600	26445
Specific fuel consumption (@ Mid-Cr)	[g/(kN*s)] [lb/hr/lbf]	N/A	14.39 508	13.88 490	13.95 492
Time to height	[min]	N/A	22.5	22.5	22.3
FAR take-off distance	[m]	N/A	2500	2480	2480
Maximum intercooler auxiliary nozzle area variation	[%]	N/A	32.0	40.0%	27.3%
HPC last stage blade height	[mm]	N/A	14.6	10.8	12.0
Engine weight	[kg]	N/A	6310	7570	7435
Stage count	[-]	N/A	1-7-9-2-4	1-6-11-2-5	1-6-10-2-5
Production cost	[k€]	N/A	5150	5825	5665

Figure 4.8. Results for the resized GTICLR concept optimised at fixed customer requirements for minimum block fuel burnt [66].

4.2 Conventional Combined Cycle Power Plants

Two, combined cycle, conventional power plants have been selected as baseline to compare the performance of the novel concepts. Section 3.1.5 provides more details on the modelling assumptions and limitations.

4.2.1 Design-point results

In the industrial world, the combined cycle configuration of both the power plants considered in this section is almost always based on a multi-pressure level steam cycle. This is confirmed also by the data available in the scientific literature [1]. Hence, a direct comparison of the combined cycle performance obtained by the simulation to the literature data will not allow a satisfactory judgement on the model soundness. This is motivated by the significant difference between the performance of a single-pressure and a multi-pressure combined cycle power plant.

Consequently, it is deemed sensible to validate in the first instance the model of the gas turbine cycle alone to perform a precise assessment of the model accuracy. When the high temperature cycle validation has proven successful, it is possible to analyse the combined cycle results starting from a solid foundation.

A list of the results obtained for the simple cycle gas turbine engine is presented in Table 4.1 where it is offered a comparison (in terms of percentage deviation) with a scientific publication [1]. A similar list of parameters for the re-heat cycle is summarised in Table 4.2.

The simulation of high temperature cycles shows satisfactory results: all quantities describing the engine performance and available for validation exhibit a deviation within one per cent.

Therefore, the design-point results for the *single-pressure* level, combined cycle power plants are compared with the open literature data [1]. Table 4.3 shows the performance of the plant based on the simple combined cycle (inspired by General Electric MS9001FA) including also the input parameters of the steam, low temperature cycle. A similar table has been created for the combined cycle arrangement with re-heat (based on Alstom GT26): Table 4.4.

As mentioned above, the difference in the performance between the simulated combined cycle and the literature data are motivated by the different layout considered for the low temperature cycle. On the other hand, the results appear coherent from a theoretical point of view considering that the data in the literature refer to a steam cycle with triple pressure level and re-heat against the simulated single pressure case.

Table 4.1. Design-point parameters of the conventional, *simple* cycle, gas turbine, power plant model. Input data and deviations are compared with the specified literature source.

Parameter	Value	Deviation
Design-point ambient temperature	298.15 K	input
Design-point ambient pressure	1.013 bar	input
Design-point inlet mass flow [1]	641 kg/s	input
Compressor pressure ratio [1]	17.0	input
Combustor outlet temperature	1600 K	input
Combustor pressure efficiency	97%	input
Compressor polytropic efficiency	88%	input
Turbine polytropic efficiency	90%	input
Turbomachinery mechanical efficiency	0.99	input
Electric generator efficiency	0.98	input
Electric power output [1]	255.06 MW	0.21%
Overall thermal efficiency [1]	37.20%	0.81%
Gas turbine exhaust temperature [1]	869.72 K	0.65%

Table 4.2. Design-point parameters of the conventional, *re-heat* cycle, gas turbine, power plant model. Input data and deviations are compared with the specified literature source.

Parameter	Value	Deviation
Design-point ambient temperature	298.15 K	input
Design-point ambient pressure	1.013 bar	input
Design-point inlet mass flow [1]	650 kg/s	input
Compressor pressure ratio [1]	33.9	input
Combustor outlet temperature	1550 K	input
Re-heater outlet temperature	1590 K	input
Combustor pressure efficiency	97%	input
Re-heater pressure efficiency	97%	input
Compressor polytropic efficiency	87.6%	input
High-pressure turbine polytropic efficiency	89%	input
Low-pressure turbine polytropic efficiency	89%	input
Turbomachinery mechanical efficiency	0.99	input
Electric generator efficiency	0.98	input
Electric power output [1]	285.93 MW	0.82%
Overall thermal efficiency [1]	38.45%	0.92%
Low-pressure turbine exhaust temperature [1]	889.66 K	0.05%

Table 4.3. Design-point parameters of the conventional, combined cycle power plant model inspired by General Electric MS9001FA.

Parameter	Value	Reference [1]
Low temperature cycle arrangement	single pressure level	triple pressure with re-heat
Steam turbine inlet pressure	28 bar	input
Condenser pressure	4 kPa	input
Evaporator pinch point temperature difference	20 K	input
Superheater pinch point temperature difference	40 K	input
Steam plant mass flow	98.0 kg/s	not available
Steam turbine overall efficiency	85%	input
Pump overall efficiency	78%	input
River water pressure	1.013 bar	input
Condenser river water inlet temperature	13 °C	input
Condenser river water outlet temperature	23 °C	input
Steam turbine power output	112.3 MW	141.8 MW
Combined cycle power output	367.4 MW	390.8 MW
Combined cycle thermal efficiency	53.9%	56.7%

Table 4.4. Design-point parameters of the conventional, combined cycle power plant model inspired by Alstom GT26.

Parameter	Value	Reference [1]
Low temperature cycle arrangement	single pressure level	triple pressure with re-heat
Steam turbine inlet pressure	30 bar	input
Condenser pressure	5.0 kPa	4.4 kPa
Evaporator pinch point temperature difference	20 K	input
Superheater pinch point temperature difference	40 K	input
Steam plant mass flow	105.3 kg/s	not available
Steam turbine overall efficiency	85%	input
Pump overall efficiency	78%	input
River water pressure	1.013 bar	input
Condenser river water inlet temperature	13 °C	input
Condenser river water outlet temperature	23 °C	input
Steam turbine power output	119.4 MW	not available
Combined cycle power output	405.3 MW	424.0 MW
Combined cycle thermal efficiency	54.9%	58.3%

4.2.2 Off-design results

An estimation of the power plant off-design performance has been obtained for

- different values of ambient temperature T_{a},
- part-load operation.

Effect of the ambient temperature Concerning the effect of the ambient temperature on the combined cycle performance, it appears clearly that the thermal efficiency (Figure 4.9) is optimal at design-point conditions.

At lower ambient temperature, although the efficiency of the high temperature cycle improves and there is an increase of mass flow at the inlet of the low temperature cycle, there is less heat available for the Heat Recovery Steam Generator (HRSG). In fact, the gas turbine exhaust temperature is lower, determining a reduction in the efficiency of the low temperature cycle.

At higher ambient temperature, the gas turbine cycle efficiency is lower and the smaller mass flow of flue gas at the inlet of the low temperature cycle dictates a reduction of the steam operating pressure and, in turn, of the steam plant efficiency.

Instead, the combined cycle power output reduces almost linearly with ambient temperature (Figure 4.10). This behaviour can be explained exactly considering the effect of the previously discussed quantities on the high and low temperature cycle power output.

Part-load operation Combined cycle part-load performance are highly dependent on the control logic of the gas turbine engine that will "drive" the low temperature cycle operating point [48]. The simple cycle gas turbine power output can be governed using compressor variable inlet guide vanes (VIGV) and reducing the firing temperature. The re-heat cycle has one additional degree of freedom allowing also the variation of the re-heater outlet temperature.

The use of compressor VIGVs to reduce the gas turbine cycle inlet mass flow at constant combustor outlet temperature is the most efficient way to reduce its power output, but the resulting increase of the flue gas temperature is unacceptable for the HRSG and the steam turbine. Thus, a reduction of the firing temperature is initially sought although at lower combustion chamber temperatures, an undesired steaming in the HRSG economiser may occur. Hence, when the outlet temperature of the economiser approaches the saturation conditions, the overall power output is reduced operating the

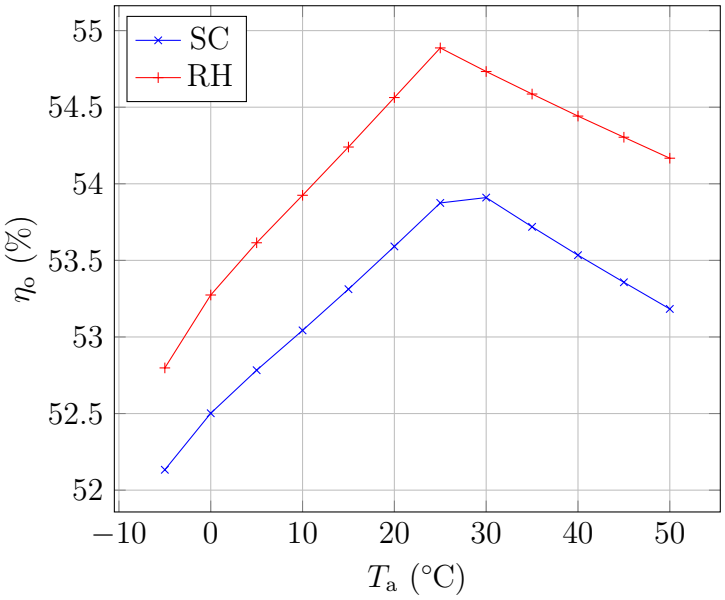

Figure 4.9. Conventional combined cycles overall efficiency η_o at different ambient temperature T_a conditions. Design-point is at $T_a = 25\,°C$. SC: simple, high temperature cycle; RH: re-heat, high temperature cycle.

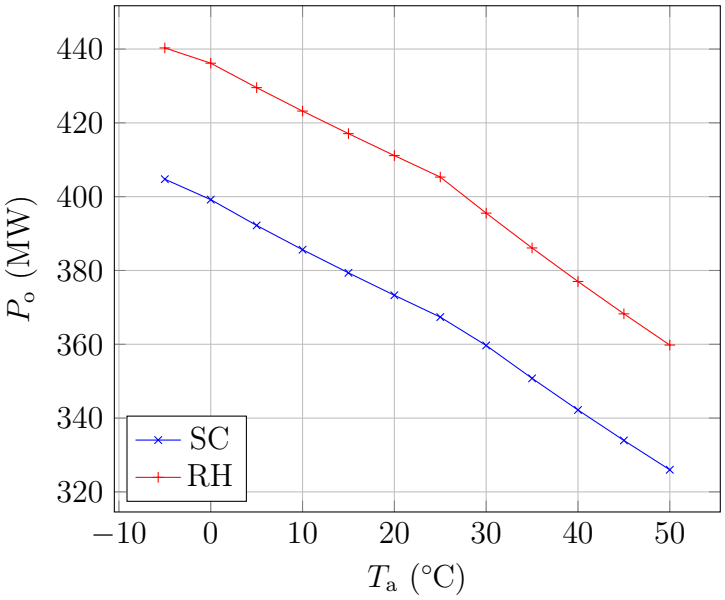

Figure 4.10. Conventional combined cycles power output P_o at different ambient temperature T_a conditions. Design-point is at $T_a = 25\,°C$. SC: simple, high temperature cycle; RH: re-heat, high temperature cycle.

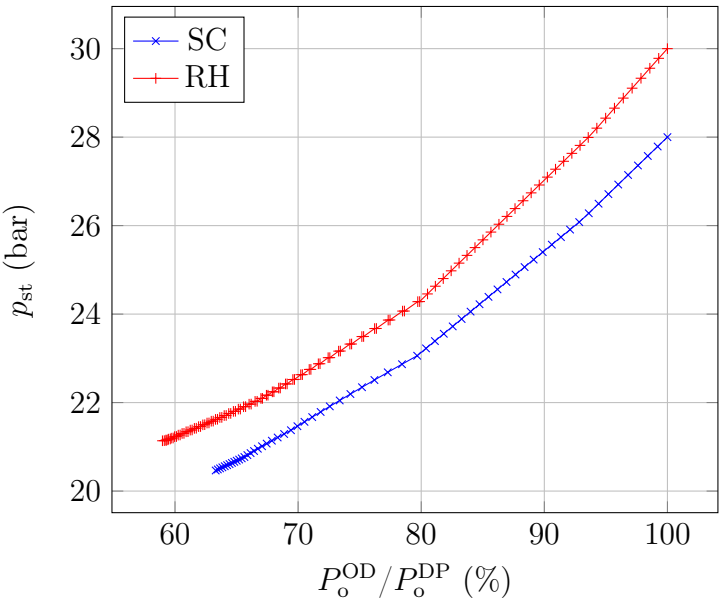

Figure 4.11. Conventional combined cycles inlet steam turbine pressure p_{st} reduction at part-load operation. SC: simple, high temperature cycle; RH: re-heat, high temperature cycle; P_o: power output; DP: design-point; OD: off-design.

compressor VIGVs that increases the sub-cooling temperature difference at the economiser outlet.

Following the previous general discussion, it is interesting to analyse, in the first instance, the relationship between the steam turbine inlet pressure (one of the main governing parameters of the low temperature cycle) and the power output reduction. Figure 4.11 shows quite clearly when a control strategy substitutes another in the high temperature cycle: this is indicated by a different trend in the steam plant pressure.

Considering the simple gas turbine cycle, after a gradual reduction of combustor outlet temperature to obtain an off-design power output 20% lower of the design-point figure, it is operated a variation of compressor VIGVs. On the other hand, the strategy for the re-heat power plant is more complicated. Similarly, until about 20% reduction of power output the re-heater firing temperature is reduced. However, afterwards the most efficient control strategy has proven to be a simultaneous reduction of the main combustor outlet temperature and compressor VIGV angle.

The superior performance of the more complicated re-heat combined cycle is shown in Figure 4.12 where the power reduction is represented against the off-design efficiency in relative terms. For example, with 30% reduction of

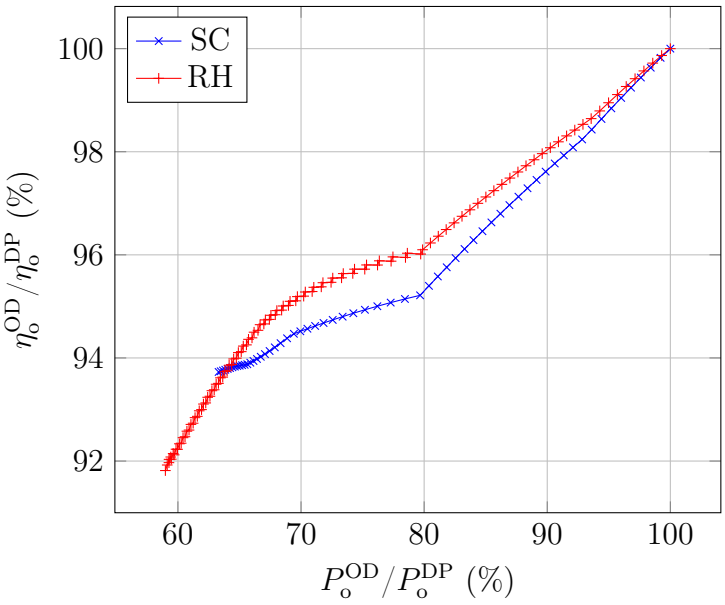

Figure 4.12. Conventional combined cycles overall efficiency η_o reduction at part-load operation. SC: simple, high temperature cycle; RH: re-heat, high temperature cycle; P_o: power output; DP: design-point; OD: off-design.

power output, the re-heat power plant retains more than 95% of its design-point efficiency. In the same conditions, the combined cycle based on a simple gas turbine has a relative off-design efficiency clearly below the 95% mark.

It is deemed interesting to conclude this section analysing the variation of the steam plant and the gas turbine exhaust mass flows. Both the conventional concepts considered show a linear trend of reduction in the steam power plant mass flow (Figure 4.13) with a negligible difference when the off-design control strategy changes.

On the contrary, the exhaust gas turbine mass flow is highly affected by the governing method adopted in the high temperature cycle. Figure 4.14 shows that changing the firing temperature has a minor effect on the exhaust mass flow, especially when compared to the clear reduction caused by the compressor VIGV control. The part-load performance of the re-heat combined cycle shows a peculiar trend of the mass flow reduction because of its combined control strategy.

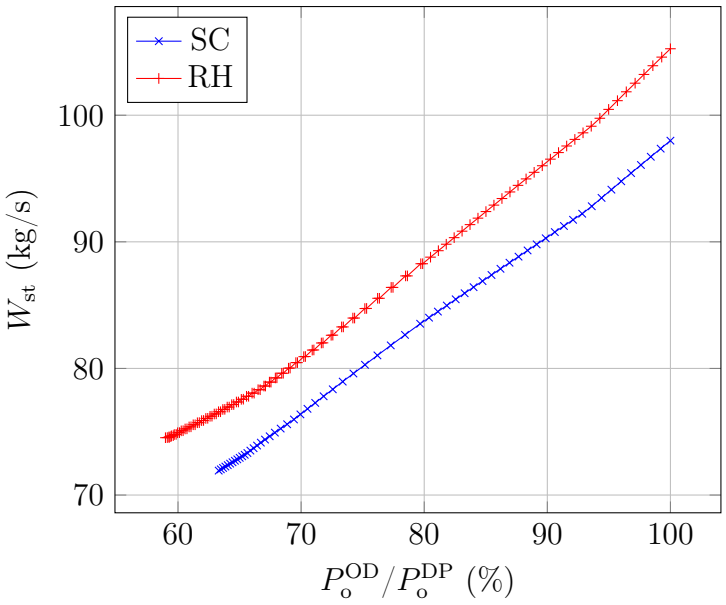

Figure 4.13. Conventional combined cycles steam cycle mass flow W_{st} reduction at part-load operation. SC: simple, high temperature cycle; RH: re-heat, high temperature cycle; P_o: power output; DP: design-point; OD: off-design.

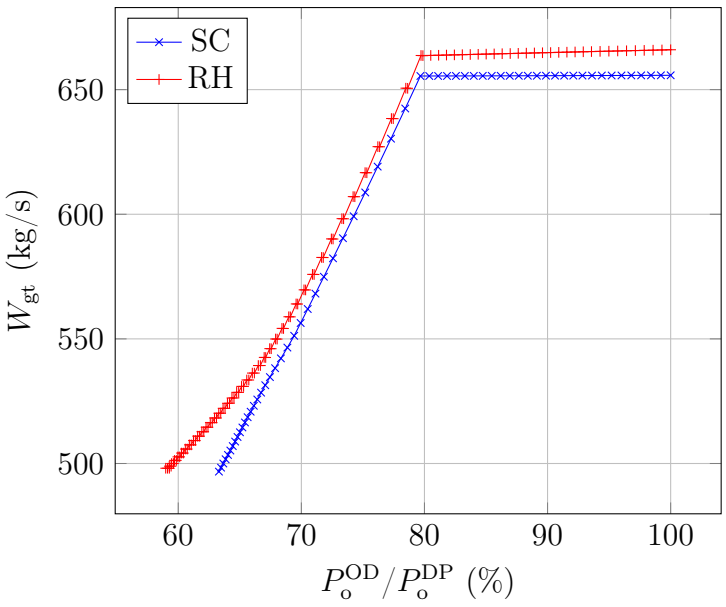

Figure 4.14. Conventional combined cycles gas turbine exhaust mass flow W_{gt} reduction at part-load operation. SC: simple, high temperature cycle; RH: re-heat, high temperature cycle; P_o: power output; DP: design-point; OD: off-design.

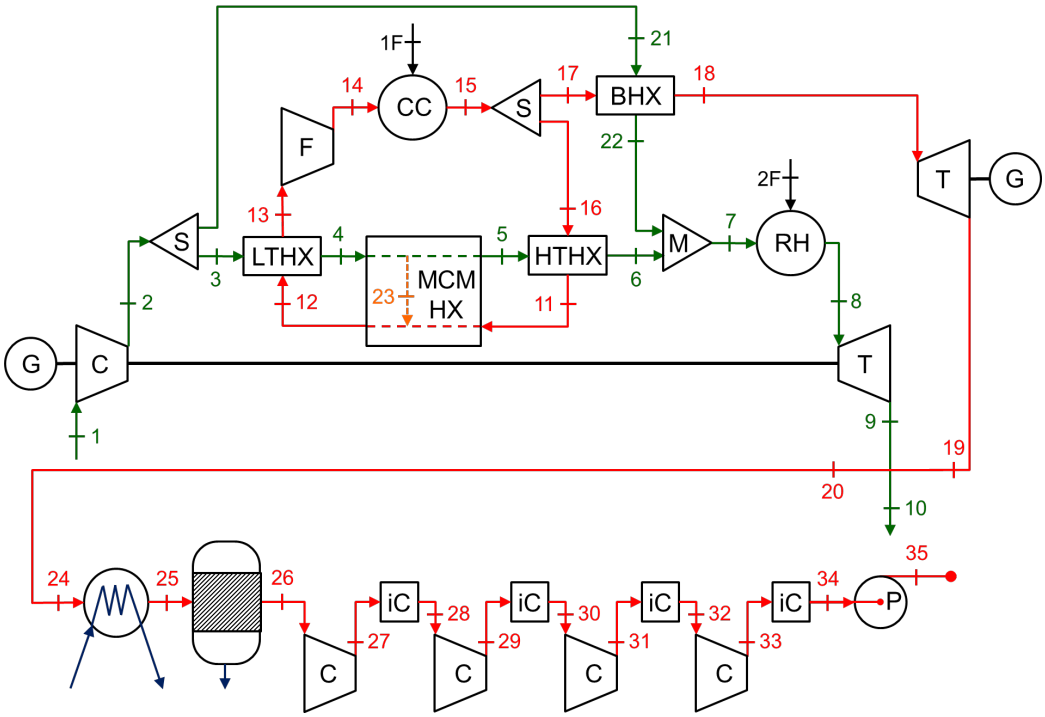

Figure 4.15. AZEP Process Flow Diagram modelled by the computer program eAZEP [34]. C: Compressor; S: Splitter; LTHX: Low Temperature Heat Exchanger; F: Recirculator Fan; CC: Catalytic Combustor; S: Splitter; HTHX: High Temperature Heat Exchanger; MCM: Mixed Conducting Membrane; BHX: Bleed Heat Exchanger; M: Mixer; T: Turbine; HRSG: Heat Recovery Steam Generator

4.3 Carbon Capture and Storage Concepts

4.3.1 Advanced Zero Emission Power Plant

The family of the Advanced Zero Emissions Power plant (AZEP) cycles has been modelled both at design-point and off-design in the AZEP 100% and AZEP 85% configuration with the computer program eAZEP (for more information, see Section 3.1.1). Figure 4.15 shows the Process Flow Diagram (PFD) implemented in eAZEP to obtain the results presented in this section.

AZEP 100%

In the AZEP 100% configuration the re-heater ("RH") is not present and, thus, stations 7 and 8 coincide.The power plant specifications of the AZEP 100% concept were inspired by the baseline, conventional, simple cycle gas turbine

Table 4.5. Design-point parameters of the AZEP 100% power plant model.

Parameter	Value
Inlet mass flow	640 kg/s
Compressor pressure ratio	17.0
Combustor outlet temperature	1570 K
Combustor pressure efficiency	99%
Compressor polytropic efficiency	84%
Turbine polytropic efficiency	88%
Turbomachinery mechanical efficiency	99.8%
Electric generator efficiency	98%
Heat exchangers pressure efficiency	98%
MCM pressure efficiency	99%
MCM minimum temperature	1173 K
MCM maximum temperature	1323 K
Exhaust gas loop mass flow rate	355.2 kg/s
Oxygen transferred by the MCM over total oxygen available	33.2%
Power output	168.833 MW
Overall thermal efficiency	27.79%

engine (Section 4.2) although the Combustor Outlet Temperature (COT) — station 15 of Figure 4.15 — has been set at a slightly lower value (1570 K against 1600 K) to reflect the different technological maturity level of the concept. The full set of design-point assumptions and main performance metrics is reported in Table 4.5. In the table are also included the parameters of the Mixed Conductive Membrane (MCM) reactor that have been carefully chosen to obtain its best performance.

The two main part-load control strategies mentioned for the conventional combined cycles were analysed — i.e. the "fuel-only" control varying the firing temperature and the mass flow control using VIGV.

However, additional control strategies were considered and applied to ensure that all the important process parameters of the cycle remain within their permissible limits. This is of particular importance in the case of the AZEP concepts because they require stringent operating conditions to allow the MCM to work effectively without quick degradation. The table presented in Figure 4.16 summarises the constraints of main AZEP components and limit the operating range.

The restraints related to the sulphur concentration in the sweep gas have not been taken into account in the present work. The reason for this choice is that keeping the sulphur concentration below the allowable limits

Process component	Constraint	Effect	Limit
Catalytic combustors	Minimum oxygen molar fraction	Performance loss and failure due to unstable and incomplete combustion	0.5 mol%
Catalyst in the catalytic combustors	Maximum sulphur concentration	Performance loss and failure due to sulphur poisoning	ppb range
Catalyst in the catalytic combustors	Maximum temperature gradients	Performance loss and failure due to thermal shocks	Depending on process conditions
GT compressor	*Maximum VIGV angle*	*Mass flow reduction by VIGVs*	*40%*
GT compressor	*Minimum surge margin*	*Performance loss and failure due to a sudden drop in pressure and detrimental aerodynamic pulsation*	*5%*
GT Turbine	*Cooling air fraction to GT turbine*	*Performance loss and failure due thermo-mechanical stresses*	*Depending on technology*
GT Turbine	*Maximum TET*	*Performance loss and failure due to thermo-mechanical stresses*	*1530K*
HTHX	Maximum temperature	Performance loss and failure due to thermo-mechanical stresses	1573K
HTHX	Maximum sulphur concentration	Performance loss and failure due to sulphur poisoning	Depending on process conditions
LTHX	Minimum temperature	Performance loss and failure due to thermo-mechanical stresses	673K
LTHX	Maximum sulphur concentration	Performance loss and failure due to sulphur poisoning	50 ppb
Dense membrane layers and porous support	Maximum temperature	Performance loss and failure due to thermo-mechanical stresses and chemical interaction	1323K (1050°C)
Dense membrane layers and porous support	Minimum temperature	Performance loss and failure due to thermo-mechanical stresses	1173K (900°C)
Dense membrane layers and porous support	Maximum sulphur concentration	Performance loss and failure due to sulphur poisoning	10 ppb
Dense membrane layers and porous support	Thermodynamic conditions with respect to membrane temperature, CO_2 and O_2 pressure in sweep gas	Performance loss and failure due to carbonate formation, oxidation and hydroxide formation	Depending on process conditions
Membrane modules and monolithic heat exchangers	Maximum total pressure difference	Performance loss and failure due to mechanical stresses	0.1 MPa

Figure 4.16. Operation and material constraints for the membrane-based combined cycle power plant. Constraints for the conventional power plant appear in italics [16].

is assumed to be duty of a fuel pre-treatment system, or alternatively, of a desulphurisation unit within the gas loop, which the current model of the plant does not include.

To the knowledge of the author, no control strategies aimed at ensuring that the MCM reactor works within permissible limits have been proposed so far in the literature. Therefore, reasonable assumptions from a physical standpoint were made and should be verified in terms of technological feasibility.

The metric adopted to control the correct working conditions of the MCM is the membrane hot inlet temperature (T_{11} in Figure 4.15). Considering the relevant limit showed in Figure 4.16 and the lumped approach adopted to model the behaviour of the MCM (Section 3.1.1), it is considered reasonable to set the following condition

$$T_{11} = 1330 \pm 3\,\mathrm{K} \tag{4.1}$$

There are two possible part-load control strategies to satisfy condition (4.1):

- variation of the firing temperature;
- variation of the mass flow rate in the flue gas loop to adjust its heat capacity.

Obviously, when the primary off-design control variable is the firing temperature ("fuel-only" control), the only possible choice between the above is to change the mass flow rate in the flue gas loop. eAZEP is able to automatically detect this situation and switch the control logic accordingly.

A number of simulations have shown very similar performance results while implementing each of the two MCM temperature control strategies. However, practical complications in adjusting the mass flow in the flue gas loop suggested to prefer the first choice, especially when compared to the simpler control of the fuel flow in the catalitic combustor. For this reason, the firing temperature is the default secondary control strategy chosen.

Additionally, other two controls were considered:

- pressure in the flue gas loop;
- excess of oxygen in the catalitic combustor.

Pressure in the flue gas loop At off-design conditions the main compressor operating point change according to its "running line" and works at different pressure ratio that determines a different value of pressure on the MCM feed side. The mechanical stress derived by the pressure difference on the feed and permeate side of the MCM can become unacceptable. Therefore, the pressure

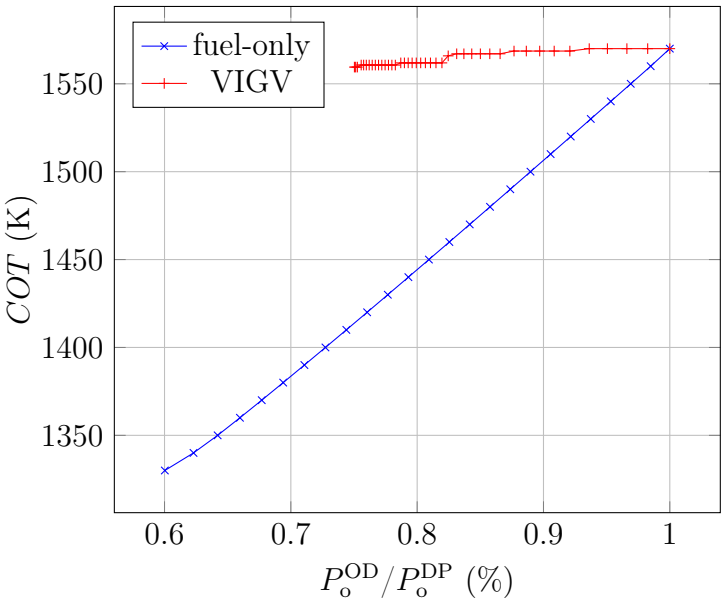

Figure 4.17. AZEP 100% off-design Combustor Outlet Temperature *COT* at part-load operation with fuel-only and mass flow control by means of Variable Inlet Guide Vanes (VIGV). P_o: power output; DP: design-point; OD: off-design.

in the flue gas loop must be adjusted to remove the mentioned pressure difference. This can be achieved operating on the splitter at the outlet of the combustor and controlling the recirculated mass flow. Although this strategy does not present any major problems for steady-state operation, it may be of interest the investigation of the power plant transient behaviour to identify potential problematic conditions (e.g. instability, resonance) related to this control.

However, unsteady simulations and analyses are beyond the scope of this work.

Excess of oxygen in the catalitic combustor Oxygen in the gas loop is transferred from the feed flow in the MCM to permit the oxidation of the natural gas in the combustor. A slight excess would guarantee a complete reaction of fuel avoiding the production of polluting species like carbon monoxide CO and Uncombusted Hydrocarbons (UHC).

The main results of the AZEP based gas turbine at part-load are shown in Figures 4.17 to 4.23. In the case of COT variation, the part load limit is applied when the combustor outlet temperature approaches the fixed membrane's hot temperature (1330 K), that is, at about 60% of the load.

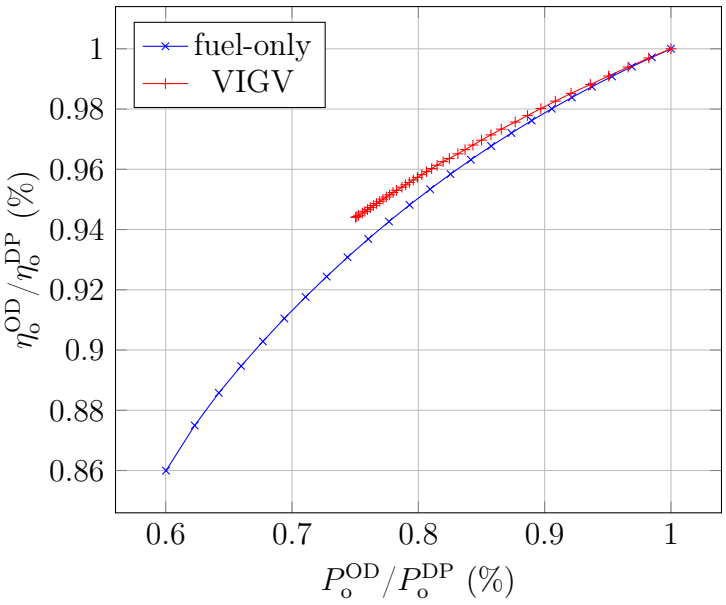

Figure 4.18. AZEP 100% overall efficiency η_o reduction at part-load operation with fuel only and mass flow control by means of Variable Inlet Guide Vanes (VIGV). P_o: power output; DP: design-point; OD: off-design.

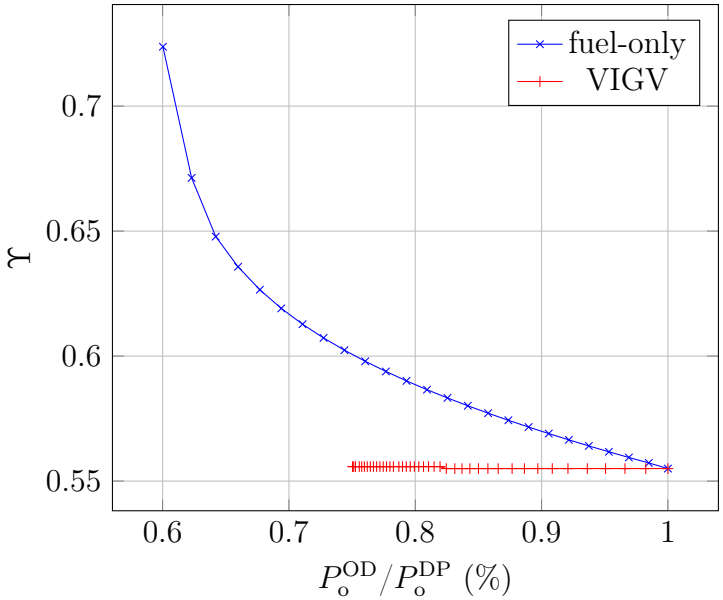

Figure 4.19. AZEP 100% fraction of the inlet mass flow rate in the flue gas loop Υ at part-load operation with fuel only and mass flow control by means of Variable Inlet Guide Vanes (VIGV). P_o: power output; DP: design-point; OD: off-design.

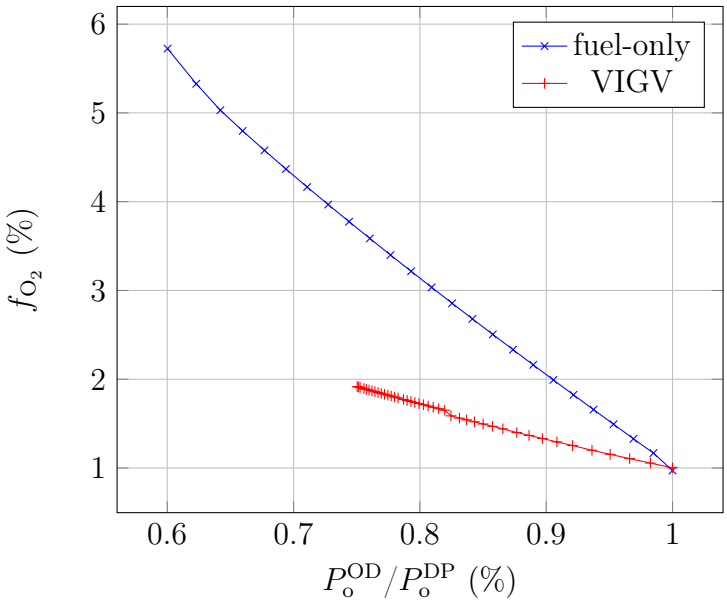

Figure 4.20. AZEP 100% mass fraction of oxygen at the outlet of the combustion chamber f_{O_2} at part-load operation with fuel only and mass flow control by means of Variable Inlet Guide Vanes (VIGV). P_o: power output; DP: design-point; OD: off-design.

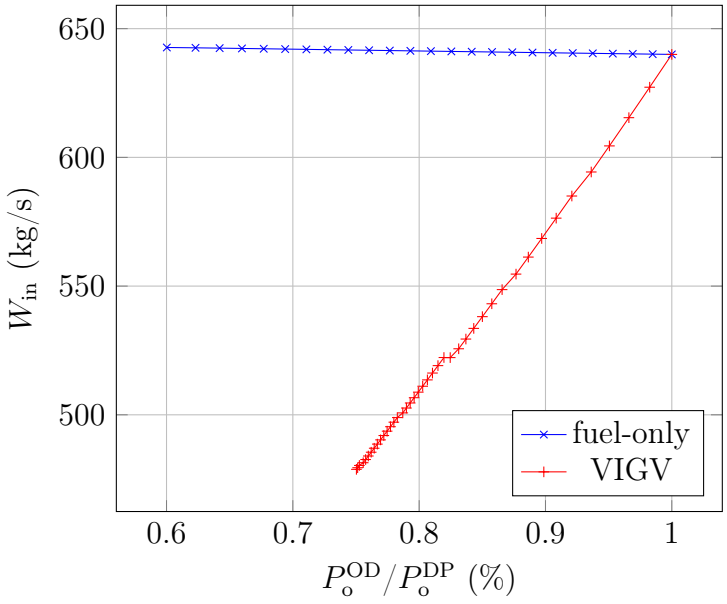

Figure 4.21. AZEP 100% inlet mass flow W_{in} at part-load operation with fuel only and mass flow control by means of Variable Inlet Guide Vanes (VIGV). P_o: power output; DP: design-point; OD: off-design.

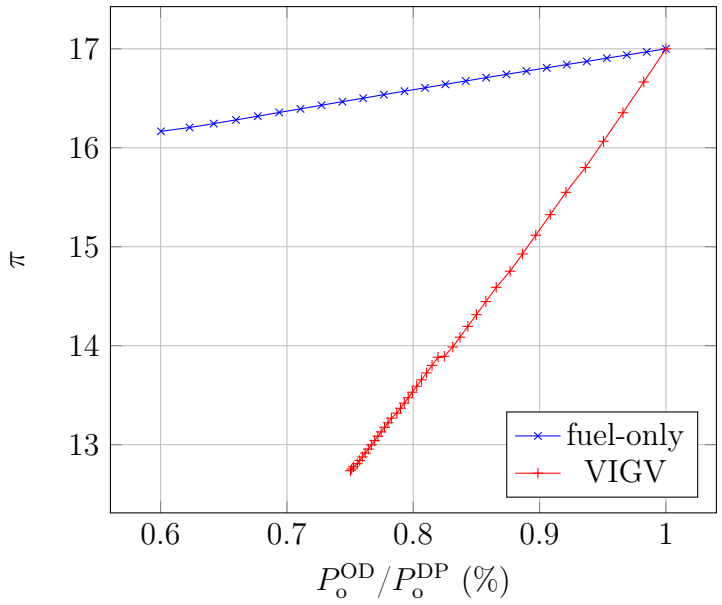

Figure 4.22. AZEP 100% compressor pressure ratio π at part-load operation with fuel only and mass flow control by means of Variable Inlet Guide Vanes (VIGV). P_o: power output; DP: design-point; OD: off-design.

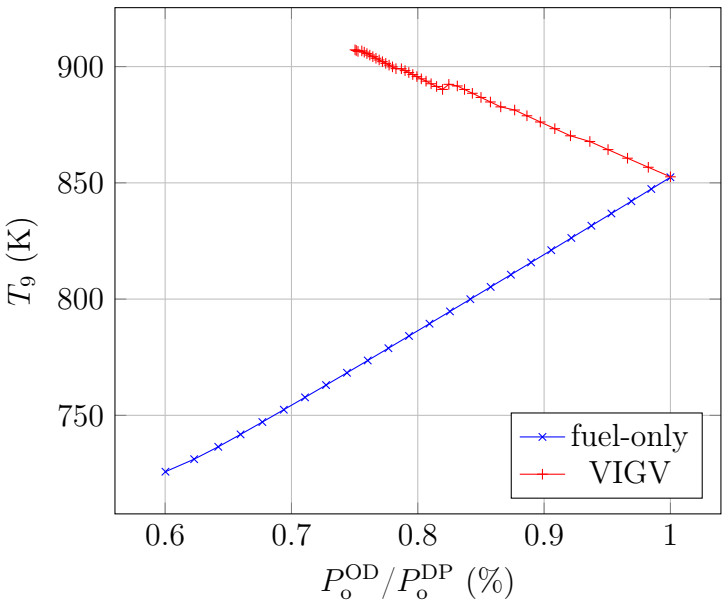

Figure 4.23. AZEP 100% turbine outlet temperature T_9 at part-load operation with fuel only and mass flow control by means of Variable Inlet Guide Vanes (VIGV). P_o: power output; DP: design-point; OD: off-design.

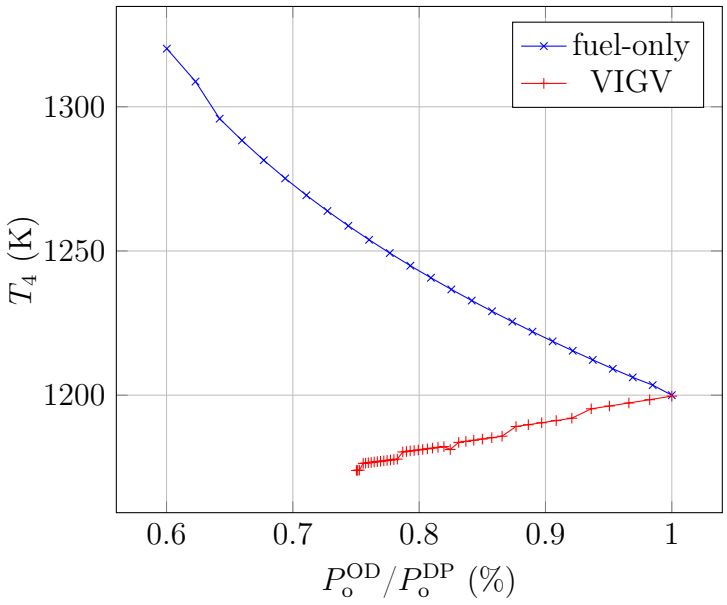

Figure 4.24. AZEP 100% MCM minimum temperature T_4 at part-load operation with fuel only and mass flow control by means of Variable Inlet Guide Vanes (VIGV). P_o: power output; DP: design-point; OD: off-design.

In the case of mass flow control with VIGV, the only modulation of the inlet mass flow is applied until the air turbine outlet temperature is too high and a reduction of COT is necessary. Even with this solution, the part load limit is reached when the stator angle is at its maximum, which occurs at about 75% of the load. The change of inclination detectable in the form of small drops of COT occurs when the mentioned control is introduced.

In both cases, the secondary control strategy is based on the variation of the mass flow rate in the flue gas loop to ensure that the optimal range of temperature for the membrane.

The results clearly show that the mass control strategy gives better performance but a narrower range of operation. With this strategy, the efficiency is higher at all load conditions and this is explainable by the higher maximum temperature reached in the cycle. The turbine outlet temperature is kept at its maximum value; therefore no degradation is expected in the bottoming steam cycle efficiency. In the fuel strategy instead, the exhaust temperature falls, causing a detrimental effect to the steam cycle performances, as well as more difficulties in controlling the steam temperature.

In the fuel-only control, the mass flow remains fairly constant, due to the small variation in the pressure ratio. Nevertheless, in the mass flow control there is a relatively large variation of mass flow and pressure ratio.

Analysing the MCM parameters it can be seen that the membrane minimum temperature is slightly decreasing below its minimum recommended value (by 10 degrees) when the mass flow control is applied. This temperature becomes constant when the COT control is introduced, because it counterbalances the previous effect.

This is better shown in the behaviour of the same parameter with the fuel control strategy. The minimum membrane temperature sharply increases, approaching the maximum value. This behaviour could seem strange at first sight, considering that the combustor outlet temperature is being reduced. The explanation is in the secondary control strategy: in order to keep the maximum membrane temperature at its constant value, the mass flow in the loop is reduced less rapidly than the main engine mass flow. Hence, the temperature variation in all the MCM components strongly decreases, leading to outlet temperatures close to the inlet one. The phenomenon is shown in Figure 4.24: the flow fraction, that is almost constant with the mass control strategy, greatly increases when the fuel control strategy is applied.

The excess oxygen at the combustor outlet increases slightly with the mass flow reduction, for the reasons explained above. In this case the increase is moderated by the constant burning temperature. Contrastingly, in the fuel only strategy this value is greatly increased as less oxygen per flow unit is consumed in the combustion process.

4.4 Nuclear Steam Turbine Cycle: Supercritical Water-cooled Reactor

A PFD of the SCWR model has been developed capturing the key features of this concept (Figure 4.25). A paper [75] selected from the open literature has provided some guidance in the regards of

- the aforementioned plant key features;
- the modelling assumptions (including the power plant parameters);
- the design criteria and control strategies.

The mentioned paper includes a useful PFD where also a number of input and output data are reported (Figure 4.26).

A comparison of the two layouts shows that the model adopted in the present work does not exhibit the complex system of steam extractions during the expansion and the relevant series of pre-heaters. Consequently, it is not

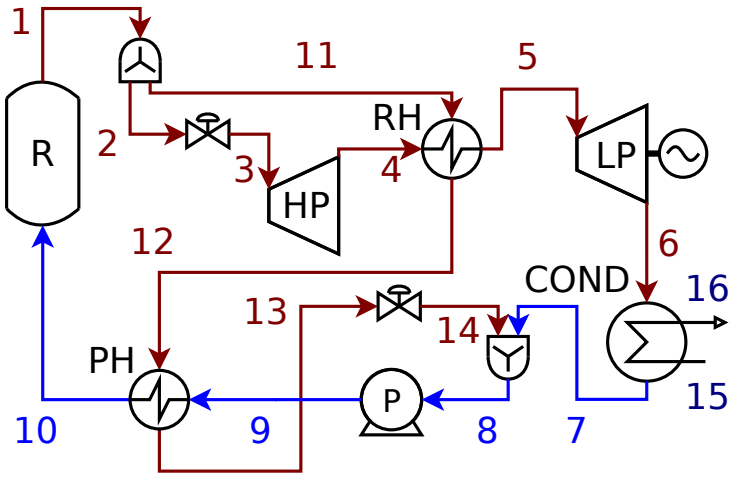

Figure 4.25. Process Flow Diagram of the SCWR cycle computational code.

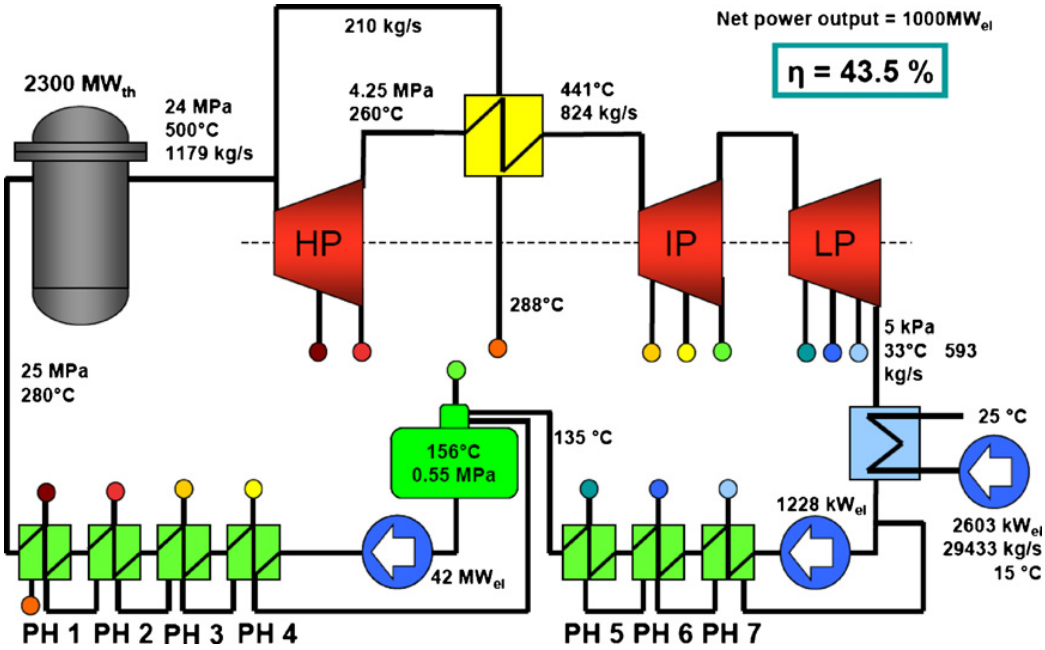

Figure 4.26. Complete layout of the SCWR concept with key parameters and performance data [75].

necessary to model separately the intermediate pressure turbine stages as well as the extraction and boiler pumps.

This simplified approach is coherent with the research objective traced and will be further analysed in the results discussion below. Although approximate, the PFD of Figure 4.25 includes all the key features of the SCWR power plant.

4.4.1 Modelling parameters

A summary of the modelling input parameters is offered in Table 4.6. The quantities coinciding with the assumptions in the mentioned paper [75] show a reference next to their name.

It is assumed to use river water at 15 °C of temperature at the condenser inlet whereas the outlet temperature is set to 25 °C [75]. The power required to pump the necessary river water mass flow through the condenser is computed and included in the overall power plant analysis.

The heat exchange design criterion for the re-heater, pre-heater, and condenser are based on the original methodology discussed in Section 3.1.2.

At design-point, it is assumed that:

- the overall mass flow equals 1179 kg/s [75];
- 230 kg/s of steam are extracted from the main flow, at the reactor outlet, to re-heat the main stream;
- the outlet temperature of the hot stream in the pre-heater is 5 °C higher than the cold inlet fluid temperature;
- the working fluid at the outlet of the condenser (station 7) is sub-cooled to a temperature necessary to guarantee the saturated liquid conditions at the inlet of the pump (station 8).

The off-design behaviour of the power plant is simulated according to the following hypotheses:

- the power output is handled by a throttling valve at the inlet of the high-pressure steam turbine keeping constant the reactor inlet pressure [75];
- the splitter handles the extracted mass flow to keep constant the re-heat temperature [75];
- all turbines work at choked conditions;
- the temperature of the river water at the condenser outlet is set constant.

Table 4.6. Input parameters of the SCWR power plant model.

Parameter	Value
Design-point overall mass flow [75]	1179 kg/s
Design-point re-heat mass flow extracted	230 kg/s
Reactor inlet pressure [75]	250 bar
Reactor outlet pressure [75]	240 bar
High-pressure turbine outlet pressure [75]	42.5 bar
Low-pressure turbine outlet pressure [75]	0.05 bar
River water pressure	1.013 bar
Reactor outlet temperature [75]	500 °C
Re-heater outlet temperature (main flow) [75]	441 °C
Condenser river water inlet temperature [75]	15 °C
Condenser river water outlet temperature [75]	25 °C
Design-point pre-heater temperature difference (hot outlet side)	5 °C
Reactor thermal efficiency	0.98
Steam turbines iso-entropic efficiency	0.88
Steam turbines mechanical efficiency	0.99
Electric generator efficiency	0.98
Overall pump efficiency (condenser and main pump)	0.78
Re-heater pressure drop efficiency (both sides)	0.98
Splitter pressure drop efficiency (main flow)	0.99
Splitter pressure drop efficiency (re-heat flow)	0.98
Condenser pressure drop efficiency (river water side)	0.98
Condenser pressure drop efficiency (steam side)	0.97
Mixer pressure drop efficiency	0.99
Pre-heater pressure drop efficiency (cold side)	0.99
Pre-heater pressure drop efficiency (hot side)	0.98
Relative numerical accuracy (order of magnitude)	10^{-10}

Table 4.7. SCWR power plant model design-point results compared to literature data.

Parameter	Value	Reference [75]
Overall efficiency	37.31%	43.5%
Net power output	1268 MW	1000 MW
Heat input	3399 MW	2300 MW
Low-pressure turbine outlet mass flow	949 kg/s	593 kg/s
Cooling river water mass flow	48 075 kg/s	29 433 kg/s
Condenser sub-cooling temperature difference	2.53 °C	/
Feed-water pumping power	38.15 MW	43.23 MW

4.4.2 Design-point results

A comparison of the main output data obtained by the simulation code (Table 4.7) with the results available in the literature [75] shows good agreement.

In fact, according to the basic theory of steam power plants, the regeneration (by means of steam extractions and pre-heaters) determines an improvement of the cycle thermal efficiency with a reduction of the power output, when compared to the simple cycle [10].

The SCWR plant simulated in this work has a single pre-heater and thus a less extensive regeneration compared to the reference case. The difference in the results shows great coherence with the different degree of approximation of the two PFDs. A further confirmation is the lower heat rate provided by the reactor in the reference case.

Another consequence of the reduced regeneration is the greater mass flow at the inlet of the condenser (on the steam side) that, in turn, requires a greater cooling water mass flow. This is again reproduced in the results obtained.

Finally, the robustness of the numerical integrator and, thus, of the heat exchange model, is clearly visible plotting the design-point results of the re-heater calculation. The temperature diagram across the heat exchanger (Figure 4.27) shows the hot fluid cooling at conditions that would have implied a change of phase of the steam if it were not at supercritical conditions.

Consequently, the relevant integrand function (see Section 3.1.2)

$$f = \frac{1}{T_{\mathrm{h}} - T_{\mathrm{c}}}$$

exhibits a fairly irregular shape that the integrator handles correctly (Figure 4.28). This observation becomes clearer plotting the same function for a

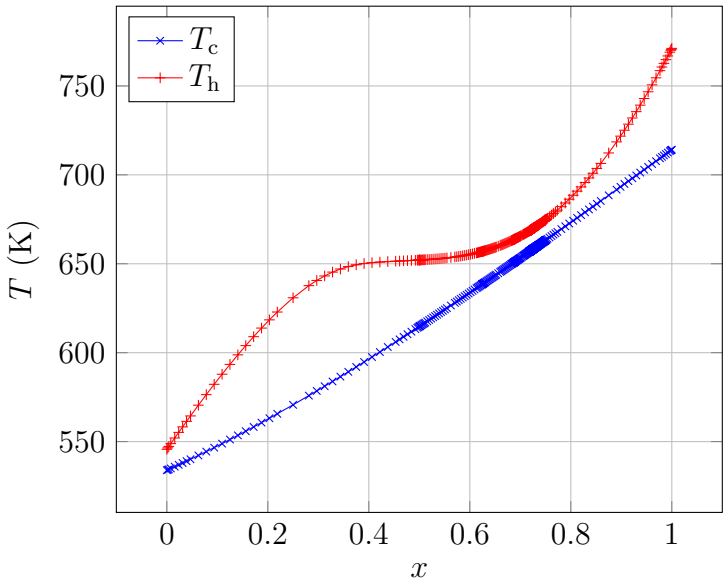

Figure 4.27. SCWR re-heater temperature chart at design-point conditions. T_c: cold fluid temperature; T_h: hot fluid temperature; x: heat exchanger abscissa.

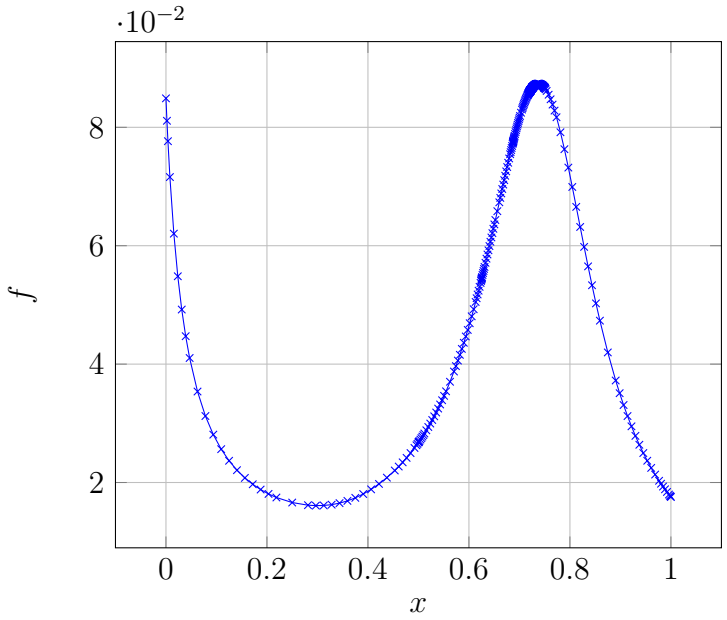

Figure 4.28. SCWR re-heater integrand function f chart at design-point conditions. x: heat exchanger abscissa.

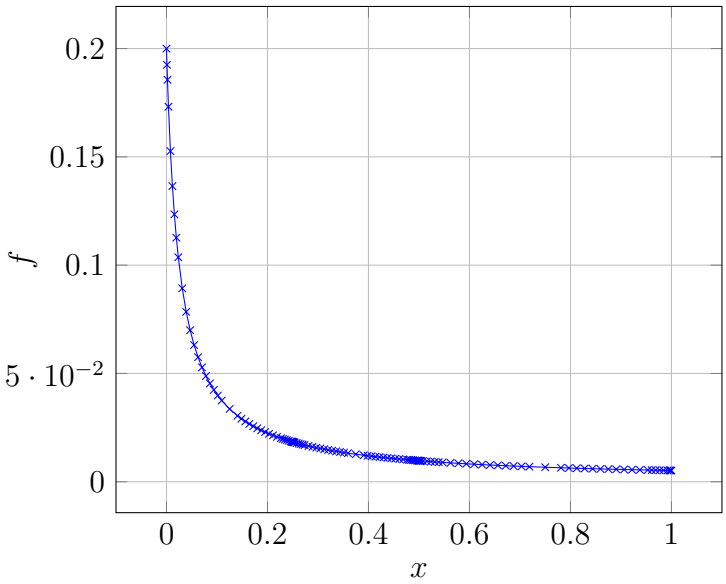

Figure 4.29. SCWR pre-heater integrand function f chart at design-point conditions. x: heat exchanger abscissa.

more typical case: e.g., Figure 4.29 shows the pre-heater design-point results.

The way the integrand function has been plotted, allows also to appreciate how the adaptative numerical integrator evaluates (correctly) more points of the function where stronger gradients are detected, minimising the numerical error and optimising the computational effort.

4.4.3 Off-design results

The main parameter to control the SCWR cycle power output P_o is the throttling valve pressure reduction Δp_t (set to zero at design-point). There is a linear reduction of the power output with the increase of the throttle setting (Figure 4.30). The off-design study has been conducted until 50 bar of pressure reduction at the high-pressure turbine inlet compared to the design-point value. In these conditions the power plant operates at 77.8% of the design-point power output (i.e., 968.78 MW).

An analysis of the overall efficiency η_o and power output off-design trends shows fairly good performance at part-load operation (Figure 4.31). At the maximum allowed reduction of power output (about 78% of the design-point value), the overall power plant efficiency is above 98% of its design-point figure. In absolute terms, the plant overall efficiency slides from 37.31% (design-point) until 36.69% ($\Delta p_t = 50$ bar) .

The cause of the power output linear reduction with the increase of the

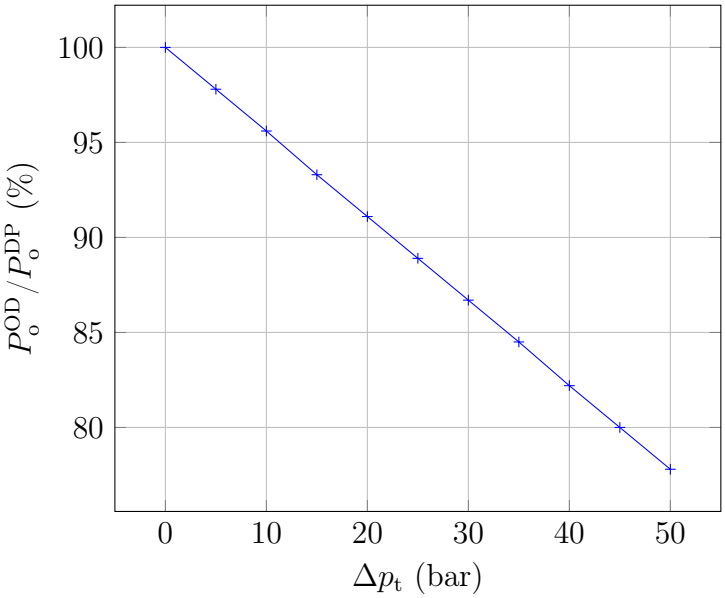

Figure 4.30. SCWR off-design power output reduction controlled by the throttling valve pressure loss Δp_t. P_o: power output; DP: design-point; OD: off-design.

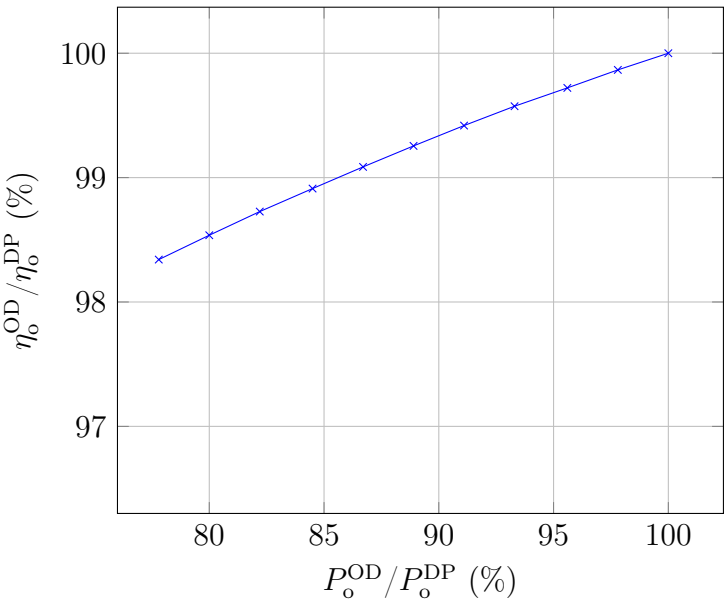

Figure 4.31. SCWR off-design overall efficiency η_o reduction at part-load operation. P_o: power output; DP: design-point; OD: off-design.

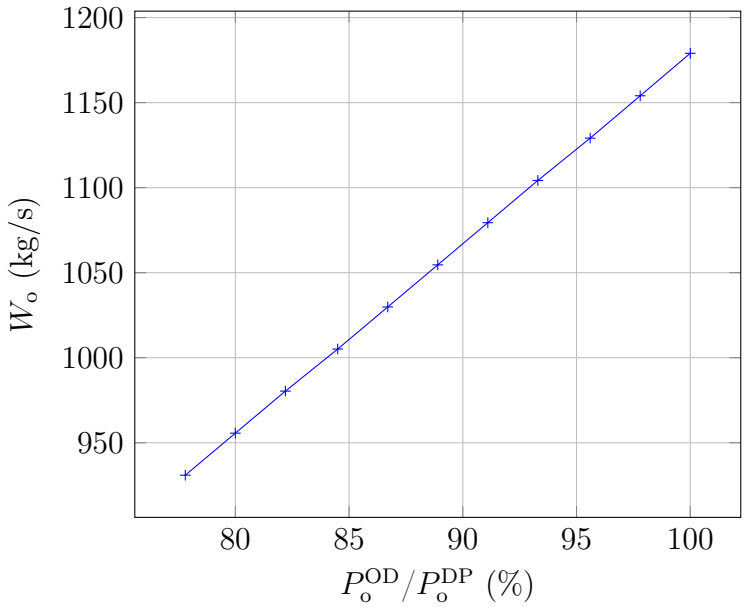

Figure 4.32. SCWR off-design overall mass flow W_o reduction at part-load operation. P_o: power output; DP: design-point; OD: off-design.

throttle setting is the reduction of the overall, working fluid mass flow W_o. This theoretical hypothesis (derived by the assumption that the turbines are working at choked conditions) is confirmed by the results (Figure 4.32).

The part-load reduction of the working fluid mass flow affects also the heat input provided by the reactor $\dot{Q}_R$ to bring the supercritical fluid to the set outlet temperature (500 °C). This is confirmed plotting the reactor heat input against the relative reduction of power output at off-design conditions (Figure 4.33).

Instead, it is not immediate to conclude that also the mass flow spillage used to re-heat the main stream W_{rh} drops linearly at part-load. However, this trend is confirmed by the results analysis (Figure 4.34).

Moreover, the condenser cooling mass flow W_w (assumed to be extracted from a river) reduces at first sub-linearly and then, below about 95% of part-load, linearly (Figure 4.35). This behaviour is explained by the dominating effect of the temperature reduction in the calculation of the condenser off-design conditions and it will be discussed further below.

Considering that all the main power plant output parameters are reducing linearly at part-load, it is interesting to perform a comparison of their variation in relative terms compared to the design-point (Figure 4.36). As theoretically predictable, the overall mass flow and the reactor heat input show superimposing trends while the re-heat bleed mass flow, energetically

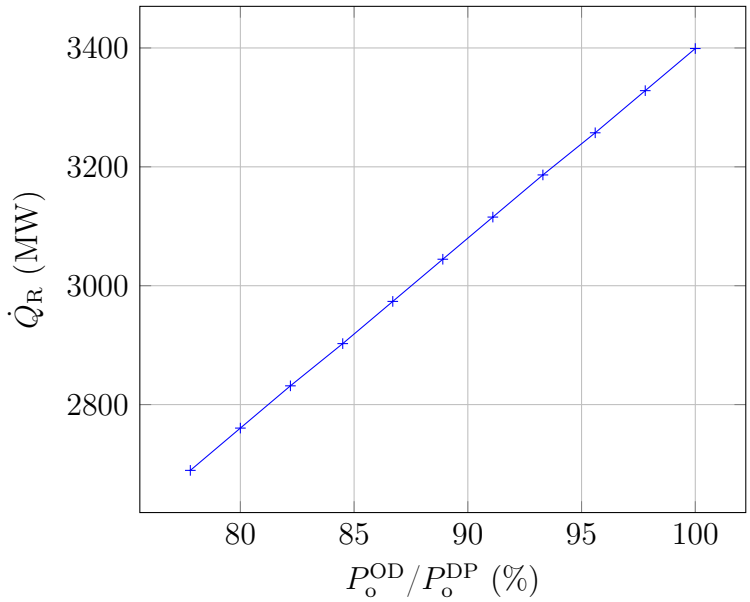

Figure 4.33. SCWR off-design reactor heat rate $\dot{Q}_{\mathrm{R}}$ reduction at part-load operation. P_{o}: power output; DP: design-point; OD: off-design.

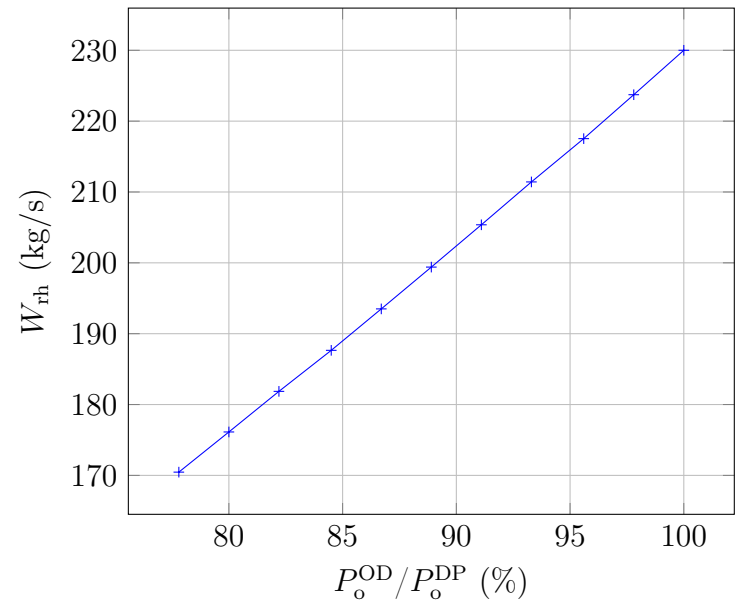

Figure 4.34. SCWR off-design re-heat mass flow W_{rh} reduction at part-load operation. P_{o}: power output; DP: design-point; OD: off-design.

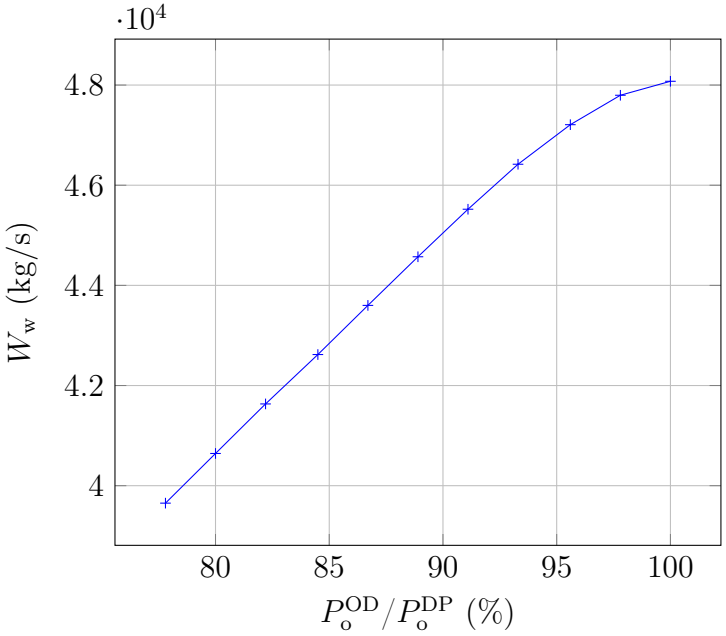

Figure 4.35. SCWR off-design condenser cooling mass flow W_w reduction at part-load operation. P_o: power output; DP: design-point; OD: off-design.

more "valuable", reduces more rapidly than the condenser cooling water. This observation explains and confirms the described good performance at part-load of the power plant overall efficiency (Figure 4.31).

The sub-cooling temperature (below the saturation point) at the condenser outlet ΔT_{sc} exhibits a rapid increase and then settles above 15 °C almost independent of the reduced load setting (Figure 4.37). This behaviour can be mostly explained analysing the condenser off-design performance.

In fact, there are two main effects that dictate the part-load behaviour of the condenser.

- The lower outlet temperature of the condensed flow. This response is triggered by the smaller inlet steam mass flow cooled through the same (design-point) heat exchange area;

- The mass flow reduction of cooling river water pumped to condensate the steam.

Both effects happen simultaneously, but the results show that the temperature reduction is dominating on the cooling mass flow reduction (Figures 4.35 and 4.37). This is better visualised plotting the condenser temperatures at different part-load settings on the cooling water outlet side (Figure 4.38). It

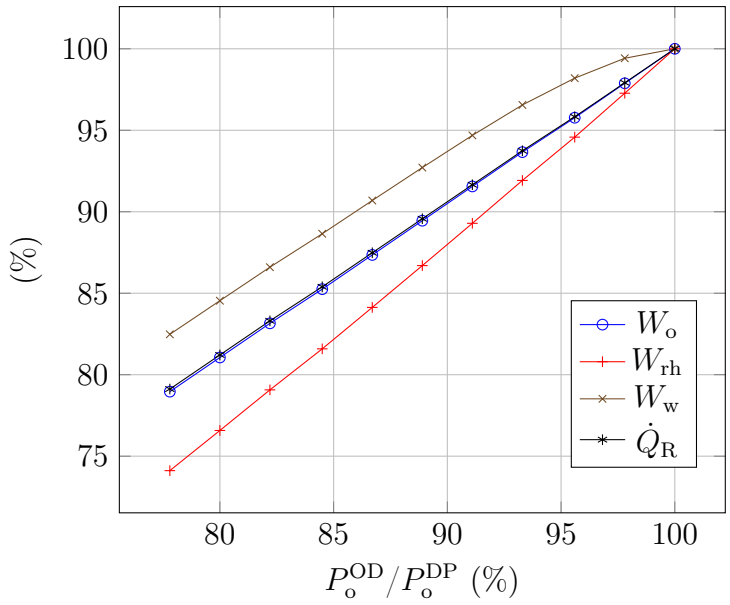

Figure 4.36. SCWR off-design relative reduction at part-load operation of some plant parameters. W_o: overall mass flow; W_{rh}: re-heat mass flow; W_w: condenser cooling mass flow; $\dot{Q}_R$: reactor heat rate; P_o: power output; DP: design-point; OD: off-design.

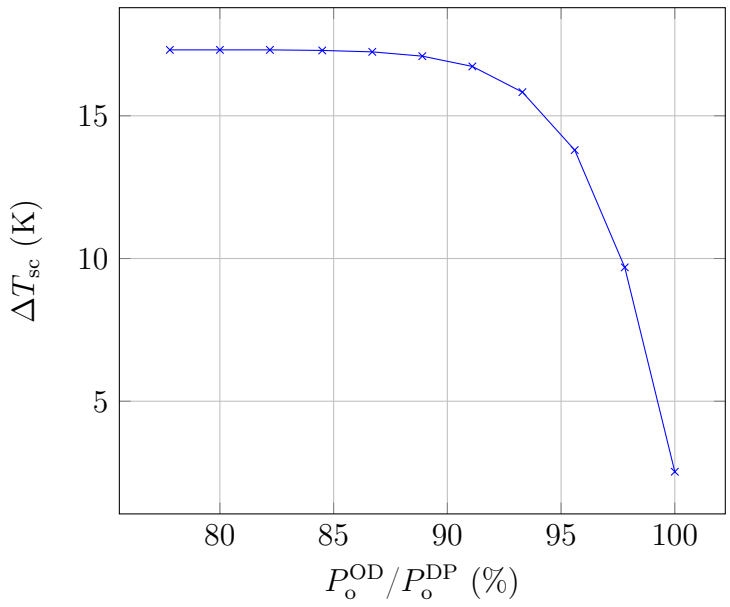

Figure 4.37. SCWR off-design condenser outlet sub-cooling temperature ΔT_{sc} at part-load operation. P_o: power output; DP: design-point; OD: off-design.

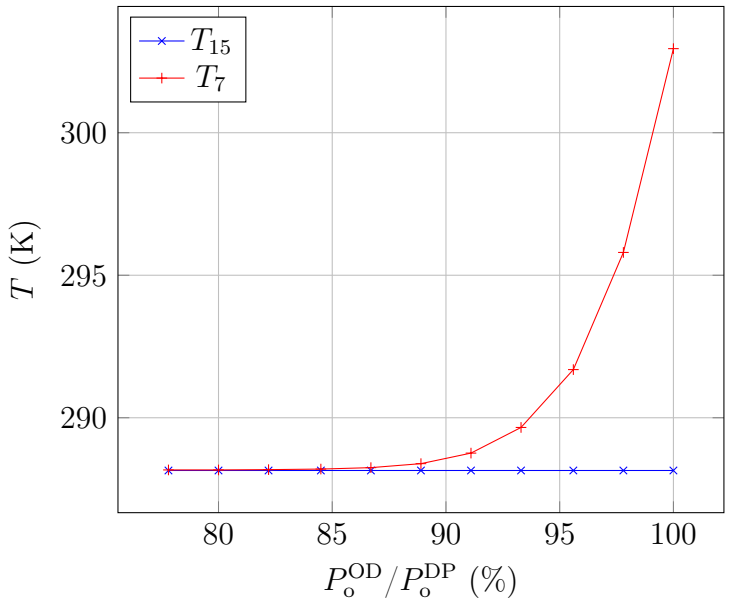

Figure 4.38. SCWR off-design condenser cooling mass flow reduction at part-load operation. T: temperature; P_o: power output; DP: design-point; OD: off-design.

is possible to see how the temperature difference reduces quickly to almost zero, markedly faster than the cooling water reduction.

Furthermore, the last considerations prove how it would be difficult to operate the power plant below 78% of design-point load, under the same set of control conditions. This could be considered another interesting finding of the present study, especially considering that in the literature it is envisaged 50% maximum reduction of the power output but it is not explicitly clarified under what control conditions [75].

4.5 Wind Farms

The integration of a wind farm with a conventional gas turbine engine has been studied in different conditions. Results are obtained for every season according to three scenarios and for a cut-in velocity of 4 m/s, a rated velocity of 15 m/s and a cut-out velocity of 25 m/s [22].

1. Electrical power for 250 000 people using the General Electric 9001FA gas turbine and a wind farm of 223 MW power output at full load. Weather conditions of London city and Aberdaron (north of Wales).

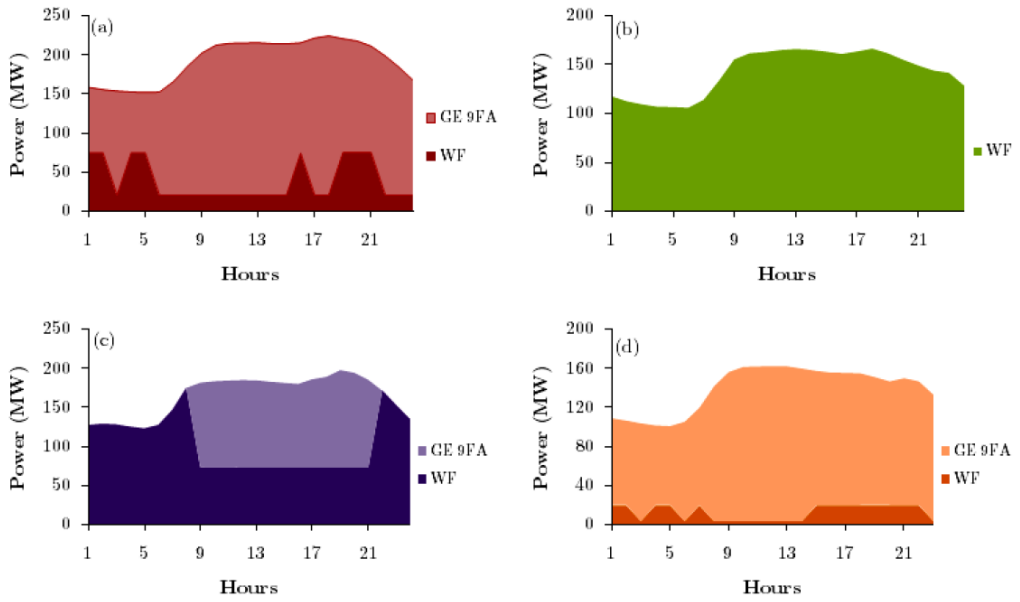

Figure 4.39. Power delivered by a wind farm and the General Electric 9001FA engine to a population of 250 000 inhabitants in a representative day of (a) winter, (b) summer, (c) autumn, (d) spring, in Aberdaron (north of Wales) [22].

2. Electrical power for 10 000 people using the General Electric 10-1 gas turbine and a wind farm of 87 MW power output at full load. Weather conditions of Aberdaron (north of Wales).

3. Electrical power for 5000 people using the Solar Mercury 50 gas turbine and a single wind turbine of 5 MW at full load. Weather conditions of Aberdaron (north of Wales).

The results for the first scenario in Aberdaron are selected (Figure 4.39).

Chapter 5

Conclusions

A background with some information about the problem of global warming and the fast, increasing consumption of natural resources has been provided. Sustainability appears a promising concept able to address these issues. A view on the possible strategies to counter-act the current trends has been produced.

Civil aviation and power generation are identified as two of the most important sectors affected by the non-sustainability of the *status quo*, being at the centre of a vibrant scientific research. Many promising, novel concepts in these fields result untested or not adequately investigated given their complexity or their plurality.

The aim of the present project was to carry out a multi-disciplinary exercise called Techno-economic Environmental Risk Analysis (TERA) on sustainable power generation concepts. The TERA strategy has been applied in two steps:

- a contribution in the integration of all TERA modules for three advanced concepts of the NEW Aero Engine Core concepts (NEWAC) project;
- the development of a reliable off-design computational code for the power generation TERA framework.

More specifically, three novel engine cycles were investigated in the aeronautical field:

- the Geared Turbofan with Counter-Rotating core for Short Range (GTCRSR) concept,
- the Geared Turbofan with Active Core for Short Range (GTACSR) concept,

- the Geared Turbofan Inter-Cooled for Long Range (GTICLR) concept.

The following electric power generation engine systems were also studied at part-load.

Carbon Capture and Storage (CCS) advanced cycles: the Advanced Zero Emissions Power plant (AZEP).

Nuclear: a supercritical steam power plant inspired by the Supercritical Water-cooled Reactor (SCWR).

Wind: a land-based wind farm working in synergy with conventional power plants.

Conventional: two combined cycle, reference engines with a simple and reheat topping cycle.

A survey of the scientific literature in the electric power generation domains highlighted above was presented isolating the areas where there is a clear lack of knowledge.

For each of the aforementioned concepts, a comprehensive description of the modelling approach has been provided. In particular, an original method developed by the author has been presented in the section regarding the SCWR concept.

The relevant results were presented showing the performance of the optimised aeronautical engine designs and the part-load behaviour of the electric power generation cycles.

Specifically, the optimised design specifications of the GTCRSR engine show a reduction of more than 7% of block fuel in comparison to the reference engine, more than 6% for the GTACSR and almost up to 5% for the GTICLR. Performance simulations at off-design condition of novel electric power generation concepts were validated against literature data at design-point, considering first principles of plant components. Multiple, specific control strategies for the fossil fuel and nuclear power plant have been identified to handle the power output down to 60% of the design point for the AZEP and slightly below 80% for the nuclear cycle. Hourly performance simulations of typical days representative of each season of the wind farm in combination to conventional gas turbine engines have been investigated for different size (from 223 MW to 5 MW at full load). Thus, a robust model of the electric power plants have been generated for the implementation in a TERA framework.

Chapter 6

Further work

A number of areas can be considered to improve the models presented in this work.

In the first instance, the Advanced Zero Emissions Power plant (AZEP) concept can be simulated in combined cycle arrangement. Several options are available in investigating this family of power plants. Considering the topping cycle, both the implementation of AZEP 100% and AZEP 95% would be of interest when coupled with a number of bottoming cycle architectures. In particular, alongside multiple pressure arrangments, multiple Heat Recovery Steam Generators (HRSGs) can be considered to capture the thermal energy of the oxygen-depleted air and the CO_2/H_2O streams. It would be of interest a systematic analysis of the off-design performance while considering different permutations of these options.

Furthermore, a few additional control strategies (as discussed in the literature review) can be investigated for the AZEP cycle. Finally, it would be interesting also to assess its transient performance searching for problematic conditions (e.g. instability, resonance).

The scientific literature about the Supercritical Water-cooled Reactor (SCWR) concept is currently limited and future publications might be helpful in further fine-tuning the current model (if proven necessary). More refined methods to model the steam turbine behaviour at off-design conditions may prove beneficial (although it is expected to have a limited impact on results) as well as a more accurate model of the pre-heating.

Concerning the wind farm model, the integration of a weather prediction model is warmly suggested.

References

[1] *Gas Turbine World 2009 GTW Handbook*, 2009. A Pequot Publication. Volume 27.

[2] Agbonzikilo, F. Advanced Low Carbon Power Systems: Performance Analysis of an Oxy-Fuel Cycle Power Plant. Master of Science in Thermal Power Thesis, Cranfield University — School of Engineering, 2009.

[3] Avila, R. Off-Design Performance Evaluation of Combined Cycle Power Plants. Master of Science in Thermal Power Thesis, Cranfield University — School of Engineering, 2011.

[4] Baxi, C. B., Perez, E., Shenoy, A., Kostin, V. I., Kodochigov, N. G., Vasyaev, A. V., Belov, S. E., and Golovko, V. F. Evolution of the power conversion unit design of the GT-MHR. In *International Congress on Advances in Nuclear Power Plants* (2006), vol. 2006, pp. 233–238.

[5] Bredesen, R., Jordal, K., and Bolland, O. High-temperature membranes in power generation with CO_2 capture. *Chemical Engineering and Processing: Process Intensification 43*, 9 (2004), 1129–1158.

[6] Brook, P., Scott, D., and Noble, C. Carbon Capture and Storage. An introduction to relevant oil and gas processes and their uses. Tech. rep., Foster Wheeler Energy Limited, Foster Wheeler Energy Limited, Shinfield Park, Reading, Berkshire, United Kingdom, November 2006.

[7] Buhl, M. L. WT_Perf User's Guide, December 2004.

[8] Burggraaf, A. J., and Cot, L. *Fundamentals of inorganic membrane science and technology.* Elsevier Science, 1996.

[9] Carrillo Romero, F. A TERA Evaluation of an Oxy-Fuel Combined Cycle Power Plant. Master of Science in Thermal Power Thesis, Cranfield University — School of Engineering, 2011.

[10] Çengel, Y. A., and Boles, M. A. *Thermodynamics: An Engineering Approach*, 7th edition ed. McGraw Hill, 2011.

[11] Cheng, X., and Schulenberg, T. Heat Transfer at Supercritical Pressures — Literature Review and Application to an HPLWR. Tech. Rep. FZKA 6609, Forschungszentrum Karlsurhe, 2001.

[12] Ciavarella, G. Off-Design Performance Analysis of the AZEP Concept. Master of Science in Thermal Power Thesis, Cranfield University — School of Engineering, 2010.

[13] Codeceira Neto, A. *Assessment of novel power generation systems for the biomass industry.* PhD thesis, Cranfield University — School of Engineering, 1999.

[14] Colmenares Quintero, R. F. *Techo-economic and Environmental Risk Assessment of Innovative Propulsion Systems for Short-Range Civil Aircraft.* PhD thesis, Cranfield University — School of Engineering, 2009.

[15] Colombo, K. E., and Bolland, O. Dynamic simulation of an oxygen mixed conducting membrane-based gas turbine power cycle for CO_2 capture. *Energy Procedia 1*, 1 (2009), 431–438.

[16] Colombo, K. E., Bolland, O., Kharton, V. V., and Stiller, C. Simulation of an oxygen membrane-based combined cycle power plant: Part-load operation with operational and material constraints. *Energy and Environmental Science 2*, 12 (2009), 1310–1324.

[17] Colombo, K. E., Imsland, L., Bolland, O., and Hovland, S. Dynamic modelling of an oxygen mixed conducting membrane and model reduction for control. *Journal of Membrane Science 336*, 1–2 (2009), 50–60.

[18] Colombo, K. E., Kharton, V. V., and Bolland, O. Simulation of an oxygen membrane-based gas turbine power plant: Dynamic regimes with operational and material constraints. *Energy and Fuels 24*, 1 (2010), 590–608.

[19] Colombo, K. E., Kharton, V. V., Viskup, A. P., Kovalevsky, A. V., Shaula, A. L., and Bolland, O. Simulation of a mixed-conducting membrane-based gas turbine power plant for CO_2 capture: System level analysis of operation stability and individual process unit degradation. *Journal of Solid State Electrochemistry 15*, 2 (2011), 329–347.

[20] Cranfield University. *The Turbomatch Scheme for Aero/Industrial Gas Turbine Engine Design-Point/Off-Design Performance Calculation.*

[21] Damen, K., van Troost, M., Faaij, A., and Turkenburg, W. A comparison of electricity and hydrogen production systems with CO_2 capture and storage. Part A: Review and selection of promising conversion and capture technologies. *Progress in Energy and Combustion Science 32*, 2 (2006), 215–246.

[22] De La Torre Mateo, I. Wind Turbine Performance Analysis with Gas Turbines as Backup. Master of Science in Thermal Power Thesis, Cranfield University — School of Engineering, 2011.

[23] Dechamps, P. J., Pirard, N., and Mathieu, P. J. Part load operation of combined cycle plants with and without supplementary firing. In *Proceedings of the 8th Congress and Exposition on Gas Turbines in Cogeneration and Utility, Industrial and Independent Power Generation* (Portland, OR, USA, 1994), vol. 9, ASME, New York, NY, United States, pp. 371–380. Conference Date: 25 October 1994 through 27 October 1994; Conference Code: 42263.

[24] Di Lorenzo, G. *Advanced Low-Carbon Power Plants: the TERA Approach.* PhD thesis, Cranfield University — School of Engineering, 2010.

[25] Dostal, V. *A Supercritical Carbon Dioxide Cycle for Next Generation Nuclear Reactors.* PhD thesis, Massachusetts Institute of Technology — Department of Nuclear Engineering, 2004.

[26] Duderstadt, J. J., and Hamilton, L. J. *Nuclear Reactor Analysis.* John Wiley & Sons, 1976.

[27] EEA (European Environment Agency). *The European environment. State and outlook 2010. Synthesis.* European Environment Agency, 2010.

[28] Eide, L. I., Anheden, M., Lyngfelt, A., Abanades, J. C., Younes, M., Clodic, D., Bill, A. A., Feron, P. H. M., Rojey, A., and Giroudière, F. Novel capture processes. *Oil and Gas Science and Technology 60*, 3 (2005), 497–508.

[29] European Union. Climate change: Commission proposes bringing air transport into EU Emissions Trading Scheme. Press Release, 20 December 2008.

[30] Favati, P., Lotti, G., and Romani, F. Algorithm 691: Improving QUADPACK Automatic Integration Routines. *ACM Trans. Math. Softw. 17*, 2 (June 1991), 218–232.

[31] Favati, P., Lotti, G., and Romani, F. Interpolatory Integration Formulas for Optimal Composition. *ACM Trans. Math. Softw. 17*, 2 (June 1991), 207–217.

[32] Fiaschi, D., Gamberi, F., Bartlett, M., and Griffin, T. The air membrane-ATR integrated gas turbine power cycle: A method for producing electricity with low CO_2 emissions. *Energy Conversion and Management 46*, 15-16 (2005), 2514–2529.

[33] Foy, K., and Yantovski, E. History and state-of-the-art of fuel fired zero emission power cycles. *International Journal of Thermodynamics 9*, 2 (2006), 37–63.

[34] Freire, J. Off-Design Performance Modelling and Analysis of an Advanced Zero Emissions Power Plant (AZEP) 85%. Master of Science in Thermal Power Thesis, Cranfield University — School of Engineering, 2011.

[35] Generation IV International Forum. GIF R&D Outlook for Generation IV Nuclear Energy Systems. Tech. rep., Generation IV International Forum, August 2009.

[36] Gomes, E. E. B. *Operational Optimisation of Gas Turbines Distributed Generation Systems in Competitive Electricity Market.* PhD thesis, Cranfield University — School of Engineering, 2007.

[37] Griffin, T., Bücker, D., and Pfeffer, A. Technology options for gas turbine power generation with reduced CO_2 emission. *Journal of Engineering for Gas Turbines and Power 130*, 4 (2008), 041801–1–041801–8.

[38] Griffin, T., Sundkvist, S. G., Åsen, K. I., and Bruun, T. Advanced zero emissions gas turbine power plant. *Journal of Engineering for Gas Turbines and Power 127*, 1 (2005), 81–85.

[39] Grochowina, F. Performance Evaluation of Gas Turbines for Nuclear Power Plants. Master of Science in Thermal Power Thesis, Cranfield University — School of Engineering, 2011.

[40] Haag, J.-C., Hildebrandt, A., Hönen, H., Assadi, M., and Kneer, R. Turbomachinery simulation in design point and part-load operation for advanced CO_2 capture power plant cycles. In *Conference of 2007 ASME Turbo Expo* (Montreal, Que., 2007), vol. 3, pp. 239–250. Conference Date: 14 May 2007 through 17 May 2007; Conference Code: 70222.

[41] Habib, M. A., Badr, H. M., Ahmed, S. F., Ben-Mansour, R., Mezghani, K., Imashuku, S., la O', G. J., Shao-Horn, Y., Mancini, N. D., Mitsos, A., Kirchen, P., and Ghoneim, A. F. A review of recent developments in carbon capture utilizing oxy-fuel combustion in conventional and ion transport membrane systems. *International Journal of Energy Research 35*, 9 (2011), 741–764.

[42] Hansen, M. O. L. *Aerodynamics of Wind Turbines*, Second Edition ed. Earthscan, 2008.

[43] Intergovernmental Panel on Climate Change (IPCC). *Climate Change 2007: Impacts, Adaptation and Vulnerability. Contribution of Working Group II to the Fourth Assessment Report of the Intergovernmental Panel on Climate Change — Summary for Policymakers*. Cambridge University Press, Cambridge, UK, 2007, pp. 7–22.

[44] International Energy Agency (IEA). *CO_2 Emissions from Fuel Combustion 2011 — Highlights*. International Energy Agency, 2011.

[45] Jie, W., Zhiyong, H., Shutang, Z., and Suyuan, Y. Design Features of Gas Turbine Power Conversion System for HTR-10GT. In *Proceedings of the Conference on High Temperature Reactors* (Beijing, China, 22–24 September 2004), I. A. E. Agency, Ed., pp. 1–12.

[46] Kakaç, S., and Liu, H. *Heat exchangers: selection, rating and thermal design*, second ed. CRC Press, Boca Raton, Florida, USA, 2002.

[47] Kato, Y., Nitawaki, T., and Muto, Y. Medium temperature carbon dioxide gas turbine reactor. *Nuclear Engineering and Design 230*, 1–3 (2004), 195–207.

[48] Kim, T. Comparative analysis on the part load performance of combined cycle plants considering design performance and power control strategy. *Energy 29*, 1 (2004), 71–85.

[49] Kulhanek, M., and Dostal, V. Supercritical Carbon Dioxide Cycles Thermodynamic Analysis and Comparison. 2007.

[50] Kvamsdal, H. M., Jordal, K., and Bolland, O. A quantitative comparison of gas turbine cycles with CO_2 capture. *Energy 32*, 1 (2007), 10–24.

[51] Kyprianidis, K. G., Colmenares Quintero, R. F., Pascovici, D. S., Ogaji, S., Pilidis, P., and Kalfas, A. I. EVA — A tool for environmental assessment of novel propulsion cycles. In *Conference of 2008 ASME Turbo Expo* (2008), vol. 2, pp. 547–556.

[52] Lennox, T. A., Millington, D. N., and Sunderland, R. E. Plutonium management and Generation IV systems. *Progress in Nuclear Energy 49*, 8 (2007), 589–596.

[53] Lienhard IV, J. H., and Lienhard V, J. H. *A Heat Transfer Textbook*, Version 2.01, Fourth ed. Phlogiston Press, Cambridge, Massachusetts, USA, January 2011.

[54] Lindfeldt, E. G., and Westermark, M. O. J. An integrated gasification zero emission plant using oxygen produced in a mixed conducting membrane reactor. In *Conference of 2006 ASME 51st Turbo Expo* (Barcelona, 2006), vol. 4, pp. 33–40. Conference Date: 6 May 2006 through 11 May 2006; Conference Code: 68506.

[55] Liu, Y., Tan, X., and Li, K. Mixed conducting ceramics for catalytic membrane processing. *Catalysis Reviews — Science and Engineering 48*, 2 (2006), 145–198.

[56] Lonneux, V. Evaluation of an Oxy-fuel Combined Cycle. Master of Science in Thermal Power Thesis, Cranfield University — School of Engineering, 2007.

[57] Lu, J., Vecchi, G. A., and Reichler, T. Expansion of the Hadley cell under global warming. *Geophysical Research Letters 34*, 6 (2007).

[58] Metz, B., Davidson, O., de Coninck, H., Loos, M., and Meyer, L. IPCC Special Report. Carbon Dioxide Capture and Storage. Tech. rep., Intergovernmental Panel on Climate Change (IPCC), 2005.

[59] Moler, C. *Numerical Computing with MATLAB*. Society for Industrial and Applied Mathematics (SIAM), Philadelphia, Pennsylvania, USA, 2004.

[60] Mucino, M. *CCGT Performance Simulation and Diagnostics for Operations Optimisation and Risk Management*. EngD thesis, Cranfield University — School of Engineering, 2007.

[61] Möller, B. F., Torisson, T., Assadi, M., Sundkvist, S. G., Sjödin, M., Klang, A., Åsen, K. I., and Wilhelmsen, K. AZEP gas turbine combined cycle power plants — Thermo-economic analysis. *International Journal of Thermodynamics 9*, 1 (2006), 21–28.

[62] National Academy of Sciences. *Understanding and Responding to Climate Change: Highlights of National Academies Reports*. National Academy Press, Wasington, D.C., 2008.

[63] NEWAC Consortium. Annex I — "Description of Work". Tech. Rep. FP6-030876, NEW Aero Engine Core conceps (NEWAC), 23 June 2010.

[64] NEWAC Consortium. Deliverable D1.3.3A — TERA2020 Optimisation of NEWAC Powerplants. Tech. rep., NEW Aero Engine Core conceps (NEWAC), 12 October 2010.

[65] NEWAC Consortium. WP1.3 GTAC — Performance Model Description and Results. Tech. rep., NEW Aero Engine Core conceps (NEWAC), 2010.

[66] NEWAC Consortium. Deliverable D1.3.2C — TERA2020 Optimisation Results the three additional NEWAC Powerplants. Tech. rep., NEW Aero Engine Core conceps (NEWAC), 5 April 2011.

[67] Ogaji, S., Pilidis, P., and Hales, R. TERA — A tool for aero-engine modelling and management. In *Second World Congress on Engineering Asset Management and Fourth International Conference on Condition Monitoring* (11th–14th June 2007).

[68] Pagone, E. Advanced low carbon power systems — The Advanced Zero Emissions Power plant. Master of Science by Research Thesis, Cranfield University — School of Engineering, 2009.

[69] Pagone, E. Gas Turbine Engine TERA (PhD first year review). Tech. rep., School of Engineering, Cranfield University, November 2011.

[70] Petrakopoulou, F., Boyano, A., Cabrera, M., and Tsatsaronis, G. Exergy-based analyses of an advanced zero emission plant. *International Journal of Low-Carbon Technologies 5*, 4 (2010), 231–238.

[71] Petrakopoulou, F., Tsatsaronis, G., and Morosuk, T. V. Exergoeconomic analysis of an advanced zero emission plant. In *Proceedings of the ASME International Mechanical Engineering Congress and Exposition* (2010), vol. 6, pp. 257–266.

[72] Press, W. H., Teukolsky, S. A., Vetterling, W. T., and Flannery, B. P. *Numerical Recipes in Fortran 77 — The Art of Scientific Computing*, second ed. Cambridge University Press, Cambridge, United Kingdom, 2001.

[73] Rackley, S. A. *Carbon Capture and Storage*. Butterworth-Heinemann, 2010.

[74] Rovira, A., Valdés, M., and Durán, M. D. A model to predict the behaviour at part load operation of once-through heat recovery steam generators working with water at supercritical pressure. *Applied Thermal Engineering 30*, 13 (2010), 1652–1658.

[75] Schulenberg, T., Starflinger, J., Marsault, P., Bittermann, D., Maráczy, C., Laurien, E., Lycklama à Nijeholt, J. A., Anglart, H., Andreani, M., Ruzickova, M., and Toivonen, A. European supercritical water cooled reactor. *Nuclear Engineering and Design 241*, 9 (2011), 3505–3513. Seventh European Commission conference on Euratom research and training in reactor systems (Fission Safety 2009).

[76] Shah, R. K., and Sekulić, D. P. *Fundamentals of heat exchanger design*. John Wiley & Sons, Hoboken, New Jersey, USA, 2003.

[77] Sunarso, J., Baumann, S., Serra, J. M. R., Meulenberg, W. A., Liu, S., Lin, Y. S., and Diniz da Costa, J. C. Mixed Ionic-Electronic Conducting (MIEC) ceramic-based membranes for oxygen separation. *Journal of Membrane Science 320*, 1–2 (2008), 13–41.

[78] Sundkvist, S. G., Griffin, T., and Thorshaug, N. P. AZEP — Development of an integrated air separation membrane–gas turbine. In *Second Nordic Minisymposium on Carbon Capture and Storage, Gothenburg, Sweden* (26th October 2001), pp. 52–57.

[79] Sundkvist, S. G., Julsrud, S., Vigeland, B., Naas, T., Budd, M., Leistner, H., and Winkler, D. Development and testing of AZEP reactor components. *International Journal of Greenhouse Gas Control 1*, 2 (2007), 180–187.

[80] Toftegaard, M. B., Brix, J., Jensen, P. A., Glarborg, P., and Jensen, A. D. Oxy-fuel combustion of solid fuels. *Progress in Energy and Combustion Science 36*, 5 (2010), 581–625.

[81] Tsoudis, E. *Technoeconomic Environmental and Risk Analysis of Marine Gas Turbine Power Plants*. PhD thesis, Cranfield University — School of Engineering, 2008.

[82] United Nations General Assembly. *Report of the World Commission on Environment and Development: Our Common Future*. United Nations, 1987.

[83] US DOE Nuclear Energy Research Advisory Committee and the Generation IV International Forum. A Technology Roadmap for Generation IV Nuclear Energy Systems. Tech. rep., Generation IV International Forum, December 2002.

[84] Vallejo Sanz, L. Techno-Economic Study of an Advanced Zero Emission Power Plant (AZEP 100%). Master of Science in Thermal Power Thesis, Cranfield University — School of Engineering, 2011.

[85] Wagner, W., Cooper, J. R., Dittmann, A., Kijima, J., Kretzschmar, H. J., Kruse, A., Mareš, R., Oguchi, K., Sato, H., Stöcker, I., Šifner, O., Takaishi, Y., Tanishita, I., Trübenbach, J., and Willkommen, T. The IAPWS Industrial Formulation 1997 for the Thermodynamic Properties of Water and Steam. *Journal of Engineering for Gas Turbines and Power 122*, 1 (2000), 150–184.

[86] Walker, B., Holling, C. S., Carpenter, S. R., and Kinzig, A. Resilience, adaptability and transformability in social-ecological systems. *Ecology and Society 9*, 2 (2004).

[87] Yadiyal, K. Off-Design Performance Analysis of Novel Combined Cycle Power Plant. Master of Science in Thermal Power Thesis, Cranfield University — School of Engineering, 2012.

[88] Yan, X., Kunitomi, K., Nakata, T., and Shiozawa, S. GTHTR300 design and development. *Nuclear Engineering and Design 222*, 2-3 (2003), 247–262.

[89] Yari, M., and Mehranpour, A. A comparative study of supercritical CO_2 (S-CO_2) recompression Brayton cycles for nuclear power plants. In *Proceedings of the 10th International Conference on Clean Energy (ICCE-2010)* (15–17 September 2010).

[90] Zehe, M. J., Gordon, S., and McBride, B. J. CAP: A Computer Code for Generating Tabular Thermodynamic Functions from

NASA Lewis Coefficients. Technical Paper NASA TP-2001-210959-REV1, NASA, National Aeronautics and Space Administration John H. Glenn Research Center at Lewis Field Cleveland, Ohio 44135-3191, February 2002. 82 pages.

Bibliography

[91] Adams, J. C., Brainerd, W. S., Martin, J. T., Smith, B. T., and Wagener, J. L. *Fortran 90 Handbook — Complete ANSI/ISO Reference*. McGraw-Hill, New York, New York, USA, 1992.

[92] Bejan, A., and Kraus, A. D. *Heat transfer handbook*. John Wiley & Sons, Hoboken, New Jersey, USA, 2003.

[93] Brandt, P. An Evaluation of the Advanced Zero Emissions Power Plant Cycle. Master of Science in Thermal Power Thesis, Cranfield University — School of Engineering, 2007.

[94] Chang, X., Zhang, C., Dong, X., Yang, C., Jin, W., and Xu, N. Experimental and modeling study of oxygen permeation modes for asymmetric mixed-conducting membranes. *Journal of Membrane Science 322*, 2 (2008), 429–435.

[95] Chapman, S. J. *Fortran 90/95 for Scientists and Engineers*. WCB/McGraw-Hill, Boston, Massachusetts, USA, 1998.

[96] Department of Trade and Industry (DTI) UK. Review of the Feasibility of Carbon Dioxide Capture and Storage in the UK, 2003.

[97] Hodge, B. K. *Analysis and design of energy systems*, second ed. Prentice-Hall, Englewood Cliffs, New Jersey, USA, 1990.

[98] Kakaç, S., Bergles, A. E., and Mayinger, F. *Heat exchangers: thermal-hydraulic fundamentals and design*, first ed. McGraw-Hill International Book, 1981. Papers from the NATO Advanced Study Institute on "Heat Exchangers — Thermal-Hydraulic Fundamentals and Design." held in Istanbul, Turkey, Aug. 4–15, 1980.

[99] Prasad, R., Gottzmann, C. F., and Drnevich, R. F. Method for Producing Oxygen and Generating Power Using a Solide Electrolyte

Membrane Integrated with a Gas Turbine. Patent, December 1998. US Patent Number 5 852 925.

[100] Reid, J. The New Features of Fortran 2003. Tech. Rep. N1579, ISO/IEC/JTC1/SC22/WG5 (International Fortran Standards Committee), Benson, United Kingdom, 2003.

[101] Ruggieri, G. Advanced low carbon power systems: Evaluation of auto thermal reformer combined cycle. Master of Science in Thermal Power Thesis, Cranfield University — School of Engineering, 2008.

[102] Smith, J. B., and Norby, T. On the steady-state oxygen permeation through $La_2NiO_{4+\delta}$ membranes. *Journal of the Electrochemical Society 153*, 2 (2006), A233–A238.

[103] Sunden, B., and Faghri, M. *Computer simulations in compact heat exchangers*, vol. 1. Computational Mechanics Publications, Southampton, United Kingdom, 1998.

[104] Winterbone, D. E. *Advanced Thermodynamics for Engineers*. Butterworth-Heinemann, 1996.

[105] Xu, S. J., and Thomson, W. J. Oxygen permeation rates through ion-conducting perovskite membranes. *Chemical Engineering Science 54*, 17 (1999), 3839–3850.

[106] Zeng, Q., Zuo, Y.-b., Fan, C.-g., and Chen, C.-s. CO_2-tolerant oxygen separation membranes targeting CO_2 capture application. *Journal of Membrane Science 335*, 1–2 (2009), 140–144.